UNIVERSITAS
FRIBURGENSIS

UNIVERSITÉ DE FRIBOURG SUISSE
UNIVERSITÄT FREIBURG SCHWEIZ

ON THE VOLUME CONJECTURE FOR HYPERBOLIC KNOTS

MASTER THESIS

submitted
by

ANNICK SCHMITGEN

Department of Mathematics
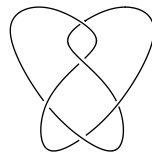
Under the supervision of
Professor Dr. Ruth Kellerhals

July 2010

ABSTRACT

This thesis presents the Volume Conjecture raised by R. Kashaev and provides proofs for the figure-eight knot 4_1 and the knot 5_2.

With the goal of constructing the colored Jones polynomial - one principal constituent of the Volume Conjecture - we first explain the main aspects of the theories of knots, tangles and braids. Hyperbolic geometry, with its volume measure, forms another essential ingredient.

Then we switch to the concept of Hopf algebras to derive the Yang-Baxter equation, whose solutions, the so-called R-matrices, will be investigated through the formalism of quantum groups.

These preliminaries culminate in a physical interpretation and their direct application to the construction of the colored Jones polynomial: consider the finite-dimensional irreducible representations of the quantum universal enveloping algebra of the Lie algebra $\mathfrak{sl}_2(\mathbb{C})$, a quantum group, and decorate the $(1,1)$-tangle diagram of a link according to certain assignment rules. This leads to the treasured colored Jones invariant. Parallel to this, the Kashaev invariant, based on the quantum dilogarithm, is introduced and shown to coincide with the colored Jones polynomial evaluated at the Nth root of unity.

Finally, the Volume Conjecture is exposed first in its original version by R. Kashaev and then in a modified formulation by H. Murakami and J. Murakami. Numerical evidence supporting the Conjecture and rigorous proofs for the cases of the knot 4_1 and the knot 5_2 are provided. The thesis concludes with a current list of links for which the Volume Conjecture has been analytically proven and with some general remarks regarding possible generalizations of the Conjecture and related methods.

Contents

1. INTRODUCTION

The genuine discovery of the Jones polynomial in 1984 sparked off a dazzling quest for other link invariants and tremendous progress in the domain of knot theory has been achieved since then. Most fascinating is the fact that these new achievements are not confined to knot theory, but appeal to many other fields ranging from topology, geometry to algebra and mathematical physics. In particular, many concepts come from the physics area leading to so-called quantum groups from which quantum invariants are derived. The Volume Conjecture, first raised by R. Kashaev in 1996, is one stunning result that unifies the world of these invariants with the world of hyperbolic geometry. Indeed, it states that the classical limit of the colored Jones polynomial of a knot evaluated at a root of unity gives the hyperbolic volume of the knot complement.

In this context, the present work not only aims to provide a survey of the Volume Conjecture, its constituent parts and proofs for two selected cases, but also to comment on the physics at the background of the theory of three-manifold invariants.

First, we explain the main features of the theories of knots, tangles and braids, which are essential notions for the construction of the colored link invariants. The first theory is necessary to understand the impact of these invariants, the second theory is indispensable to prove their mere existence and finally the third theory enters into the link invariant definition. Besides, a seemingly completely different subject is treated in the second part of chapter 2, namely hyperbolic geometry. Of particular interest is the computation of hyperbolic volume as well as the Gromov norm of the three-manifold given by the link complement.

Switching over to algebra and physics in chapter 3, we derive, by a purely abstract method involving Hopf algebras, the Yang-Baxter equation. This equation stands at the basis of the link invariants we are heading for and is of significant relevance in physics. A fundamental role is played by the quantum inverse scattering method. Moreover, we study quantum groups that were originally conceived as a machinery for producing solutions to the Yang-Baxter equation by the so-called R-matrices. This approach gradually found applications in other areas, particularly in the theory of link invariants. The quantum universal enveloping algebra of a Lie algebra represents one of the most important classes of quantum groups. We investigate the case of the Lie algebra $\mathfrak{sl}_2(\mathbb{C})$, whose finite-dimensional irreducible representations are required for coloring the Jones polynomial.

This alludes to chapter 4, which is dedicated to the colored Jones polynomial J_N, a generalization of the well-known Jones polynomial. Its general construction is explained, followed by the definition of the link invariant $\langle - \rangle_N$ introduced by R. Kashaev in the framework of quantum groups. With the goal of clarifying Kashaev's invariant from a mathematical point of view, H. Murakami and J. Murakami revised the colored Jones polynomial evaluated

at the Nth root of unity and this in the framework of enhanced Yang-Baxter operators. In this way, they succeeded to show the equivalence between both invariants.

In chapter 5, we turn to the famous Volume Conjecture, exposing first its original formulation by R. Kashaev and then a modified version by H. Murakami and J. Murakami. Main evidence to the Conjecture is provided by a numerical method. However, this one is not entirely satisfactory for a stout-hearted mathematician but stimulates the search for a general algorithm in order to show the Volume Conjecture rigorously. Up to now, such a method is still not available, and henceforth the Conjecture needs to be studied for each link individually. We illustrate the difficulties through the proofs for the figure-eight knot 4_1 and the knot 5_2. A current list of links for which the Volume Conjecture has been analytically proven is attached. Finally, we conclude with some remarks on possible generalizations as well as on a potential global algorithm to prove the Conjecture.

2. Preliminaries

Although the present work, motivated by physical arguments, involves features of knot theory, algebra as well as geometry, we are not able to give here an elaborate introduction to these vast fields. With the objective of being self-explanatory, this thesis should not overflow the reader with certainly interesting, but not vital information for the sequel. Therefore, we briefly introduce the main notions in the areas of:

- knots, links, braids and tangles (2.1, 2.2),
- hyperbolic geometry (2.3).

2.1. Knots and Links

The roots of knot theory lie back in the 19$^{\text{th}}$ century, when C.F. Gauss dedicated to them a first mathematical study. Significant stimulus to the field was then brought by Lord Kelvin, who had the conviction that atoms were knots in the aether. By that time, tabulation of knots was of major concern and cumulated in Tait's knot tables. Through the following century, knot theory gained further interest and established as part of the subject of topology. Despite this tremendous gain in popularity, the major and most exciting breakthroughs in the field date from the past thirty years and inconceivable jewels are yet to be discovered. Proper understanding of the complicated knotting phenomena in DNA helices or other polymers are just some of the numerous yet open questions that keep research in knot theory extremely active.

Here, we concentrate primarily on invariants, whose breakthrough came with the discovery of the Jones polynomial and the work of other distinguished mathematicians and theoretical physicists, as well as on the volume of the knot complement in the 3-sphere. We refer to [Ada94], [Lic97], [PS97] and [Tur09] for more details.

2.1.1. Polygonal and smooth approaches. Intuitively, we would define a knot as a subspace of $\mathbb{R}^3$ homeomorphic to the circle $\mathbb{S}^1$. However this definition is not satisfactory, because it allows knots with infinitely many crossings, the so-called *wild knots*. As a consequence, we rely on the polygonal ap-
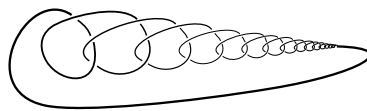

Figure 1: *Example of a wild knot*

proach in order to define knots without being confronted to such problems.

Definition 2.1.
A *polygonal knot* is a subset of $\mathbb{R}^3$ homeomorphic to $\mathbb{S}^1$ and expressible as

a disjoint union of finitely many points (vertices) and open straight lines (edges).

Remark. Imagine a physical knot K in $\mathbb{R}^3$. Clearly, a *knot diagram* corresponds to the planar representation (standard projection on the xy-plane) of K with additional information recorded (over/under-crossings) (see Figure 2). However, we need to be careful while drawing a knot diagram: knots must be in *general position* before being projected. In general position means that the pre-image of every point in the projected knot consists of either one or two points and in the latter case, neither being a vertex of K. In other words, in the 3-dimensional knot picture, there are no edges above edges, no vertical edges (that is parallel to the z-axis), no tangencies and no triple (or "higher") points. It turns out that any knot can be put into general position (by a small perturbation of the vertices). Hence, every knot disposes of a representing diagram.
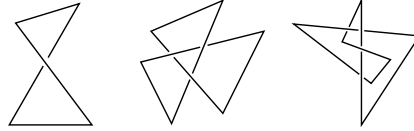
Figure 2: *polygonal knots: unknot, trefoil and figure-eight knot*

Even though this definition is mathematically compliant, it does not reflect our intuitive perception of a tangled rope. Thus, we invoke the smooth approach. In the sequel, we denote by $\mathbb{S}^1$ and $\mathbb{S}^3$ the 1-sphere and the 3-sphere respectively, that is

$$\mathbb{S}^1 = \{x \in \mathbb{R}^2 \mid \|x\| = 1\},$$
$$\mathbb{S}^3 = \{x \in \mathbb{R}^4 \mid \|x\| = 1\} \cong \mathbb{R}^3 \cup \{\infty\}.$$

Definition 2.2.
Let $f : \mathbb{S}^1 \longrightarrow \mathbb{S}^3$ be an infinitely differentiable embedding with non-vanishing differential. Then $K := f(\mathbb{S}^1)$ is called a *(smooth) knot*.

Remarks.
- These two approaches of definitions 2.1 and 2.2 give rise to the same theory. Indeed, there is a 1-to-1 correspondence, called *smoothing*, that takes polygonal knots to smooth knots. Thus, from now on, we consider all knots to be polygonal, but we are going to think about them as being drawn smoothly.
- An *oriented knot* is obtained by specifying a direction on it.
- Two oriented knots K_1 and K_2 may be added in the way Figure 5 illustrates. This process is called *connected sum* (we write $K_1 \# K_2$) and is well defined, since it does not depend on where the addition takes place. Moreover, the unknot plays the role of neutral element.
- In the study of the existence of an additive inverse for a non-trivial knot,

the notion of *prime knot* is indispensable. In fact, a knot is said to be *prime* if it is not the unknot and if it is not the connected sum of two non-trivial knots. Similarly to numbers, every knot can be expressed uniquely, up to recording of summands, as a finite sum of prime knots (Schubert's theorem). Consequently, the answer to the question on additive inverses is negative. We are going to work merely with prime knots in the sequel.

Here are some examples of prime knots. Those are denoted by an indexed integer N_m, where N is the number of crossings in the knot diagram and m is the tabulation parameter, distinguishing knots with same N.
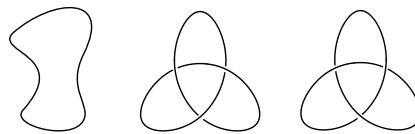
Figure 3: *Unknot, right- and left- handed trefoil*
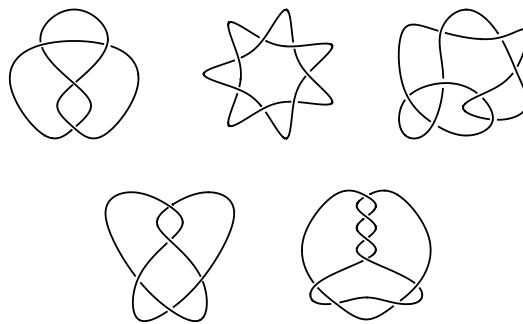
Figure 4: *Figure-eight knot 4_1, knot 5_2, knot 7_2, knot 8_3 and knot 8_8*
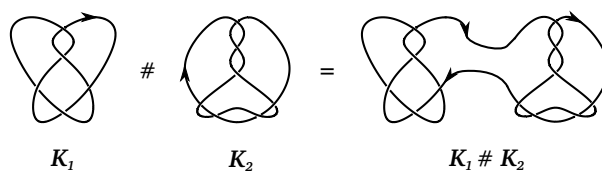
Figure 5: *Connected sum of two knots K_1 and K_2*

The notion of a knot generalizes to that of a link.

Definition 2.3.
A *link L* of m components is a collection of m disjoint knots.

Remarks.
- A one-component link is a knot.
- The notions of general position and diagrams are defined for links as for

knots.

- An *oriented link* is a choice of direction for each component.
- The *connected sum* does not exist for links, since it is not well defined.
- There exist many types of links (and knots). One important class (for which the Volume Conjecture holds) contains the so-called *torus links* $T(p, q)$, where $p \in \mathbb{N}^*, q \in \mathbb{Z}$ are coprime. They are constructed in the following way: place p strands equally along the length of a cylinder and rotate the latter by $\frac{2\pi q}{p}$ in the anti-clockwise direction if $q > 0$ and in the clockwise direction if $q < 0$. Then, join up the ends of the cylinder in order to make a torus. Finally, throw away the torus, but keep the strands. The result is the torus link $T(p, q)$. The class of torus knots constitutes an important example of prime knots. For instance the right-handed trefoil correponds to $T(3, 2)$, the left-handed trefoil to $T(3, -2)$ and the knot 7_2 from Figure 4 is the torus knot $T(7, 2)$.
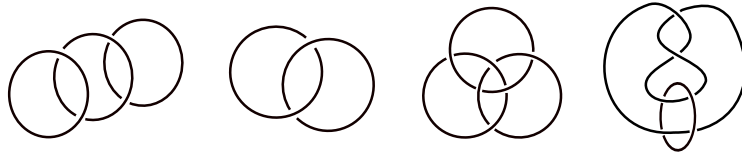
Figure 6: *3-component unlink, Hopf link, Borromean rings and Whitehead link*

2.1.2. Equivalence.   The aim of this section consists in explaining the notions of *equivalent knots* and *equivalent links*. For the sake of legibility, we are going to talk only about links in the sequel, but the whole theory is of course applicable to knots.

The projection of a link is not an injective process. Indeed, a link, depending on how it is embedded in 3-dimensional space, can have various link diagrams. A natural question that arises is the following: Given a set of links, which of them can be deformed by stretching and twisting (without cutting up any strand) one into the other? To answer this question, we need a precise definition of the deformation process.

Definition 2.4.

Suppose a closed triangle ABC in $\mathbb{R}^3$ meets a polygonal link L such that the sides AC and BC of the triangle are edges of the link L that does not intersect the triangle ABC at any other points. Replace the two edges AC and BC by the edge AB obtaining a new link L'. Such a move or its reverse is called a Δ-*move*.

Definition 2.5.

Two links L and L' are *equivalent* or *isotopic* if they can be joined by a sequence of links $L_0 = L, L_1, ..., L_n = L'$ in which each pair (L_i, L_{i+1}) $(0 \leq i \leq n - 1)$ is related by a Δ-move.
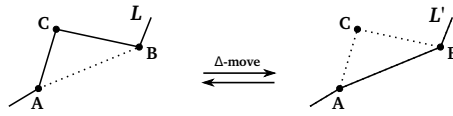
Figure 7: Δ-*move*

Remarks.

- In general, two links L and L' are said to be equivalent in $\mathbb{S}^3$ if there exists an (orientation preserving, if orientation is involved) piecewise linear homeomorphism $h : \mathbb{S}^3 \longrightarrow \mathbb{S}^3$ such that $h(L) = L'$.

- This implies that the *complements* to the links L and L', that is the sets $\mathbb{S}^3 \setminus L$ and $\mathbb{S}^3 \setminus L'$ are homeomorphic. Caution is needed for the converse statement: for knots it is true, but not for links. Indeed, there exist non-isotopic links with homeomorphic complements.

2.1.3. Reidemeister's Theorem. In 1926, K. Reidemeister succeeded in establishing a sequence of moves, called *Reidemeister moves*, that are needed and sufficient to take equivalent links one into the other. More precisely, consider the following local Reidemeister moves.

(R0)   (R1)   (R2)   (R3)
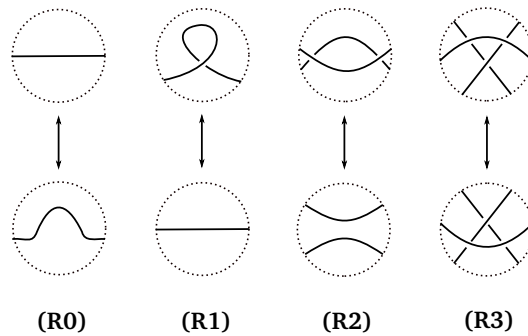
Remark. Link diagrams related by a sequence of moves of type (R0) are said to be *planar isotopic*, that is, the underlying graph structure remains unchanged.

Definition 2.6.
Two diagrams D and D' representing the links L and L' respectively, are *Reidemeister equivalent* if they can be joined by a sequence of diagrams $D_0 = D, D_1,..., D_n = D'$ in which each pair (D_i, D_{i+1}) $(0 \leq i \leq n - 1)$ is related by one of the moves (R0)-(R3).

THEOREM 2.7 (Reidemeister's Theorem)
Let L and L' be two links with corresponding diagrams D and D'. Then L and L' are isotopic if and only if D and D' are Reidemeister equivalent.

Proof. A proof can be found in [PS97] p.11-12.   □

2.1.4. Invariants.   In section 2.1.2 we addressed the problem of comparing links, that is of how to detect if two links are equivalent or not. The Reidemeister moves give us the transformations needed to deform one link into the other if they are equivalent. But still we lack a convenient tool to decide whether or not two links are equivalent and only then, we seek for the appropriate Reidemeister sequence. Another natural question that occurs is the unknotting problem: given a link, is it isotopic to the m-component unlink? The quest for solutions to these essential problems in knot theory motivates the introduction of *link invariants*: we assign to each link diagram an algebraic object, such as a number or a polynomial, that depends only on the link isotopy class. If the value of the invariant for the considered link differs from the value for the unlink, then the link is not isotopic to the latter one. In general, if the values of such an invariant for two links do not coincide, then they are not equivalent. However, the converse does not hold (even though we wish it to do so), that is if the invariants issue identical values, then the links are not necessarily equivalent. Certainly, this method is effective only if there is a simple algorithm for computing the invariant from the link diagram.

2.1.5. The Jones polynomial.   The famous Jones polynomial, discovered by V. Jones in 1984, is such an invariant for oriented links. Its construction involves the so-called bracket polynomial due to L. Kauffman, which associates to every unoriented link diagram D a Laurent polynomial in one variable A with integer coefficients.

Definition 2.8.
The *Kauffman bracket* or *bracket polynomial* is a function

$$\langle - \rangle : \{\text{link diagrams } D\} \longrightarrow \mathbb{Z}[A^{\pm 1}] \quad \text{defined by}$$

  (i) invariance under planar isotopy (R0),
 (ii) $\langle \text{ unknot } \rangle = 1$,
(iii) $\langle D \sqcup \bigcirc \rangle = (-A^{-2} - A^2)\langle D \rangle$,
(iv) $\langle \asymp \rangle = A\langle)(\rangle + A^{-1}\langle \asymp \rangle$.

Remarks.
-   (iv) is referred to as *skein relation* and defines the bracket inductively.
-   Besides, the Kauffman bracket can be expressed as a *state sum*. This will be useful for the physical interpretation we give in chapter 3. A *state S* of a diagram is an assignment of $+1$ or -1 to each crossing; indeed we can resolve each crossing by the rule

$$)(\xleftarrow{\;+1\;} \times \xrightarrow{\;-1\;} \asymp .$$

As a result, each state S gives a collection of circles in the plane, $\kappa(S)$ being the number of these circles. The Kauffman bracket can now be reformulated as follows

$$\langle D \rangle = \sum_S A^{\varsigma(S)}(-A^2 - A^{-2})^{\kappa(S)-1}, \tag{2.1}$$

where $\varsigma(S)$ is the sum of the assignment values ± 1. A straightforward calculation using this new definition of the bracket then shows that

$$\langle D_1 \# D_2 \rangle = \langle D_1 \rangle \langle D_2 \rangle. \tag{2.2}$$

The Kauffman bracket has one main deficiency: it is not invariant under Reidemeister move (R1), whereas (R0),(R2),(R3)-invariance is guaranteed. This makes us wondering if there exists a slight modification which transforms the bracket into a new polynomial, invariant under all Reidemeister moves. The answer is yes and the result is the Jones polynomial. The modification occurs in 2 steps.

1. We need to introduce the notion of *writhe* $\omega(D)$ of an oriented link diagram, which corresponds to the sum of the signs of all the crossings; the sign of a crossing being defined as follows
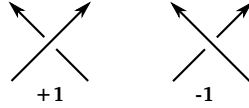
Figure 8: *Sign associated to a crossing*

   It turns out that ω is invariant under (R0), (R2) and (R3) and changes by ± 1 under (R1).

2. For an oriented link diagram D, we define

$$f_D(A) := (-A^3)^{-\omega(D)} \langle D \rangle \in \mathbb{Z}[A^{\pm 1}]. \tag{2.3}$$

Clearly, $f_D(A)$ is invariant under (R0), (R2) and (R3) since both $\omega(-)$ and $\langle - \rangle$ are. A short calculation shows that (R1)-invariance is also satisfied by $f_D(A)$. This enables us to define the Jones polynomial.

Definition 2.9.
The *Jones polynomial* $V(L)$ of an oriented link L is the polynomial $f_D(A)$ for any diagram D representing L with the substitution $A = t^{-\frac{1}{4}}$.

Examples 2.10.

$$V(\bigcirc) = (-A^3)^{-\omega(\bigcirc)}\langle\bigcirc\rangle \;\Big|_{A\to t^{-\frac{1}{4}}} \overset{\text{(ii)}}{=} (-A^3)^0 \cdot 1 \;\Big|_{A\to t^{-\frac{1}{4}}} = 1$$

$$V(\bigcirc \sqcup \bigcirc) = (-A^3)^{-\omega(\bigcirc\sqcup\bigcirc)}\langle\bigcirc \sqcup \bigcirc\rangle \;\Big|_{A\to t^{-\frac{1}{4}}}$$

$$\overset{\text{(iii)}}{=} (-A^3)^0(-A^{-2}-A^2)\langle\bigcirc\rangle \;\Big|_{A\to t^{-\frac{1}{4}}}$$

$$\overset{\text{(ii)}}{=} (-A^{-2}-A^2) \;\Big|_{A\to t^{-\frac{1}{4}}} = -t^{\frac{1}{2}}-t^{-\frac{1}{2}}$$

$$V(\circledS) = (-A^3)^{-\omega(\circledS)}\langle\circledS\rangle \;\Big|_{A\to t^{-\frac{1}{4}}} = \ldots = -t^4+t^3+t$$

$$V(\circledS) = (-A^3)^{-\omega(\circledS)}\langle\circledS\rangle \;\Big|_{A\to t^{-\frac{1}{4}}} = \ldots = -t^{-4}+t^{-3}+t^{-1}$$

Similarly to the Kauffman bracket, the Jones polynomial satisfies a skein relation.

Theorem 2.11
Let L_+, L_- and L_0 be three oriented links differing only locally according to the diagrams

$$L_+ \qquad\qquad L_- \qquad\qquad L_0$$
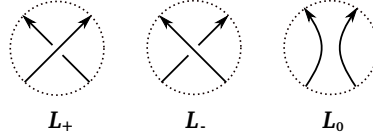
Then the following skein relation is satisfied

$$t^{-1}V(L_+) - tV(L_-) = (t^{\frac{1}{2}}-t^{-\frac{1}{2}})V(L_0). \tag{2.4}$$

Proof. The calculations for the proof may be found in [Lic97] p.28. □

Properties 2.12.

1. $V(L) \in \mathbb{Z}[t^{-\frac{1}{2}}, t^{\frac{1}{2}}]$ for any link L.

2. As a result of (2.3), we get $V(L \sqcup \bigcirc) = (-t^{-\frac{1}{2}}-t^{\frac{1}{2}})V(L)$ for any link L.

3. (2.2) implies that $V(K_1 \# K_2) = V(K_1)V(K_2)$ for any two knots K_1, K_2.

4. As a consequence of the previous property and theorem 2.11 we have that $V(K_1 \sqcup K_2) = (-t^{-\frac{1}{2}}-t^{\frac{1}{2}})V(K_1)V(K_2)$ for any two knots K_1, K_2.

5. If $\bar{L}$ is the mirror image of L (that is, the link obtained by reversing all over-/undercrossings), then $V(\bar{L}) = V(L)\big|_{t\to t^{-1}}$.

6. It can be shown that the Jones polynomial is the only polynomial invariant in $\mathbb{Z}[t^{-\frac{1}{2}}, t^{\frac{1}{2}}]$ of oriented links featuring property (2.4) and a normed value for the unknot, namely 1.

In fact, the efficiency of a link invariant is not only measured by the computational costs, but simultaneously by the 'degree of accuracy' of the statement that identical invariants yield equivalent links. The Jones polynomial is excellent at distinguishing knots and links, but unfortunately not infallible. For instance for the knots 5_1 and 10_{132}, that cleary are not equivalent (different crossing numbers), the Jones polynomials coincide. Another related problem with the Jones polynomial is the open question whether there exists a non-trivial knot K (that is, different from the unknot) such that $V(K) = 1$.

Attempts to generalize or to improve the Jones polynomial lead to the Kauffman polynomial and the HOMFLY-PT polynomial, invariants of oriented links given by Laurent polynomials with integer coefficients and in two variables. They are independent invariants in the sense that they distinguish different pairs of knots (for instance the knots 11_{255} and 11_{257} have the same Kauffman polynomial but different HOMFLY-PT polynomials). We remark that by a subtle change of variables, these polynomials can be reduced to the Jones polynomial. We will not give further details to these and other polynomial invariants here. However, notice that the procedure in chapter 4, used to define the *colored Jones polynomial*, leads to the HOMFLY-PT polynomial with a particular choice of enhanced Yang-Baxter operator (cf. 4.5).

2.1.6. The link group. In addition to the scalar and polynomial invariants, there exist other invariants of links that do not rely on their diagrams and bear powerful techniques of algebraic topology and homology (two interesting vast fields, that we are however not going to specify in this work, since they are not of main concern). The group of a link provides such an example. Its definition involves the *link complement* or the *link exterior*.

Definition 2.13.
Let L be a link in $\mathbb{S}^3$. The *link exterior* X is defined to be

$$X := \mathbb{S}^3 \setminus \{\text{open neighbourhood of } L\}.$$

Remarks.
- X is a compact 3-manifold with boundary a torus.
- X is homeomorphic to $\mathbb{S}^3 \setminus L$.

Definition 2.14.
The *link group* of a link $L \subset \mathbb{S}^3$ is defined to be the fundamental group of its exterior, that is $\Pi_1(\mathbb{S}^3 \setminus L)$.

We are not going to specify presentations of the link group. We refer to [Tur09] for an overview on the *Wirtinger presentation* and on *Van Kampen's Theorem*. Even though, let us have a glance at two examples.

Examples 2.15.
- $\Pi_1(\mathbb{S}^3 \setminus \bigcirc) \cong \mathbb{Z}$.
- $\Pi_1(\mathbb{S}^3 \setminus T(p,q)) \cong \langle a, b : a^p = b^q \rangle$.

2.2. Braids and Tangles

The study of braid groups turns out to be essential for defining an important class of link invariants, namely the colored Jones polynomials. Furthermore, we are going to see in section 3 that the braid point of view establishes a connection between the Yang-Baxter equation and knot theory. The following initiation is based on [PS97].

2.2.1. Geometrical interpretation of braids. We start by defining braids geometrically. For an integer $n \geq 1$, we imagine $2n$ points $A_i = (i, 0, 0)$ and $B_i = (i, 0, 1)$ ($i = 1, 2, ..., n$) in $\mathbb{R}^3$. A polygonal line joining one of the points A_i with one of the points B_j is called *ascending* if in the motion of a point from A_i to B_j along this line, its z-coordinate increases monotonically. A *braid in n strands* is defined as a set of pairwise non-intersecting ascending polygonal lines *(strands)* joining the points $A_1, ..., A_n$ to the points $B_1, ..., B_n$.
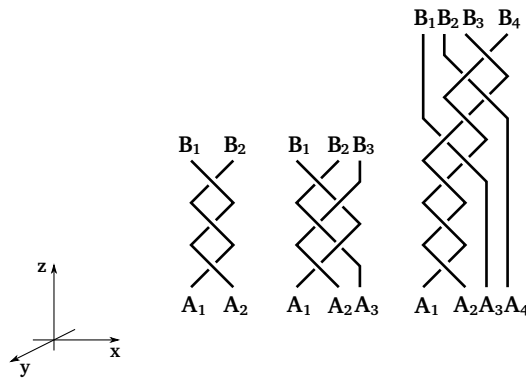
Figure 9: *Examples of braids*

Two braids are said to be *equivalent* if one can be deformed into the other using the Reidemeister moves with the additional condition that the line ABC shown below is ascending. Similarly, if we consider braids whose strands are ascending smooth lines, then equivalence is defined as isotopy, that is as a smooth deformation (the Reidemeister moves can be considered as smooth deformations instead of the polygonal approach) in the class of braids.
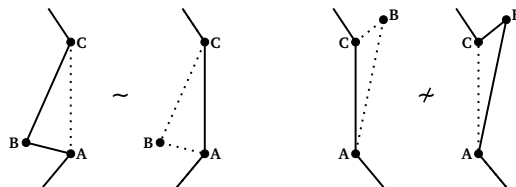
Figure 10: *Additional requirement for equivalence between braids*

2.2.2. Group structure of braids. The set of equivalence classes of braids in n strands has a natural group structure, namely

- the product of two braids σ and ρ in n strands is given by their concatenation; the associativity of this multiplication is an immediate consequence of the definition,
- the unit element simply corresponds to the braid in n parallel vertical strands,
- the inverse σ^{-1} of a braid σ is given by its mirror image with respect to the plane in $z = \frac{1}{2}$ that is parallel to the xy-plane.

The following figures illustrate these properties.
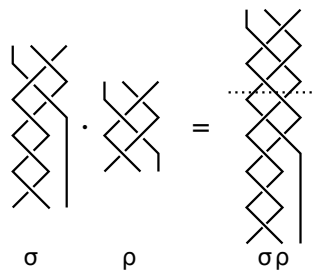
Figure 11: *Product of two braids σ and ρ*
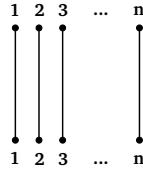
Figure 12: *Unit element in the braid group*
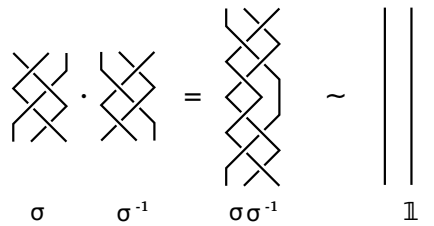
Figure 13: *Inverse of a braid*

The set of equivalence classes of braids in n strands together with this operation is called *braid group* and is denoted by $\mathcal{B}_n$. Our next goal consists in determining a presentation for the braid group and accordingly, we will give a formal definition of $\mathcal{B}_n$.

2.2.3. Presentation of braid groups. First, let us look at the generators of the braid group in n strands. In every equivalence class, we choose one representative with the following projective behaviour

  (i) the projections of the strands on the xz-plane are not tangent to each other;
 (ii) no point in the xz-plane is the projection of 3 or more points from different strands;
(iii) all the crossings occur at different altitudes above the xy-plane.

With respect to these restrictions, the xz-plane projection of a braid in $\mathcal{B}_n$ will be given by a product of generators $\sigma_1, ..., \sigma_{n-1}$ and their inverses.
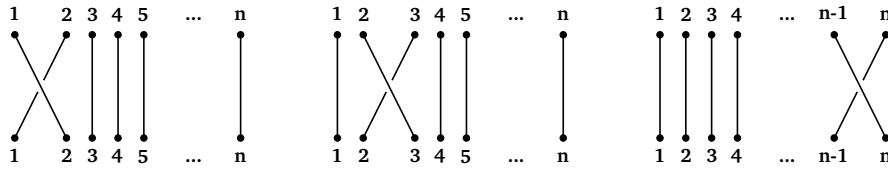
Figure 14: Generators $\sigma_1, \sigma_2, \sigma_{n-1}$
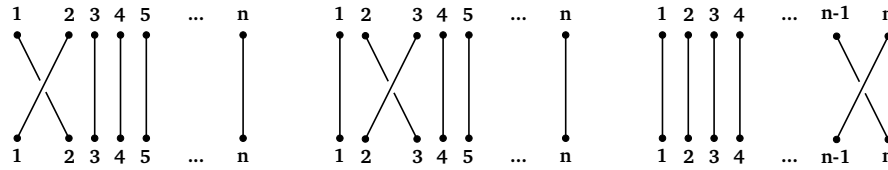
Figure 15: Inverses of generators $\sigma_1^{-1}, \sigma_2^{-1}, \sigma_{n-1}^{-1}$

Now, we are heading for relations among these generators. To this end, we need to consider braid transformations under which the conditions (i) to (iii) break down. It turns out that these transformations correspond mainly to the Reidemeister moves (we exclude (R1), since it does not preserve the braid character), as we want the braid projections to be equivalent. From the pictures below, the following relations result:

$$\sigma_i \sigma_i^{-1} \quad = \quad \mathbb{1}, \tag{2.5}$$

$$\sigma_i \sigma_{i+1} \sigma_i \quad = \quad \sigma_{i+1} \sigma_i \sigma_{i+1}, \tag{2.6}$$

$$\sigma_i \sigma_j \quad = \quad \sigma_j \sigma_i \quad \text{whenever } |i - j| \geq 2. \tag{2.7}$$

The second condition is also called *Artin* or *braid relation*, whereas the last one stands for *far commutativity*, because it states that generators commute, only if they are sufficiently far from each other.
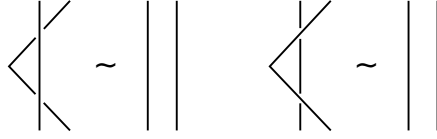
Figure 16: *Illustration of relation (2.5) - result from (R2). (i) breaks down under this transformation.*
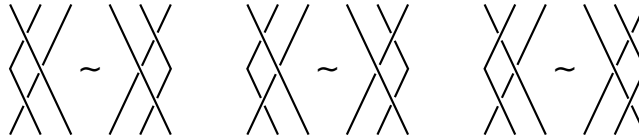
Figure 17: *Illustration of relation (2.6) - Result from (R3). (ii) breaks down under this transformation.*
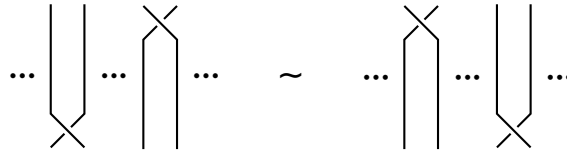
Figure 18: *Illustration of relation (2.7). (iii) breaks down under this transformation.*

Let us summarize these properties in a formal definition for $\mathcal{B}_n$.

Definition 2.16.
Fix an integer $n \geq 3$. The *braid group* with n strands is the group $\mathcal{B}_n$ generated by $n - 1$ generators $\sigma_1, ..., \sigma_{n-1}$ that satisfy the relations

$$
\begin{aligned}
\sigma_i \sigma_j &= \sigma_j \sigma_i \quad \text{whenever } |i - j| \geq 2, \\
\sigma_i \sigma_{i+1} \sigma_i &= \sigma_{i+1} \sigma_i \sigma_{i+1},
\end{aligned}
$$

for any $1 \leq i, j \leq n - 1$.

Remarks.
- For $n = 1$, we get the trivial group: $\mathcal{B}_1 = \{\mathbb{1}\}$,
- For $n = 2$, we get the free group on one generator: $\mathcal{B}_2 \cong \mathbb{Z}$,
- For $n \geq 2$, $\mathcal{B}_n$ is an infinite group.

2.2.4. Mechanical interpretation. In classical mechanics, the space of all possible positions that a physical system, possibly subject to external constraints, may attain is called the *configuration space*. For typical systems, this space is endowed with the structure of a manifold and is also referred to as

configuration manifold (e.g. the configuration manifold of a system of n particles progressing in $\mathbb{R}^3$ corresponds to $\mathbb{R}^{3n}$ or a subspace of $\mathbb{R}^{3n}$ depending on the kinematical properties of the system). Generally, the configuration space of n particles moving in a manifold $\mathcal{M}$ can be regarded as $\mathcal{M}^n$.

With the aim of linking braid theory to mechanics, we limit our study to the case where the physical system is composed of n identical distinct particles in the plane. The configuration space $\mathcal{C}_n \mathbb{R}^2$ is given by

$$\mathcal{C}_n \mathbb{R}^2 = \mathcal{F}_n \mathbb{R}^2 / \mathfrak{S}_n,$$

where $\mathcal{F}_n \mathbb{R}^2 = \{(x_1, x_2, \ldots, x_n) \in (\mathbb{R}^2)^n | x_i \neq x_j, \forall i \neq j\}$ and $\mathfrak{S}_n$ is the symmetric group acting by permuting the coordinates of $\mathcal{F}_n \mathbb{R}^2$. Henceforth, $\mathcal{C}_n \mathbb{R}^2$ consists of unordered n-tuples of points in $\mathbb{R}^2$ and is endowed with the natural topology (see [PS97]).

It turns out that in $\mathcal{C}_n \mathbb{R}^2$ the homotopy classes of loops based at ω_0, where we choose the base point to be $\omega_0 = \{(1,0), (2,0), \ldots, (n,0)\}$, correspond bijectively to the isotopy classes of braids in n strands. Indeed, suppose that at some moment in time t_0, $0 \leq t_0 \leq 1$, a loop passes through an element $X(t_0)$ of the configuration space $\mathcal{C}_n \mathbb{R}^2$. Viewing $X(t_0)$ as a horizontal cut in $\mathbb{R}^3$ at $z = t_0$, $X(t_0)$, as a set, contains n distinct points marked on it. The result of considering these planes for all $t_0 \in [0, 1]$ is a braid in n strands. To exemplify, we look at a physical system of 3 distinct particles in the plane. One possible time evolution of their trajectories is illustrated below. It cleary corresponds to a braid in 3 strands. Furthermore, as a consequence of the correspondence
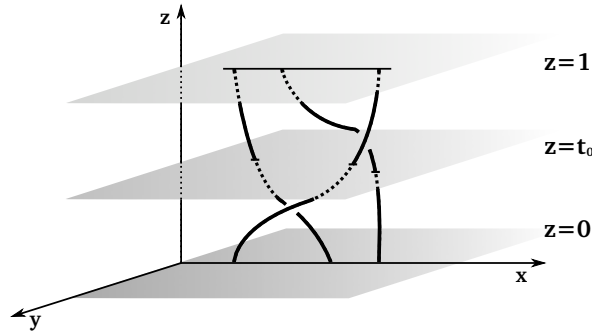
Figure 19: *Braid in 3 strands corresponding to a loop in $\mathcal{C}_3 \mathbb{R}^2$*

between the product of braids and the composition of loops, the fundamental group of the configuration space of n identical distinct particles in the plane is isomorphic to the braid group in n strands

$$\Pi_1(\mathcal{C}_n \mathbb{R}^2) \cong \mathcal{B}_n.$$

2.2.5. Relationship between braids and links. Up to now, we have not yet established any relationship between braids and links. A natural way for

doing so is provided by the closure map $\Omega : \mathcal{B}_n \longrightarrow \{\text{links}\}$. Given a braid σ, we join the upper points of its strands to the lower ones and thus get a link or even a knot. Two questions immediately arise:

1. For what braids does the closure map Ω produce a knot rather than a link?

2. Is Ω a bijective map, that is, is there a 1-to-1 correspondence between the braid group and the set of all possible links?
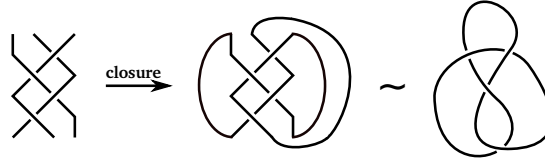
Figure 20: *Illustration of the closure map for the figure-eight knot*

The answer to the first question is given by considering the following map between the braid group $\mathcal{B}_n$ and the permutation group $\mathfrak{S}_n$

$$\xi : \mathcal{B}_n \longrightarrow \mathfrak{S}_n$$
$$\sigma_i \longmapsto (i, i+1) =: \tau_{i,i+1}.$$

In other words, regarding the geometrical interpretation of braids, the ith strand from a braid σ originating from A_i ends up at $B_{\xi(\sigma)(i)}$. The following properties hold for ξ:

- ξ is surjective (as the permutation group is generated by transpositions),

- ξ is a group homomorphism: it is sufficient to show that $\xi(\sigma_i\sigma_j) = \xi(\sigma_i)\xi(\sigma_j)$ for $1 \leq i, j \leq n$. Actually, we have:

$$\xi(\sigma_i\sigma_j) = \begin{cases} 1 = \tau_{i,i+1}^2 = \xi(\sigma_i)^2 & \text{if } i = j, \\ \tau_{i,i+1}\tau_{j,j+1} = \xi(\sigma_i)\xi(\sigma_j) & \text{if } |i - j| \geq 1. \end{cases}$$

Now we are able to answer our first question: the closure of a braid $\sigma \in \mathcal{B}_n$ is a knot if and only if the associated permutation is cyclic of order n, otherwise there will be more components either linked or unlinked. Thus, we have

PROPOSITION 2.17
The closure of a braid $\sigma \in \mathcal{B}_n$ is a knot $\Longleftrightarrow \langle \xi(\sigma) \rangle \cong \mathbb{Z}_n$.

Let us turn to our second question on the bijective character of the closure map. By looking for example at the closures of $\sigma_1, \sigma_1^{-1} \in \mathcal{B}_2$, we get in both cases the unknot, although $\sigma_1 \neq \sigma_1^{-1}$. Thus injectivity already fails. However, the closure map is surjective.

THEOREM 2.18 (Alexander's Braiding Theorem)
Any link, in particular any knot, is the closure of some braid.

Proof. A proof may be found in [KT08] p.59-60 or in [Bir74] p.55-56. □

Ω not being a bijection, we want to know in what cases the closures of different braids produce isotopic links. This problem has been solved by Markov. Before exposing his result, we need to introduce the following algebraic transformations of braids, called *Markov moves*:

1. For braids $\sigma, \rho \in \mathcal{B}_n$, exchange σ by $\rho\sigma\rho^{-1}$ (*first Markov move*);

2. For a braid $\sigma \in \mathcal{B}_n \subset \mathcal{B}_{n+1}$ and $\sigma_n \in \mathcal{B}_{n+1}$ (n^{th} generator of $\mathcal{B}_{n+1}$), exchange σ by $\sigma\sigma_n^{\pm 1}$ (*second Markov move*) or exchange $\sigma\sigma_n^{\pm 1}$ by σ (*inverse second Markov move*).
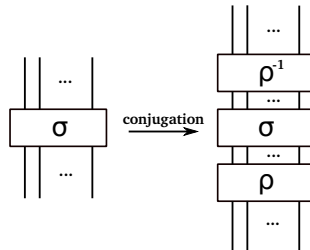
Figure 21: *First Markov move: conjugation*
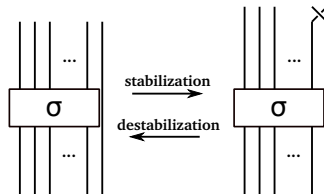
Figure 22: *Second Markov move and its inverse: (de-)stabilization*

THEOREM 2.19 (Markov's Theorem)
The closures of two braids are isotopic if and only if one braid can be deformed into the other by a finite sequence of Markov moves.

Proof. For a proof, we refer to [KT08] p.69-90. The first published proof may be read in [Bir74] p.51-69. □

2.2.6. Tangles. In addition to the theories of knots, links and braids, there is another interesting related concept - the concept of tangles, which generalizes the notion of links. In this section, we will just give a brief introduction

to the theory of tangles in order to be appropriately equipped for the sequel. For further details [KM91], [KRT97] and [Kass95] may be consulted.

In the following, we denote by I the closed unit interval $[0, 1]$ and by $\mathcal{M}^1$ a 1-manifold (that is a circle or an arc or here a finite collection of them).

Definition 2.20.

Let $f : \mathcal{M}^1 \longrightarrow I^3 \subset \mathbb{R}^3$ be a proper embedding such that $\partial T \subset \frac{1}{2} \times I \times \partial I$, where $T := f(\mathcal{M}^1)$. Define $\partial_- T := T \cap (I^2 \times 0), \partial_+ T := T \cap (I^2 \times 1)$ as well as $m := |\partial_- T|$ and $n := |\partial_+ T|$ for $m, n \in \mathbb{N}$. Then T is called an (m, n)-*tangle*.

Remarks.

- As a consequence of the definition, a link is a $(0, 0)$-tangle. Any general tangle consists of a link together with a finite collection of proper (pairwise disjoint) arcs.
- Braids constitute a special class of tangles. For any integer $n \geq 1$, a braid on n strands can be considered as an (n, n)-tangle T with the additional properties that T does not contain any closed circles and that the intersection of T with $I^2 \times z, \forall z \in I$, consists of exactly n distinct points. Henceforth, in the following chapters, although we are going to work exclusively with braids, we can apply results from the theory of tangles.
- Unless explicitly stated, we do not assume tangles to be oriented.
- Similary to links and braids, we study tangles by their 2-dimensional diagrams D in the square I^2, where $\partial D \subset I \times \partial I$.

Examples 2.21.

The $(2, 2)$-tangle does not correspond to a braid in $\mathcal{B}_2$, because there is a variable number of intersection points of the tangle with $I^2 \times z, z \in I$.
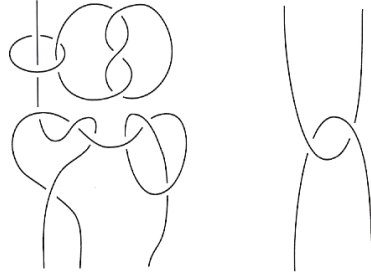
Figure 23: *(3,1)-tangle and (2,2)-tangle (extracted from [KRT97])*

Finally, we look for an adequate equivalence relation on the set of all (m, n)-tangles, which, by the way, form a complex vector space (see [KRT97] p.54 for more details). It turns out that any tangle diagram can be split into elementary diagrams denoted by $I, R, L, \cap, \cup$ (with all possible orientations if required) using the composition $\circ$ (when defined) and the tensor product $\otimes$ of diagrams (see Figure 24).

$$I \qquad R \qquad L \qquad \cap \qquad \cup$$

$$\boxed{T_1} \circ \boxed{T_2} = \boxed{\begin{array}{c} T_1 \\ \hline T_2 \end{array}} \qquad \boxed{T_1} \otimes \boxed{T_2} = \boxed{T_1 \,|\, T_2}$$
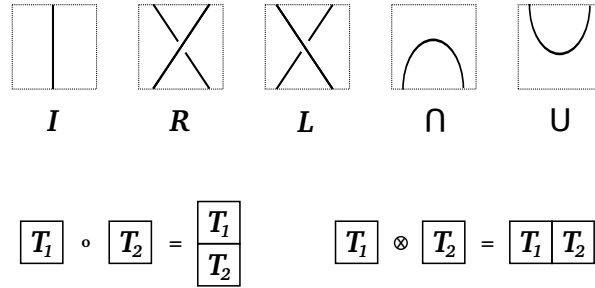
Figure 24: *Elementary diagrams; composition and tensor product of tangles*

Similarly to links, the Reidemeister moves defined in 2.1.3 apply to tangle diagrams as well (clearly, they do not move the endpoints of the arcs). Thus, two (m, n)-tangles S and T are said to be *equivalent* or *isotopic* if their component diagrams are related by a sequence of Reidemeister moves together with the implicit associativity and identity relations and $(S_1 \circ T_1) \otimes (S_2 \circ T_2) = (S_1 \otimes S_2) \circ (T_1 \otimes T_2)$.

In chapter 4, we will consider $(1, 1)$-tangles in order to define link invariants.

2.3. Hyperbolic Geometry

The discovery of hyperbolic geometry was stimulated by the criticism of the parallel (fifth) postulate of Euclidean geometry, which states that for any point outside a given infinite straight line, there exists only one infinite straight line running parallel to the first line and passing through that point. On one side, this criticism was nourished by the fact that in comparison to the four other postulates of Euclidean geometry, the fifth was of infinitesimal nature and less axiomatic. On the other side, Euclid showed in one of the books of his famous work *Elements* the converse of the parallel postulate (that is that the sum of the angles of a triangle is less than 180°), which is curious because the postulate itself seemed to be unprovable. Combined with the fact that most of plane geometry can be proved without the fifth postulate, these arguments militated in favour of the unnecessity of the latter.

In the 18th and at the beginning of the 19th century, C.F. Gauss, J. Bolyai and N. Lobachevsky studied a theory based on the Euclidean axioms apart from the fifth postulate. These investigations led to the unexpected and remarkable discovery of a new consistent, non-Euclidean geometry, today known as *hyperbolic geometry*. As a result for this progress, E. Beltrami succeeded finally in 1868 to show the independence of the fifth postulate.

In order to work in hyperbolic geometry, we need an appropriate model, an equivalent to the unit sphere for spherical geometry. There are at least four models: the *Beltrami-Klein model* (*projective disc model*), the *Poincaré ball model* (*conformal ball model*), the *Poincaré half-space model* and the *Lorentz model* (*hyperboloid model*). We are going to treat briefly the last three ones

with the aim of exposing how to compute the volume of a hyperbolic 3-manifold.

The following introduction is not exhaustive (we omit all proofs), but will be sufficiently helpful for the sequel. For further reading, especially for proofs, we may refer to [Rat06], [Kel08] and [Kel10].

2.3.1. The hyperboloid model. The hyperboloid model or Lorentz model is often used as basic model for hyperbolic geometry, since it most naturally exhibits the duality between spherical and hyperbolic geometries.

In a first step, we need to define a new inner product on $\mathbb{R}^{n+1}$ (suppose $n > 1$) beside the habitual one. Let E^n be the Euclidean n-space with the standard basis $\{e_1, e_2, \ldots, e_n\}$ and let $E^{n,1}$ be the real vector space $\mathbb{R}^{n+1}$ endowed with the following bilinear form

$$\langle x, y \rangle_{n,1} := \sum_{k=1}^n x_k y_k - x_{n+1} y_{n+1},$$

where $x = (x_1, x_2, \ldots, x_{n+1}), y = (y_1, y_2, \ldots, y_{n+1}) \in \mathbb{R}^{n+1}$. $E^{n,1}$ is called *Lorentzian n-space* with signature $(n, 1)$. Notice that this new inner product is not a scalar product and induces the norm $\|x\|_{n,1} := \sqrt[+]{\langle x, x \rangle_{n,1}}$ which allows for complex lengths. Thus, we may distinguish three types of vectors in $E^{n,1}$, namely $x \in E^{n,1}$ is said to be

$$\begin{cases} \textit{light-like} & \Longleftrightarrow & \|x\|_{n,1} = 0, \\ \textit{space-like} & \Longleftrightarrow & \|x\|_{n,1} > 0, \\ \textit{time-like} & \Longleftrightarrow & \|x\|_{n,1} < 0. \end{cases}$$

A time-like vector is called *positive* if and only if $x_{n+1} > 0$.

What is more, equivalently to the orthogonal transformations defined on $\mathbb{R}^{n+1}$ with respect to the Euclidean inner product, we may define endomorphisms Φ of $\mathbb{R}^{n+1}$ featuring the same property with respect to the Lorentzian inner product. Such a map is called *Lorentz transformation* and satisfies

$$\langle \Phi(x), \Phi(y) \rangle_{n,1} = \langle x, y \rangle_{n,1}.$$

A matrix $A \in \mathrm{Mat}(n+1, \mathbb{R})$ is said to be *Lorentzian* if and only if the associated linear transformation $A : \mathbb{R}^{n+1} \longrightarrow \mathbb{R}^{n+1}$ defined by $A(x) = Ax$ is Lorentzian. The set of all Lorentzian $(n+1) \times (n+1)$-matrices together with matrix multiplication forms a group, called the *Lorentz group* and is denoted by $\mathrm{O}(n, 1)$. The set

$$\mathrm{PO}(n, 1) := \{A \in \mathrm{O}(n, 1) | A \text{ positive}\}$$

is a subgroup of $\mathrm{O}(n, 1)$ and is called *positive Lorentz group*.

In order to define the hyperboloid model explicitly, we need the following result.

PROPOSITION 2.22
Let $x, y \in E^{n,1}$ be positive time-like vectors. Then there is a unique nonnegative

real number $\eta(x, y)$ such that

$$\langle x, y \rangle_{n,1} = \|x\|_{n,1} \|y\|_{n,1} \cosh \eta(x, y).$$

$\eta(x, y)$ *is called the Lorentzian time-like angle between x and y.*

$\square$

Definition 2.23.
The *hyperboloid model* or *Lorentz-Minkowski model* for hyperbolic n-space $\mathbb{H}^n$ is defined by

$$H^n := \{x \in E^{n,1} \mid \|x\|_{n,1} = -1, x_{n+1} > 0\}.$$

For $x, y \in H^n$, a distance is given by

$$d_H(x, y) := \eta(x, y),$$

d_H is called the *hyperbolic distance* between x an y on H^n.

Remarks. Let us summarize some important facts on (H^n, d_H).

- The group of *isometries* of H^n is isomorphic to the positive Lorentz group, that is $\mathrm{Iso}(H^n) \cong \mathrm{PO}(n, 1)$.

- In order to study *geodesics* in H^n, we shall recall the notions of geodesic (line) and hyperbolic line. Indeed a *geodesic line* λ of (H^n, d_H) is a locally distance preserving continuous function $\lambda : \mathbb{R} \longrightarrow H^n$. A *geodesic* g in H^n is the image of a geodesic line λ, that is $g := \lambda(\mathbb{R})$. Finally, a *hyperbolic line* of H^n is defined to be the intersection of H^n with a 2-dimensional time-like vector subspace of $\mathbb{R}^{n+1}$. It can be shown that the geodesics of H^n are precisely its hyperbolic lines.

- The *element of hyperbolic volume* of H^n with respect to the Euclidean coordinates $x_1, x_2, \ldots, x_n$ is given by

$$\mathrm{dVol}_n = \frac{dx_1 dx_2 \ldots dx_n}{\sqrt{1 + x_1^2 + x_2^2 + \cdots + x_n^2}}.$$

$\square$

2.3.2. The conformal ball model. Another model for hyperbolic geometry is provided by the conformal ball model. The great advantage of this model lies in the fact that its angles agree with the Euclidean angles and that it exhibits Euclidean rotational symmetry with respect to its Euclidean centre. However, this is only achieved at the expense of distortion.

Rather than H^n, we now choose the unit ball $B^n := \{x \in \mathbb{R}^{n+1} \mid \|x\| < 1, x_{n+1} = 0\}$ for our model ($\|-\|$ describing the Euclidean norm). By conformal stereographic projection p of B^n onto H^n via

$$\mathrm{p} : B^n \longrightarrow H^n$$

$$x \longmapsto \left(\frac{2x_1}{1 - \|x\|^2}, \frac{2x_2}{1 - \|x\|^2}, \ldots, \frac{2x_n}{1 - \|x\|^2}, \frac{1 + \|x\|^2}{1 - \|x\|^2} \right),$$

we sense that B^n inherits the metric d_H of H^n. Indeed, we have for $x, y \in B^n$

$$d_B(x, y) := d_H(\mathrm{p}(x), \mathrm{p}(y))$$

is a metric. This leads us to

Definition 2.24.

The *conformal ball model* for hyperbolic n-space $\mathbb{H}^n$ is defined by

$$B^n := \{x \in \mathbb{R}^{n+1} | \|x\| < 1, x_{n+1} = 0\}.$$

For $x, y \in B^n$ and p the stereographic projection of B^n onto H^n, a distance is given by

$$d_B(x, y) := d_H(\mathrm{p}(x), \mathrm{p}(y)),$$

and satisfies

$$\cosh d_B(x, y) = 1 + \frac{2\|x - y\|^2}{(1 - \|x\|^2)(1 - \|y\|^2)}.$$

d_B is called the *hyperbolic distance* between x an y on B^n.

Remarks.

- As a consequence to this metric, we have $d_B(x, 0) \xrightarrow{x \to q \in \partial B^n} \infty$, which suggests that points situated at the boundary of B^n actually form the set of points at infinity.

- The group of *isometries* of B^n is isomorphic to the group of Möbius transformations of B^n, that is $\mathrm{Iso}(B^n) \cong \mathrm{M}(B^n)$.

- The *geodesics* of B^n are composed of the open diameters of B^n (all crossing the centre 0) and circular segments of B^n that are orthogonal to ∂B^n.

- The *element of hyperbolic volume* of B^n with respect to the Euclidean coordinates $x_1, x_2, \ldots, x_n$ is

$$\mathrm{dVol}_n = 2^n \, \frac{dx_1 dx_2 \ldots dx_n}{(1 - \|x\|^2)^n}.$$

$\square$

2.3.3. The upper half-space model. Continuing our walk along the models for hyperbolic space, we now arrive at the upper half-space model, which features conformal Euclidean angles and Euclidean translational symmetry - again at the expense of an unlimited amount of distortion. Similarly to the previous method in the conformal ball model, we pass from B^n to the upper half-space $U^n := \{x \in \mathbb{R}^n | x_n > 0\}$ via a particular map and then transfer the metric. In this case, we choose the *Cayley transformation* c (c is a conformal diffeomorphism) of B^n onto U^n given by

$$c : B^n \longrightarrow U^n$$

$$x \longmapsto -e_n + \left(\frac{\sqrt{2}}{\|x + e_n\|}\right)^2 (x + e_n).$$

This map corresponds to the inversion with respect to the sphere $S(-e_n, \sqrt{2})$, hence satisfies $c^2 = \text{id}$. The metric induced by B^n on U^n reads for $x, y \in U^n$

$$d_U(x, y) := d_B(c(x), c(y)).$$

Definition 2.25.
The *upper half-space model* for hyperbolic n-space $\mathbb{H}^n$ is defined by

$$U^n := \{x \in \mathbb{R}^n | x_n > 0\}.$$

For $x, y \in U^n$ and c the Cayley map from B^n onto U^n, a distance is given by

$$d_U(x, y) := d_B(c(x), c(y)),$$

and satisfies

$$\cosh d_U(x, y) = 1 + \frac{\|x - y\|^2}{2x_n y_n}.$$

d_U is called the *Poincaré metric* on U^n.

Remarks.

- The group of *isometries* of U^n is isomorphic to the group of Möbius transformations of U^n, that is $\text{Iso}(U^n) \cong \text{M}(U^n)$.

- The *geodesics* of U^n are composed of vertical (Euclidean) lines in U^n and semicircles centered in E^{n-1} (thus orthogonal to E^{n-1}).

- The *element of hyperbolic volume* of U^n with respect to the Euclidean coordinates $x_1, x_2, \ldots, x_n$ is

$$\text{dVol}_n = \frac{dx_1 dx_2 \ldots dx_n}{(x_n)^n}.$$

$\square$

2.3.4. Hyperbolic triangles. Instead of exposing a general theory on hyperbolic polytopes and their volume, we concentrate on the cases in 2 and 3 dimensions. For the sake of coherence, we start with some explanations on hyperbolic triangles until switching over to the 3-dimensional case.
Analogous to Euclidean geometry, a hyperbolic triangle originates from the connection of three noncollinear points. Let x, y be distinct points of H^n. Then x, y span a 2-dimensional time-like vector space $V(x, y) \subset \mathbb{R}^{n+1}$ and we have that

$$L(x, y) := H^n \cap V(x, y)$$

is the unique hyperbolic line of H^n crossing both x and y.

Definition 2.26.
Three points $x, y, z \in H^n$ are *hyperbolically collinear* if and only if there is a hyperbolic line L of H^n containing x, y, z.

Definition 2.27.

Let x, y, z be three hyperbolically noncollinear points of H^2. Further, let $L(x, y)$ be the unique hyperbolic line of H^2 containing x and y and let $H_z(x, y)$ be the closed half-plane of H^2 with $L(x, y)$ as its boundary and z in its interior. The *hyperbolic triangle* $\Delta(x, y, z)$ with vertices x, y, z is defined to be

$$\Delta(x, y, z) := H_z(x, y) \cap H_x(y, z) \cap H_y(z, x).$$

A *generalized hyperbolic triangle* in H^2 is a hyperbolic triangle that may have some of its vertices at infinity (the corresponding angle(s) being 0), that is *ideal vertices*. A hyperbolic triangle with three ideal vertices is called an *ideal hyperbolic triangle*.
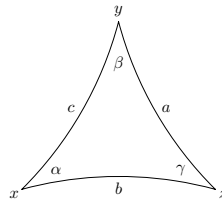
Figure 25: *Hyperbolic triangle in H^2 (extracted from [Rat06])*

Remark. By virtue of the theorem of *angular defect*, we have the following relation for a hyperbolic triangle $\Delta(x, y, z)$ in H^2 with angles α, β, γ

$$\alpha + \beta + \gamma < \pi.$$

Besides the definition of a hyperbolic triangle with respect to the hyperboloid model, we can adopt the point of view of the upper half-plane model, where a triangle is characterized by its angles rather than its vertices. If at least one vertex is at infinity (and thus admits an angle 0), we speak of an *asymptotic triangle* in the upper half-space model U^2, described by $\Delta_\infty(\frac{\pi}{2}, \alpha, 0)$. For an illustration, see the figure below. Although having at least one vertex at in-
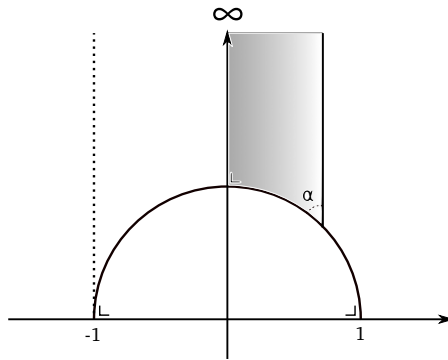
Figure 26: *Asymptotic triangles $\Delta_\infty(\frac{\pi}{2}, 0, 0)$ and $\Delta_\infty(\frac{\pi}{2}, \alpha, 0)$ in U^2*

finity, an asymptotic triangle exhibits a finite area. The general area formula

for a hyperbolic triangle in H^2 is sustained after a right parametrisation of x, y, z by hyperbolic coordinates and integration.

Theorem 2.28
The area of a hyperbolic triangle $\Delta(x, y, z)$ in H^2 with angles α, β, γ is given by

$$Vol_2(\Delta(x, y, z)) = \pi - (\alpha + \beta + \gamma).$$

$\square$

Remark. Consequently, for an asymptotic triangle in U^2, we get

$$\mathrm{Vol}_2\left(\Delta_\infty\left(\frac{\pi}{2}, \alpha, 0\right)\right) = \frac{\pi}{2} - \alpha < \infty.$$

2.3.5. Hyperbolic orthoschemes and tetrahedra. Next, we shall concentrate on hyperbolic orthoschemes and tetrahedra. In fact, the key idea behind this study is that the volume of any hyperbolic 3-manifold obtained by gluing together a finite family of disjoint, convex, finite-sided polyhedra in $\mathbb{H}^3$ of finite volume can be computed by knowing only the gluing pattern. More precisely, the volume of the latter is nothing else than the sum of the volumes of the involved hyperbolic tetrahedra.

Definition 2.29.
A *generalized orthoscheme* or *orthotetrahedron S* in $\mathbb{H}^3$ with angles α, β, γ is a generalized tetrahedron in $\mathbb{H}^3$ with three right dihedral angles and whose four sides can be ordered F_1, F_2, F_3, F_4 so that $\theta(F_1, F_2) = \alpha, \theta(F_2, F_3) = \beta, \theta(F_3, F_4) = \gamma, \theta(F_i, F_j)$ being dihedral angles ($1 \le i < j \le 4$).

Remark. An orthoscheme can be seen as the 3-dimensional analogue of a right triangle, since its four sides are right triangles. Any tetrahedron can be expressed as the algebraic sum of orthoschemes.
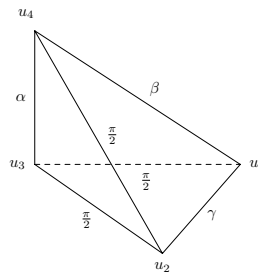
Figure 27: *Orthoscheme in $\mathbb{H}^3$ (extracted from [Rat06])*

Definition 2.30.
A *hyperbolic tetrahedron* is the hyperbolic convex hull of 4 points (possibly at infinity) which do not lie in a 2-dimensional hyperbolic subspace. A vertex at infinity is called an *ideal vertex*. A hyperbolic tetrahedron with four ideal vertices is said to be an *ideal tetrahedron*.
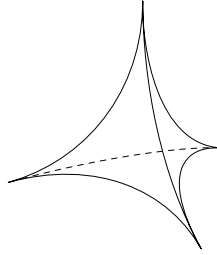
Figure 28: *Regular ideal tetrahedron in B^3 (extracted from [Rat06])*

A classification of ideal tetrahedra is achieved by studying horospheres. A *horosphere* Σ of B^n based at a point b of ∂B^n is the intersection of B^n with of a Euclidean sphere in $\overline{B}^n$ tangent to ∂B^n at b. Its convex interior is referred to as *horoball* centered at b. In 3 dimensions, the visualization of Σ in U^3 is easier, since it inherits a canonical Euclidean structure in an obvious way. Henceforth, we consider a horosphere Σ based at an ideal vertex v of an ideal tetrahedron T that does not meet the opposite side of T. Then $L(v) := \Sigma \cap T$ is a Euclidean triangle and is called the *link* of v in T. It turns out that the link of T does not depend on the choice of vertex and that

THEOREM 2.31
An ideal tetrahedron in $\mathbb{H}^3$ is determined, up to congruence, by the three dihedral angles α, β, γ of the edges incident to a vertex of T. Moreover, $\alpha + \beta + \gamma = \pi$ and the dihedral angles of opposite edges of T are equal. Conversely, if α, β, γ are positive real numbers such that $\alpha + \beta + \gamma = \pi$, then there is an ideal tetrahedron in $\mathbb{H}^3$ with dihedral angles α, β, γ. Such an ideal tetrahedron is denoted by $T(\alpha, \beta, \gamma)$.

$\square$
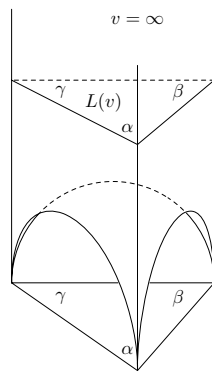
Figure 29: *Ideal tetrahedron in U^3 (extracted from [Rat06])*

Contrary to the previous section, the integration of the volume differential involves more complicated functions.

2.3.6. Dilogarithm, Lobachevsky and Bloch-Wigner functions.   In order to compute the hyperbolic volume of simplices of the type we encountered in the previous section, we need three important functions, namely the Euler dilogarithm, the Lobachevsky function and the Bloch-Wigner function. We start with the study of the Euler dilogarithm.

Definition 2.32.
For $z \in \mathbb{C}$ such that $|z| \leq 1$, the *Euler dilogarithm* is defined by

$$\mathrm{Li}_2(z) := \sum_{r=1}^{\infty} \frac{z^r}{r^2}.$$

Remarks.
- There is an integral form of the Euler dilogarithm, that extends the domain of Li_2 to the whole complex plane. More precisely, for $z \in \mathbb{C}$ such that $|\arg(z)| < \pi$, the analytic continuation of the dilogarithm function is given in a unique way by

$$\mathrm{Li}_2(z) := -\int_0^z \frac{\log(1-t)}{t} dt, \tag{2.8}$$

  with $0 < \arg(1-z) < 2\pi$. In the sequel, if we mention the Euler dilogarithm, we always refer to its analytic continuation.

- For $z = 1$, we obtain the Riemann zeta function ζ evaluated at 2

$$\mathrm{Li}_2(1) = \sum_{r=1}^{\infty} \frac{1}{r^2} = \zeta(2) = \frac{\pi^2}{6}.$$
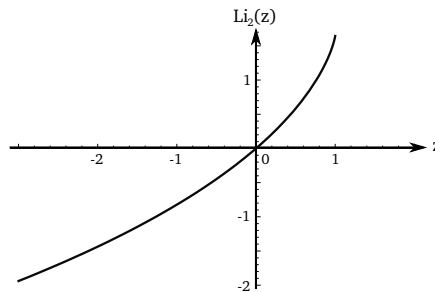
Figure 30: *Euler dilogarithm for real arguments z*

Next, we turn to the Lobachevsky function.

Definition 2.33.
For $\theta \in \mathbb{R}$, the *Lobachevsky function* is defined by the formula

$$\Lambda(\theta) := \frac{1}{2} \Im\left(\mathrm{Li}_2\left(\exp\left(2\theta \mathrm{i}\right)\right)\right) = \frac{1}{2} \sum_{r=1}^{\infty} \frac{\sin\left(2r\theta\right)}{r^2}.$$

Remark. As for the Euler dilogarithm, the Lobachevsky function can be expressed in the form of an integral, more precisely

$$\Lambda(\theta) = -\int_0^\theta \log|2\sin(t)| \, dt. \qquad (2.9)$$
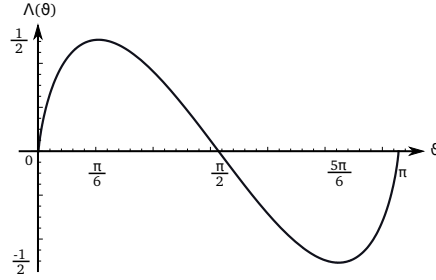
Figure 31: *One period of the Lobachevsky function*

THEOREM 2.34
The Lobachevsky function satisfies the following properties:

(i) *Λ is well defined and continuous for all $\theta \in \mathbb{R}$.*

(ii) *Λ is an odd function.*

(iii) *Λ is π-periodic.*

(iv) *For each positive integer n, Λ satisfies the identity*

$$\Lambda(n\theta) = n\sum_{k=0}^{n-1}\Lambda\left(\theta + \frac{k\pi}{n}\right).$$

$\square$

Remarks.

- Λ attains its maximum value at $\frac{\pi}{6}$ and its minimum value at $\frac{5\pi}{6}$ in $[0, \pi]$.

- By virtue of the previous theorem, we deduce for $\theta = \frac{\pi}{6}$

$$\frac{1}{2}\Lambda\left(2\frac{\pi}{6}\right) \overset{(iv)}{=} \Lambda\left(\frac{\pi}{6}\right) + \Lambda\left(\frac{\pi}{6} + \frac{\pi}{2}\right) \overset{(iii)}{=} \Lambda\left(\frac{\pi}{6}\right) + \Lambda\left(\frac{\pi}{6} - \frac{\pi}{2}\right)$$
$$\overset{(ii)}{=} \Lambda\left(\frac{\pi}{6}\right) - \Lambda\left(\frac{\pi}{3}\right),$$

which leads to the following equality, that will be helpful in section 5.

$$\Lambda\left(\frac{\pi}{3}\right) = \frac{2}{3}\Lambda\left(\frac{\pi}{6}\right) \qquad (2.10)$$

Finally, let us introduce the Bloch-Wigner function.

Definition 2.35.
For $z \in \mathbb{C} \setminus \mathbb{R}$, the *Bloch-Wigner function* is defined by the formula

$$D(z) := \Im\left(\mathrm{Li}_2(z)\right) + \arg(1-z)\log|z|. \qquad (2.11)$$

For $z \in \mathbb{R} \cup \{\infty\}$, $D(z) = 0$.

Remark. Note that for $\theta \in \mathbb{R}$, we have the following relation between the Euler dilogarithm, the Lobachevsky and the Bloch-Wigner functions

$$\mathrm{D}\left(\exp\left(\mathrm{i}\theta\right)\right) = \Im\left(\mathrm{Li}_2(\exp\left(\mathrm{i}\theta\right))\right) = 2\Lambda\left(\frac{\theta}{2}\right).$$

LEMMA 2.36

The Bloch-Wigner function satisfies the following properties for $z \in \mathbb{C} \setminus \mathbb{R}$:

  (i) $D(z) + D(1 - z) = 0$,

  (ii) $D(z) + D(z^{-1}) = 0$,

  (iii) $D(z) + D(z^*) = 0$,

where z^* denotes the complex conjugate of z, $z^* = \bar{z}$.

<div align="right">□</div>

The way these three functions are related to the hyperbolic volume will be explained in the next section.

2.3.7. Hyperbolic volume.   Using the previous functions, particularly the Lobachevsky function, we can give the essential volume formulas for an orthoscheme and an ideal tetrahedron.

THEOREM 2.37

Let S be an orthoscheme in H^3 with angles α, β, γ, and let $\delta \in \left[0, \frac{\pi}{2}\right]$ be defined by

$$\tan\delta := \frac{\sqrt{\cos^2\beta - \sin^2\alpha\sin^2\gamma}}{\cos\alpha\cos\gamma}.$$

Then the volume of S is given by

$$\begin{aligned}
Vol_3(S) =& \frac{1}{4}\left[\Lambda(\alpha + \delta) - \Lambda(\alpha - \delta) + \Lambda(\gamma + \delta) - \Lambda(\gamma - \delta)\right] \\
&+ \frac{1}{4}\left[-\Lambda\left(\frac{\pi}{2} - \beta + \delta\right) + \Lambda\left(\frac{\pi}{2} - \beta - \delta\right) + 2\Lambda\left(\frac{\pi}{2} - \delta\right)\right].
\end{aligned}$$

<div align="right">□</div>

THEOREM 2.38

Let $T(\alpha, \beta, \gamma)$ be an ideal tetrahedron in U^3 with dihedral angles α, β, γ. The volume of $T(\alpha, \beta, \gamma)$ is given by

$$Vol_3(T(\alpha, \beta, \gamma)) = \Lambda(\alpha) + \Lambda(\beta) + \Lambda(\gamma). \tag{2.12}$$

Suppose that $T(\alpha, \beta, \gamma)$ is parametrized in a way such that its vertices correspond to $0, 1, \infty$ and $z \in \mathbb{C}$ with positive imaginary part (this is possible by applying an appropriate isometry of $\mathbb{H}^3$). The tetrahedron is then denoted by $T(z)$ and the previous formula becomes

$$Vol_3(T(z)) = D(z). \tag{2.13}$$

$\square$

Returning to knots, we say that a knot is *hyperbolic* if its complement is equipped with a complete hyperbolic structure.

Example 2.39.
A hyperbolic structure on the complement of the figure-eight knot in $\mathbb{S}^3$ can be obtained by gluing together two copies of $T\left(\frac{\pi}{3}, \frac{\pi}{3}, \frac{\pi}{3}\right)$. For details about the gluing, we refer to [Rat06, chapter 10.3] or [Thu02, chapters 1,3,4]. With regard to formula (2.12) from the previous theorem, its volume is given by

$$\mathrm{Vol}\left(T\left(\frac{\pi}{3}, \frac{\pi}{3}, \frac{\pi}{3}\right)\right) = 6\Lambda\left(\frac{\pi}{3}\right). \tag{2.14}$$

This result is crucial in section 5 while proving the Volume Conjecture for the figure-eight knot.

2.3.8. The Gromov norm. In this section the Gromov norm of a closed, connected, orientable, hyperbolic manifold will be considered.

Definition 2.40.
Let X be a topological space with k^{th} homology group $\mathrm{H}_k(X, \mathbb{R})$ ($k \geq 1$) and α be a homology class in $\mathrm{H}_k(X, \mathbb{R})$. The *simplicial norm* of α is defined to be the real number

$$\|\alpha\| = \inf\{\|c\| \,|\, c \text{ is a } k\text{- cycle representing } \alpha\}.$$

Definition 2.41.
The *Gromov norm* of a closed, connected, orientable n-manifold $\mathcal{M}^n$ is the simplicial norm of a fundamental class of $\mathcal{M}^n$ in $\mathrm{H}_n(\mathcal{M}^n, \mathbb{R})$. The Gromov norm of $\mathcal{M}^n$ is denoted by $\|\mathcal{M}^n\|$.

An important result on the Gromov norm for the proof of the Volume Conjecture for torus knots, that are not hyperbolic, is

THEOREM 2.42
If $\mathcal{M}^n$ is a closed, connected, orientable, spherical or Euclidean n-manifold ($n > 0$), then $\|\mathcal{M}^n\| = 0$.

$\square$

Furthermore, it is worth evoking *Gromov's theorem* that establishes the connection between its norm and the hyperbolic volume.

THEOREM 2.43
Let $\mathcal{M}^n$ be a closed, connected, orientable, hyperbolic n-manifold with $n > 1$, and let υ_n be the volume of a regular ideal n-simplex in H^n. Then

$$\|\mathcal{M}^n\| = \frac{Vol_n(\mathcal{M}^n)}{\upsilon_n}.$$

$\square$

3. The Yang-Baxter Equation and Quantum Groups

After this introduction to the world of knots, links, braids and tangles, and of hyperbolic geometry, we could immediately go on by defining the link invariants we are actually heading for and investigate the Volume Conjecture. However, for the sake of coherence, we choose another option, that not only maintains some suspense, but mainly motivates the steps we are going to take. In this chapter, we concentrate on:

- exposing the Yang-Baxter equation via the concept of Hopf algebras and explaining the relationship with knot theory (3.1),

- presenting an overview on the physical significance of the Yang-Baxter equation (3.2),

- alluding to quantum groups with their physical and mathematical interpretations (3.3),

- studying the Lie algebra $\mathfrak{sl}_2(\mathbb{C})$, which will be the key algebra in chapter 4 for defining link invariants (3.4).

3.1. The Yang-Baxter equation

As already announced, the Yang Baxter equation plays an important role in different domains. Originally motivated by physics, it has become the subject of abstract Hopf algebra theory. We will start with that point of view until switching to a survey on the evolution of the physical significance of the Yang-Baxter equation. As references, we use [KM91], [Kass95] and [PS97].

3.1.1. Hopf algebra. The motivation for introducing Hopf algebras will be emphasized in the subsequent chapter when dealing with quantum groups. For the time being, we need the definition in order to understand the maps that will be used in the following. We start with some definitions.

Definition 3.1.
Let $\mathcal{A}$ be a vector space over the field $\mathbb{F}$ and let $\zeta : \mathcal{A} \otimes \mathcal{A} \longrightarrow \mathcal{A}$, $\eta : \mathbb{F} \longrightarrow \mathcal{A}$, $\phi : \mathbb{F} \otimes \mathcal{A} \longrightarrow \mathcal{A}$ and $\tilde{\phi} : \mathcal{A} \otimes \mathbb{F} \longrightarrow \mathcal{A}$ be the linear maps defined by $\zeta(a_1 \otimes a_2) := a_1 a_2$, $\eta(k) := k \operatorname{id}_{\mathcal{A}}$, $\phi(k \otimes a) := ka$ and $\tilde{\phi}(a \otimes k) := ak$ respectively, $\operatorname{id}_{\mathcal{A}}$ being the identity map on $\mathcal{A}$, such that

$$
\begin{aligned}
\zeta(\zeta \otimes \operatorname{id}_{\mathcal{A}}) &= \zeta(\operatorname{id}_{\mathcal{A}} \otimes \zeta) \quad \text{(Associativity)}, \\
\zeta(\eta \otimes \operatorname{id}_{\mathcal{A}}) &= \phi_{\mathcal{A}} \qquad\quad \text{(Unitality)}, \\
\zeta(\operatorname{id}_{\mathcal{A}} \otimes \eta) &= \tilde{\phi}_{\mathcal{A}} \qquad\quad \text{(Unitality)}.
\end{aligned}
$$

Then the triple $(\mathcal{A}, \zeta, \eta)$ is called an *algebra*. If in addition, for the permutation (or flip) map $P : \mathcal{A} \otimes \mathcal{A} \longrightarrow \mathcal{A} \otimes \mathcal{A}$ defined by $P(a_1 \otimes a_2) := a_2 \otimes a_1$, we have

$$
\zeta(P) = \zeta \quad \text{(Commutativity)},
$$

then $\mathcal{A}$ is said to be a *commutative algebra*.

Remark. Given two algebras $\mathcal{A}_1$ and $\mathcal{A}_2$, the tensor product $\mathcal{A}_1 \otimes \mathcal{A}_2$ inherits an algebra structure by putting $(a_1 \otimes a_2)(a_1' \otimes a_2') = a_1 a_1' \otimes a_2 a_2'$, for any $a_1, a_1' \in \mathcal{A}_1, a_2, a_2' \in \mathcal{A}_2$.

Example 3.2.
$\mathrm{Mat}(N, \mathbb{F})$, where $\mathbb{F}$ is a field, forms an algebra under matrix multiplication and addition. More generally, any ring of matrices with coefficients in a commutative ring $\mathcal{R}$ forms an algebra.

Example 3.3.
Every polynomial ring $\mathcal{R}[x_1, x_2, \ldots, x_n]$, where $\mathcal{R}$ is a commutative ring, is a commutative algebra (called the *free commutative algebra on the set* $\{x_1, x_2, \ldots, x_n\}$).

Definition 3.4.
Let $\mathcal{C}$ be a vector space over the field $\mathbb{F}$ and let $\Delta : \mathcal{C} \longrightarrow \mathcal{C} \otimes \mathcal{C}$, $\epsilon : \mathcal{C} \longrightarrow \mathbb{F}$, $\psi : \mathcal{C} \longrightarrow \mathbb{F} \otimes \mathcal{C}$ and $\tilde{\psi} : \mathcal{C} \longrightarrow \mathcal{C} \otimes \mathbb{F}$ be linear maps such that $\psi(c) := \mathbb{1}_{\mathbb{F}} \otimes c$, $\tilde{\psi}(c) := c \otimes \mathbb{1}_{\mathbb{F}}$ and such that the following diagrams commute

$$
\begin{array}{ccc}
\mathcal{C} & \xrightarrow{\ \Delta\ } & \mathcal{C} \otimes \mathcal{C} \\
\Delta \downarrow & & \downarrow \mathrm{id} \otimes \Delta \\
\mathcal{C} \otimes \mathcal{C} & \xrightarrow[\Delta \otimes \mathrm{id}]{} & \mathcal{C} \otimes \mathcal{C} \otimes \mathcal{C}
\end{array}
$$

$$
\begin{array}{ccc}
\mathcal{C} \otimes \mathcal{C} & \xrightarrow{\ \epsilon \otimes \mathrm{id}\ } & \mathbb{F} \otimes \mathcal{C} \\
{}^{\Delta}\nwarrow & & \uparrow {}^{\psi} \\
& \mathcal{C} &
\end{array}
\qquad
\begin{array}{ccc}
\mathcal{C} \otimes \mathcal{C} & \xrightarrow{\ \mathrm{id} \otimes \epsilon\ } & \mathcal{C} \otimes \mathbb{F} \\
{}^{\Delta}\nwarrow & & \uparrow {}^{\tilde{\psi}} \\
& \mathcal{C} &
\end{array}
$$
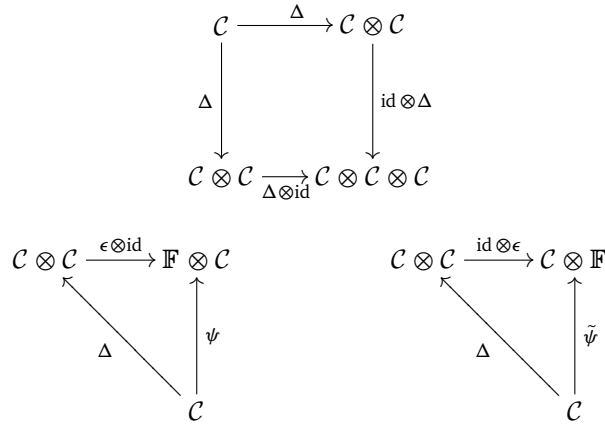
that is

$$
\begin{aligned}
(\Delta \otimes \mathrm{id}_{\mathcal{C}})\Delta &= (\mathrm{id}_{\mathcal{C}} \otimes \Delta)\Delta && \text{(Coassociativity)}, \\
(\epsilon \otimes \mathrm{id}_{\mathcal{C}})\Delta &= \psi && \text{(Counitality)}, \\
(\mathrm{id}_{\mathcal{C}} \otimes \epsilon)\Delta &= \tilde{\psi} && \text{(Counitality)}.
\end{aligned}
$$

Then the triple $(\mathcal{C}, \Delta, \epsilon)$ is called a *coalgebra*. If in addition, for the permutation map $P : \mathcal{C} \otimes \mathcal{C} \longrightarrow \mathcal{C} \otimes \mathcal{C}$ defined by $P(c_1 \otimes c_2) := c_2 \otimes c_1$, we have

$$
P(\Delta) = \Delta \quad \text{(Cocommutativity)},
$$

then $\mathcal{C}$ is said to be a *cocommutative algebra*.

Remarks.
   - The map Δ is called *comultiplication* or *coproduct*, whereas ϵ is referred to as *counit*.

- In analogy to algebras, the tensor product $\mathcal{C}_1 \otimes \mathcal{C}_2$ of two coalgebras $(\mathcal{C}_1, \Delta_1, \epsilon_1)$ and $(\mathcal{C}_2, \Delta_2, \epsilon_2)$ has a coalgebra structure with comultiplication $(\mathrm{id}_{\mathcal{C}_1} \otimes P \otimes \mathrm{id}_{\mathcal{C}_2})$ (P being the permutation map from $\mathcal{C}_1 \otimes \mathcal{C}_2$ to $\mathcal{C}_2 \otimes \mathcal{C}_1$) and counit $\epsilon_1 \otimes \epsilon_2$.

Example 3.5.
Consider a field $\mathbb{F}$ and the maps $\Delta(k) := k \otimes k$ and $\epsilon(k) = k$, $k \in \mathbb{F}$. The triple $(\mathbb{F}, \Delta, \epsilon)$ has a coalgebra structure (called the *ground coalgebra*).

Example 3.6.
Given a finite set $X = \{x_1, x_2, \ldots, x_n\}$ and a field $\mathbb{F}$, the following vector space is generated by X

$$\mathcal{C} := \bigoplus_{k=1}^{n} \mathbb{F} x_k.$$

$(\mathcal{C}, \Delta, \epsilon)$ is then a coalgebra if we define $\Delta(x_k) := x_k \otimes x_k$ and $\epsilon(x_k) := \mathbb{1}_{\mathbb{F}}$ for any $x_k \in X$ (it is sufficient to define the maps on the generator set of $\mathcal{C}$, because of the bilinearity and associativity properties of the tensor product).

Example 3.7.
The dual of the algebra $\mathrm{Mat}(N, \mathbb{F})$ is a coalgebra, called the *matrix coalgebra*. This can be seen by defining

$$\Delta(x_{ij}) := \sum_{k=1}^{N} x_{ik} \otimes x_{kj} \quad \text{and} \quad \epsilon(x_{ij}) := \delta_{ij},$$

where $\{E_{i,j} | 1 \leq i, j \leq N\}$, $E_{i,j}$ being the matrix with all entries equal to 0 except for the $(i, j)^{\text{th}}$ entry which is 1, is a basis for $\mathrm{Mat}(N, \mathbb{F})$ and $\{x_{i,j} | 1 \leq i, j \leq N\}$ is the associated dual basis.

Remark. In general, the dual vector space of a finite-dimensional algebra is a coalgebra. The converse, that is the dual vector space of a coalgebra is an algebra, holds for all dimensions. (see [Kass95] p.41)

Definition 3.8.
A *bialgebra* is a quintuple $(\mathcal{H}, \zeta, \eta, \Delta, \epsilon)$ where $(\mathcal{H}, \zeta, \eta)$ is an algebra and $(\mathcal{H}, \Delta, \epsilon)$ is a coalgebra satisfying the equivalent conditions

  (i) ζ and η are morphisms (linear maps) of coalgebras,

  (ii) Δ and ϵ are morphisms of algebras.

Remark. The equivalence between these two conditions needs actually to be proved. This can be done by looking at the commutative diagrams illustrating each statement. Details may be found in [Kass95] p.45-46.

Example 3.9.
Recall from example 3.6 that for a finite set $X = \{x_1, x_2, \ldots, x_n\}$ and a field $\mathbb{F}$,

$(\mathcal{C}, \Delta, \epsilon)$ is a coalgebra with $\mathcal{C} := \bigoplus\limits_{k=1}^{n} \mathbb{F}x_k$, $\Delta(x_k) := x_k \otimes x_k$ and $\epsilon(x_k) := \mathbb{1}_{\mathbb{F}}$ for any $x_k \in X$. Suppose we have an associative map from $\rho : X \times X \longrightarrow X$ with a right and left unit. This map then induces an algebra structure on $\mathcal{C}$ with $\zeta(x_k \otimes x_l) := x_k x_l = \rho((x_k, x_l))$. It is sufficient to show that Δ and ϵ are morphisms of algebras (see the equivalence in definition 3.8) in order to conclude that $(\mathcal{C}, \zeta, \eta, \Delta, \epsilon)$ is a bialgebra. In fact, we have

$$\begin{aligned}
\Delta(x_k x_l) &= x_k x_l \otimes x_k x_l = (x_k \otimes x_k)(x_l \otimes x_l) = \Delta(x_k)\Delta(x_l), \\
\epsilon(x_k x_l) &= \mathbb{1}_{\mathbb{F}} = \mathbb{1}_{\mathbb{F}}\mathbb{1}_{\mathbb{F}} = \epsilon(x_k)\epsilon(x_l),
\end{aligned}$$

which proves the statement.

Definition 3.10.
Let $(\mathcal{A}, \zeta, \eta)$ be an algebra and $(\mathcal{C}, \Delta, \epsilon)$ a coalgebra. The *convolution* of two maps $f, g \in \mathrm{Hom}(\mathcal{C}, \mathcal{A})$ is the bilinear map

$$\begin{aligned}
\star : \mathrm{Hom}(\mathcal{C}, \mathcal{A}) \times \mathrm{Hom}(\mathcal{C}, \mathcal{A}) &\longrightarrow \mathrm{Hom}(\mathcal{C}, \mathcal{A}) \\
(f, g) &\longmapsto f \star g := \zeta((f \otimes g)(\Delta)).
\end{aligned}$$

Eventually, we are able to define

Definition 3.11.
A *Hopf algebra* is a bialgebra $(\mathcal{H}, \zeta, \eta, \Delta, \epsilon)$ together with a map $\mathrm{S} \in \mathrm{End}(\mathcal{H})$, called *antipode for* $\mathcal{H}$ and satisfying

$$\mathrm{S} \star \mathrm{id}_{\mathcal{H}} = \mathrm{id}_{\mathcal{H}} \star \mathrm{S} = \eta \circ \epsilon.$$

We therefore write $(\mathcal{H}, \zeta, \eta, \Delta, \epsilon, \mathrm{S})$.

Remark. The antipode of a bialgebra $\mathcal{H}$ - if it does exist - is unique: suppose S and S' being antipodes of $\mathcal{H}$, then

$$\mathrm{S} = \mathrm{S} \star (\eta\epsilon) = \mathrm{S} \star (\mathrm{id}_{\mathcal{H}} \star \mathrm{S}') = (\mathrm{S} \star \mathrm{id}_{\mathcal{H}}) \star \mathrm{S}' = (\eta\epsilon) \star \mathrm{S}' = \mathrm{S}'.$$

Example 3.12.
$(\mathcal{C}, \zeta, \eta, \Delta, \epsilon)$ from example 3.9 is not a Hopf algebra. Without any additional structure on the set X, we do not know anything about the existence of multiplicative inverses, thus we are not able to define an antipode.
However, if the set X is endowed with a group structure (in this case, we write $X =: G$) and the bialgebra $\mathcal{C}$ corresponds to the group algebra $\mathbb{F}G$, $(\mathbb{F}G, \zeta, \eta, \Delta, \epsilon)$ becomes a Hopf algebra where the morphisms are defined by

$$\zeta\left(\sum_{g \in G} \alpha_g g \otimes \sum_{g \in G} \beta_g g\right) := \sum_{h \in G}\left(\sum_{\substack{x,y \in G \\ xy=h}} \alpha_x \beta_y h\right),$$

$$\eta(\alpha_g) := \alpha_g \mathbb{1}_{\mathcal{C}}, \quad \Delta(g) := g \otimes g, \quad \epsilon(g) := \mathbb{1}_{\mathbb{F}}, \quad \mathrm{S}(g) := g^{-1},$$

for any $\alpha_g, \beta_g \in \mathbb{F}$ and for any $g \in G$.

3.1.2. The Yang-Baxter equation.   Using the notations from the previous section, we are able to introduce the notions of quasitriangular Hopf algebra, R-matrix and the Yang-Baxter equation.

Definition 3.13.
Let $\mathcal{H}$ be a Hopf algebra and $R \in \mathcal{H} \otimes \mathcal{H}$ an invertible element satisfying

$$
\begin{align}
\check{\Delta}(h) \quad &:= \quad P(\Delta(h)) = R\Delta(h)R^{-1}, \tag{3.1}\\
(\Delta \otimes \mathrm{id}_{\mathcal{H}})(R) \quad &= \quad R_{13}R_{23}, \tag{3.2}\\
(\mathrm{id}_{\mathcal{H}} \otimes \Delta)(R) \quad &= \quad R_{13}R_{12}, \tag{3.3}
\end{align}
$$

where $h \in \mathcal{H}$, $R_{12} = R \otimes \mathrm{id}_{\mathcal{H}}$, $R_{23} = \mathrm{id}_{\mathcal{H}} \otimes R$ and $R_{13} = (P \otimes \mathrm{id}_{\mathcal{H}})(R_{23})$. Then the pair $(\mathcal{H}, R)$ is called a *quasitriangular Hopf algebra*. If in addition $R_{12}R_{21} = \mathrm{id}_{\mathcal{H}^{\otimes 3}}$, then $(\mathcal{H}, R)$ is said to be *triangular*. R is called a *universal R-matrix* for $\mathcal{H}$. $\check{R} = P \circ R$ is referred to as *Ř-matrix*.

We consider now such a universal R-matrix in $\mathcal{H} \otimes \mathcal{H}$ as described in the previous definition. The composition of the linear maps R_{12}, R_{23}, R_{13} satisfies the following relation

$$
\begin{align}
R_{12}R_{13}R_{23} &\stackrel{(3.2)}{=} R_{12}(\Delta \otimes \mathrm{id}_{\mathcal{H}})(R) = (R \otimes \mathrm{id}_{\mathcal{H}})(\Delta \otimes \mathrm{id}_{\mathcal{H}})(R)\\
&\stackrel{(3.1)}{=} (\check{\Delta} \otimes \mathrm{id}_{\mathcal{H}})(R)(R \otimes \mathrm{id}_{\mathcal{H}}) \stackrel{(3.2)}{=} (P \otimes \mathrm{id}_{\mathcal{H}})(R_{13}R_{23})R_{12}\\
&\stackrel{(\clubsuit)}{=} R_{23}R_{13}R_{12}
\end{align}
$$

This identity is called the *Yang-Baxter equation* for the R-matrix. Similarly, we may derive the Yang-Baxter equation for the $\check{R}$-matrix. Indeed, by means of the following identity for the linear map P

$$
(P \otimes \mathrm{id}_{\mathcal{H}})(\mathrm{id}_{\mathcal{H}} \otimes P)(P \otimes \mathrm{id}_{\mathcal{H}}) = (\mathrm{id}_{\mathcal{H}} \otimes P)(P \otimes \mathrm{id}_{\mathcal{H}})(P \otimes \mathrm{id}_{\mathcal{H}}),
$$

and the above equation, we establish the second version of the Yang-Baxter equation, namely

$$
\check{R}_{12}\check{R}_{23}\check{R}_{12} = \check{R}_{23}\check{R}_{12}\check{R}_{23}.
$$

This leads us to the formal definition.

Definition 3.14.
Let V be a complex vector space, id_V the identity map on V and $R \in \mathrm{End}(V \otimes V)$ an invertible map. The following equation for R

$$
(R \otimes \mathrm{id}_V)(\mathrm{id}_V \otimes R)(R \otimes \mathrm{id}_V) = (\mathrm{id}_V \otimes R)(R \otimes \mathrm{id}_V)(\mathrm{id}_V \otimes R) \tag{3.4}
$$

is called the *Yang-Baxter equation* (YBE). The solution R is called *R-matrix*.

Remarks.
  - With respect to the above vocabulary, we should have chosen the $\check{R}$-notation in this definition. However, for convenience, we always write

R-matrix in the sequel and specify - if not clear - what we are referring to.

- There exists a classical version of the YBE, that uses solely the Lie algebra structure of $\text{End}(V)$. For $r \in \text{End}(V \otimes V)$ and $r_{12} = r \otimes \text{id}_V, r_{23} = \text{id}_V \otimes r, r_{13} = (P \otimes \text{id}_V)r_{23}$, this equation reads

$$[r_{12}, r_{13}] + [r_{12}, r_{23}] + [r_{13}, r_{23}] = 0.$$

- The YBE is sometimes called *star-triangle relation*, which is a motivation for the name (quasi-)triangular Hopf algebra. However, in order to explain the origin of the "star-triangle" denomination, we need to lean on physics. A deeper investigation on this subject is given in paragraph 3.2.2.

Example 3.15 ([Tur88]).
Take $V = \mathbb{C}^2$ with basis $\{v_1, v_2\}$, $q \in \mathbb{C}$ and define

$$R := -q \sum_j E_{j,j} \otimes E_{j,j} + \sum_{j \neq k} E_{j,k} \otimes E_{k,j} + (q^{-1} - q) \sum_{j<k} E_{j,j} \otimes E_{k,k},$$

with $E_{j,k} : \mathbb{C}^2 \longrightarrow \mathbb{C}^2$ defined by $E_{j,k}(v_l) = \delta_{j,l} v_k$ for $1 \leq j, k, l \leq 2$. R satisfies the YBE. To show this, we use the associated matrices with respect to the basis $\{v_1 \otimes v_1 \otimes v_1, v_1 \otimes v_1 \otimes v_2, \dots, v_2 \otimes v_2 \otimes v_2\}$ of $\mathbb{C}^2 \otimes \mathbb{C}^2 \otimes \mathbb{C}^2$. First, we get for R and $\text{id}_{\mathbb{C}^2}$

$$\overline{R} = \begin{pmatrix} -q & 0 & 0 & 0 \\ 0 & q^{-1} - q & 1 & 0 \\ 0 & 1 & 0 & 0 \\ 0 & 0 & 0 & -q \end{pmatrix}, \qquad \mathbb{1}_2 = \begin{pmatrix} 1 & 0 \\ 0 & 1 \end{pmatrix}.$$

With the help of Mathematica, we calculate the Kronecker products $\overline{R} \otimes \mathbb{1}_2$ and $\mathbb{1}_2 \otimes \overline{R}$ respectively. The matrix products $(\overline{R} \otimes \mathbb{1}_2)(\mathbb{1}_2 \otimes \overline{R})(\overline{R} \otimes \mathbb{1}_2)$ and $(\mathbb{1}_2 \otimes \overline{R})(\overline{R} \otimes \mathbb{1}_2)(\mathbb{1}_2 \otimes \overline{R})$ each lead to the same result

$$\begin{pmatrix} -q^3 & 0 & 0 & 0 & 0 & 0 & 0 & 0 \\ 0 & q - q^3 & -1 + q^2 & 0 & -q & 0 & 0 & 0 \\ 0 & -1 + q^2 & -q & 0 & 0 & 0 & 0 & 0 \\ 0 & 0 & 0 & q - q^3 & 0 & -1 + q^2 & -q & 0 \\ 0 & -q & 0 & 0 & 0 & 0 & 0 & 0 \\ 0 & 0 & 0 & -1 + q^2 & 0 & -q & 0 & 0 \\ 0 & 0 & 0 & -q & 0 & 0 & 0 & 0 \\ 0 & 0 & 0 & 0 & 0 & 0 & 0 & -q^3 \end{pmatrix}.$$

Consequently R defined as above is an R-matrix.

3.1.3. The Yang-Baxter equation in knot theory. Up to now, all the descriptions have been very abstract and the connections to knot theory that we are going to establish below are purely mathematical. However, it should

be emphasized that all the basic ingredients are due to physicists.

The first bridge between the YBE and knot theory is the Artin braid relation, which can be understood in the following way. To each strand of an n-braid, we associate a vector space V such that the whole braid is related to the n-fold tensor product $V^{\otimes n}$. The braiding between initial and endpoints can be viewed as a composition of endomorphisms of $V^{\otimes n}$, according to the following identification of the generators $\sigma_1, \sigma_2, \ldots, \sigma_{n-1}$

$$\sigma_j \longleftrightarrow \mathrm{id}_V^{\otimes j-1} \otimes R \otimes \mathrm{id}_V^{\otimes n-j-1} := R_j,$$

for $1 \leq j \leq n-1$ and for $R \in \mathrm{Aut}(V \otimes V)$. It turns out that the braid relation in terms of the previous description writes as

$$R_j R_{j+1} R_j = R_{j+1} R_j R_{j+1},$$

which is nothing but the YBE.
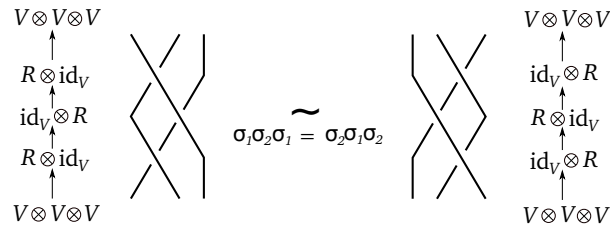
Figure 32: *Illustration for $n=3$*

Since the braid relation emerged from the condition on the third Reidemeister move, as seen in chapter 2 (Figure 17), it is obvious that the previous identification combined with (R3) leads to the YBE too.

Finally, a connection between the YBE and knot invariants can be drawn by referring to representation theory. Indeed any irreducible representation of a simple Lie algebra can be used to produce an R-matrix in the sense that it sets up the involved vector spaces. In order to produce a link invariant, we go back to the braid representation of the link and thus associate it with a composition of endomorphisms R_j, each containing the R-matrix. Now taking the trace (or a version of the trace operator) we get a well defined invariant of links. This procedure is explained in more details in 4.3 for the case of the simple Lie algebra $\mathfrak{sl}_2(\mathbb{C})$ and will lead to the colored Jones polynomials.

3.2. Physical Interpretation.

The YBE is an equation that comes from two totally distinct sources which are statistical physics and quantum mechanics. It takes its name from the independent work of C.N. Yang from 1968 and R.J. Baxter from 1971. Recent

progress in other fields such as link invariants, quantum groups, quantum field theories shed new light to the significance of the YBE. We start by its very first manifestation, our resources being [KaM98], [Ada94], [Jim94], [PS97], [Fad95] and [Akt09].

3.2.1. Bethe's Ansatz. A few years after the formulation of quantum mechanics (1923-1927), W. Heisenberg and P. Dirac succeeded to uncover the old mystery of *ferromagnetism*. As a consequence to the laws of quantum mechanics, they observed the existence of an effective interaction between electron spins on neighbouring atoms with overlapping orbital wave functions, caused by the combined effect of the Coulomb repulsion and the Pauli exclusion principle. A model for the study of critical points and phase transitions of magnetic systems had been provided by the *quantum Heisenberg model*. In the 1-dimensional case for an N-body system with periodic boundary conditions (spins: $\mathbf{S_{N+1}} = \mathbf{S_1}$) and under the assumption of solely magnetic interactions between adjacent dipoles, the Hamiltonian in the spin $\frac{1}{2}$ Heisenberg model takes the following form

$$H = -J \sum_{j=1}^{N} \mathbf{S_j} \, \mathbf{S_{j+1}},$$

where J is the coupling constant and $\mathbf{S_j} = (S_j^x, S_j^y, S_j^z)$ is the spin. This Hamiltonian acts on a 2^N-dimensional Hilbert space spanned by the orthogonal basis vectors $|s_1, s_2, \ldots, s_N\rangle$ with s_j being either spin up $\uparrow$, either spin down $\downarrow$. The commonly used method to solve this model consists in determining the Hamiltonian matrix (occasionally, for the sake of diminishing the computational efforts, it can be rewritten in block diagonal by performing basis transformations) and the eigenvectors via diagonalization leading to the acquaintance of the physical quantities of interest.

Opposite to this mechanism, Bethe exposed in 1931 another method for the computation of the exact eigenvalues and eigenvectors of H. It is based on a parametrization of the eigenvectors, also called *Bethe Ansatz* and features two main advantages: all eigenstates are characterized by a set of quantum numbers which can be used to distinguish them according to specific physical properties and in many cases the eigenvalues and the physical properties derived from these numbers can be evaluated in the thermodynamic limit (i.e. $N \gg 1$). For the application of the Bethe Ansatz, two symmetries in the Heisenberg model are essential:

- rotational symmetry around the quantization axis z implying the conservation of $S_{\text{tot}}^z := \sum_{j=1}^{N} S_j^z$. The action of H on $|s_1, s_2, \ldots, s_N\rangle$ yields a linear combination of the basis vectors, each of which has the same number of spins $\downarrow$.

- translational symmetry of H with respect to discrete translations by any number of lattice spacings.

Hence, sorting the basis vectors according to the quantum number $S_{\text{tot}}^z = \frac{N}{2} - r$, r being the number of $\downarrow$ spins, the Hamiltonian matrix will be block diagonalized. To get the idea, here are the steps for the easiest case, that is $r = 1$.

1. Bethe Ansatz for the eigenstates: $|\psi\rangle = \sum\limits_{j=n}^{N} a(n)|n\rangle$.

2. $|\psi\rangle$ is a solution to the eigenvalue equation $H|\psi\rangle = E|\psi\rangle$. Considering the action of H on the basis and denoting by $E_0 = \frac{-JN}{4}$ the energy of the state with all spins $\uparrow$, we get the equations

$$2(E - E_0)a(n) = J[2a(n) - a(n-1) - a(n+1)].$$

3. Using the periodic boundary conditions $a(n + N) = a(n)$, N linearly independent solutions will be given by

$$a(n) = \exp(ikn), \quad k = \frac{2\pi m}{N}, \quad m = 0, 1, \ldots, N - 1.$$

k is called the *momentum* of the Bethe Ansatz.

4. After normalization, we obtain the so-called *magnon states* and energy eigenvalues

$$|\psi\rangle = \frac{1}{\sqrt{N}} \sum\limits_{j=n}^{N} \exp(ikn)|n\rangle, \quad E - E_0 = J(1 - \cos k).$$

This method can be generalized for $2 \leq r \leq \frac{N}{2}$. Nowadays, the procedure introduced by Bethe has been tremendously extended in a way that many other quantum many-body systems have been solved in the meantime.

What is the importance of the YBE in this system? The answer is given by the *scattering matrix* S, short S-matrix, which is the unitary operator that describes the evolution of the physical interacting system. Suppose the system passes from t_0 to t, then the S-matrix is defined to be

$$S = \lim_{\substack{t_0 \to -\infty \\ t \to \infty}} U(t, t_0),$$

where $U(t, t_0)$ is the evolution operator defined by

$$U(t, t_0) := \exp(iH_0 t) \exp(-iH(t - t_0)) \exp(-iH_0 t_0),$$

$H = H_0 + H_I$ with H_0 the free and H_I the interacting part of the Hamiltonian. This leads then to the calculation of the transition probability. It can be shown that this S-matrix factorizes to that of the two-body problem and can be determined exactly. The YBE appears as consistency condition for this factorization.

Another picture to visualize more concretely the occurrence of the YBE in

quantum mechanical systems is given by a 1-dimensional 3-body problem. Suppose the result of the interaction of the three aligned particles is the permutation (13) of their positions (particle 2 stays at its site). There are two possibilities for the intermediate process:

1. $1 \longleftrightarrow 2$, $1 \longleftrightarrow 3$, $2 \longleftrightarrow 3$,

2. $2 \longleftrightarrow 3$, $1 \longleftrightarrow 3$, $1 \longleftrightarrow 2$.

According to the Heisenberg indeterminacy principle, we can never learn, which process actually occured. The two are equiprobable, which translates by the following equation

$$R_{12}R_{13}R_{23} = R_{23}R_{13}R_{12},$$

where R_{jk} are the endomorphisms as defined above and describe the interaction of the jth and k^{th} particles. We rediscovered the YBE equation, sometimes also referred to as *quantum Yang-Baxter equation*, since it appears in the context of quantum mechanics.
We continue by commenting on statistical mechanics.

3.2.2. Ising and Potts models.   Invented by W. Lenz for the study of ferromagnetism in statistical mechanics, the *Ising model* was developed for particles that interact only with nearest neighbours, similarly to the Heisenberg model. It was already solved for the 1-dimensional case in 1925 by E. Ising, student of W. Lenz. Despite this fast success, the 2-dimensional square lattice Ising model turned out to be a much harder nut to crack. In the case of zero magnetic field, it was given a complete analytic description much later in 1944 by L. Onsager. This model corresponds to one of the simplest statistical models with a phase change, since the 1-dimensional model does not have this property. The solution of the model with non zero magnetic field has yet to be found. In more than 2 dimensions, the Ising model becomes complicated, inaccurate and computations very intractable. Let us shortly explain the square lattice model with its significance to the YBE, omitting the solution of the model.
We imagine the molecules in the metal we investigate arranged in a lattice, that is, we get a graph with vertices illustrating the particles and edges denoting the interaction between adjacent neighbours. Since metals are built up more or less in such a 3-dimensional lattice, this model is quite relevant in practice. Each vertex, that is each particle, is assigned a spin, either $+1$ ($\uparrow$) or -1 ($\downarrow$). Among the 2^N possible states of a system composed of N molecules, a particular one is represented by a vector $S = (s_1, s_2, \ldots, s_N)$. The goal consists in the determination of the *partition function* of the system defined by

$$Z := \sum_{\text{states S}} \exp\left(\frac{-E(S)}{k_B T}\right) = \sum_{\text{states S}} \prod_{1 \le j,k \le N} \omega(s_j, s_k), \qquad (3.5)$$

where $E(S)$ is the energy of the state S, k_B is the Boltzmann constant, T is the temperature and $\omega(s_j, s_k) := \exp\left(\frac{-E(s_j, s_k)}{k_B T}\right)$ is the weight of the edge joining particles j and k (again, there are only two possible values). This function is actually a crucial quantity in order to calculate the value of different observables, for instance the expected value for the total energy or the probability to find the system in a given state $\tilde{S}$

$$P(\tilde{S}) = \frac{\exp\left(\frac{-E(\tilde{S})}{k_B T}\right)}{Z}.$$

Henceforth we need to calculate the energy of the system. At the basis, this is not difficult, since every edge in the lattice, representing the interaction (only source of energy) between the vertices at its ends, can have only two possible values E_+, if the adjacent vertices have same spins, or E_- in the contrary case. The total energy is just the sum of these energies $E(s_j, s_k)$. Things become more complicated when reintroducing $E(S)$ in (3.5) and aiming the explicit computation. The immediate evaluation of this sum is impossible, except for a system with very few particles. Unfortunately, in practice the number of particles is much bigger (studying a metal involves moles) and thus the number of states becomes enormous.

The remedy is found in the *star-triangle relation* or *Yang-Baxter equation* introduced by Onsager in 1944. Instead of restricting to lattices, we consider all kinds of planar graphs with no edges crossing over one another. The key
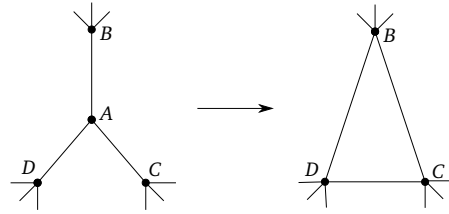
Figure 33: *Illustration of the star-triangle exchange*

to the alleviate partition function is to replace a star in the graph by a triangle, reducing the number of vertices by 1, but halfening the number of states in Z! The condition for this exchange is that there exist new energy weights ω' along the three edges between B, C and D, such that their product equals the total weights of interaction between the centered vertex A and B, C and D, summed over the possible states of A. In the case under consideration, this condition, that is the star-triangle relation, becomes

$$\omega(1, s_B)\omega(1, s_C)\omega(1, s_D) + \omega(-1, s_B)\omega(-1, s_C)\omega(-1, s_D)$$
$$= \omega'(s_B, s_C)\omega'(s_C, s_D)\omega'(s_D, s_B).$$

Consequently, if this equation holds, then we calculate the partition function of the new graph with the star replaced by a triangle, which coincides with

the partition function of the prior graph.

Furthermore, the connection between statistical mechanics and knot theory, more precisely invariants of links, becomes obvious once we remember the state sum expression of the Kauffman bracket introduced in (2.1). In fact, a link diagram can be seen as a planar graph as in the Ising model, where the vertices represent particles and the edges represent interaction energies. A state of the graph, that is a choice of spin for each site, corresponds to the assignment ± 1 to the crossings in the link diagram following the rule from section 2.1.5. The Kauffmann bracket can thus be seen as the state model's partition function. Despite the fact that the partition function itself is not a link invariant due to (R1) which it does not respect (the Kauffman bracket bears the same problem), it can be modified by addition of some factor such that the final "partition function" becomes invariant under all three Reidemeister moves. In the case of the Ising model, this invariant is called *Arf invariant*.

The *Potts model* from 1952 is a generalization of the Ising model where the particles can have more than 2, say $q \geq 1$ possible states. Its partition function generates a link invariant in two variables q and t when t satisfies $t = \exp\left(-\frac{1}{k_B T}\right) - 1$. This invariant is known as *dichromatic polynomial* $Z_G(q, t)$ (G standing for the underlying graph), since we may think of the particles as being colored rather than being in some undefined state. With the appropriate choice of interaction energies in the Potts model, the partition function generates the Jones polynomial $V(t)$, with q and t related via $2 + t + t^{-1}$.

3.2.3. Inverse scattering method. At the origin of the *inverse scattering method* (ISM) stands the *Korteweg-de Vries equation* (KdV) from 1895

$$\frac{\partial u(x,t)}{\partial t} - 6u(x,t)\frac{\partial u(x,t)}{\partial x} + \frac{\partial^3 u(x,t)}{\partial x^3} = 0.$$

This dispersive, nonlinear, partial differential equation (NPDE) depicts a model of waves on shallow water surfaces. Since a general theory on how to solve NPDEs didn't (actually doesn't) seem to exist, an algorithm was to be invented for its individual resolution. The fruit of these investigations was the *inverse scattering method* (ISM), that allowed to find an exact solution of the KdV equation. It can be seen as the nonlinear analogue of the Fourier transform. With this impulse, other scientists adapted the method quite quickly to other exactly solvable models/NPDEs. More recent research in the field appealed to the quantum version of this process, which leads to surprising results and involves commutation relations of operators that are described by a solution to the YBE.

The precise presentation of the ISM is far too technical and elaborate for the current framework, therefore we shall just briefly give the different steps of

the method and refer to [Fad95] and [Akt09] for more details.

1. We begin with a linear ordinary differential equation (LODE) which is known to be associated to the NPDE that has to be solved. It turns out that such an LODE is integrable if its corresponding initial value problem (IVP) can be treated with the help of an IST. The procedures retained for establishing this association LODE → NPDE are either the *Lax method*, or the *AKNS method*. For example, if we start with the LOD Schrödinger equation

$$-\frac{d^2\psi}{dx^2} + u(x,t)\psi = k^2\psi,$$

these methods lead to the KdV equation. The function $u(x,t)$ has the property of vanishing for $x \to \infty$.

2. Consider the LODE at an initial time, say $t = 0$, where $u(x,0)$, perceived as potential, is known. By *direct scattering method*, we determine from the potential the scattering data $S(\lambda, 0)$ at time $t = 0$, also called *Jost solutions*.

3. The study of the time evolution of the previous solutions by means of Lax or AKNS method leads to the knowledge of the time evolution of the scattering data, thus of $S(\lambda, t)$.

4. The last step consists then in solving the LODE for $u(x,t)$, knowing the scattering data $S(\lambda, t)$. This is precisly the IST and is effectuated by the *Marchenko integral*.

Stunningly, the resulting function $u(x,t)$ satisfies the NPDE and has the property that $\lim_{t\to 0} u(x,t)$ agrees with the initial profile $u(x,0)$.

It is interesting to notice that the solutions to NPDEs include examples of *solitons*, which have zero *reflection coefficient* in the corresponding scattering data. More precisely, solitons are self-reinforcing solitary waves, that demonstrate particle-like behaviour and interact with each other nonlinearly, but come out of interactions unaffected in size or shape except for some phase shifts. Since at the beginning, the particle interpretation of solitons was rather obscure, L. Faddeev and collaborators were motivated to consider the quantization of these wave-like excitations. Progressively, the ISM was adapted to the quantum domain (founding the QISM), raising new commutation relations that could be described by solutions of YBE (1978-1983). The QISM emerged to be a very powerful tool since all classical models were imbedded into the realm of this method.

From a mathematical point of view, the quantization of integrable models is related to the representation of the corresponding Lie algebra (of involved operators). This more algebraic and abstract attitude was worked out by V. Drinfeld and led to the introduction of *quantum groups* (see 3.3).

Remark. It were the founders of the QISM (Faddeev, Takhtajan et al.) that gave the YBE its denomination (previously only known as star-triangle relation), since the works of Yang and Baxter inspired them for the establishment of the commutation relations. Being born in the context of QISM, the solutions to the YBE could not be described as *S*-matrices, since this name was reserved for the solutions of the direct scattering method, so they were referred to as *R*-matrices, *R* being the next letter in the inverse alphabetical order (according to our interpretation).

3.3. Quantum Groups

3.3.1. Physical approach. In the same spirit as we presented the physical motivations for the YBE in the previous paragraph, we will give here a physical introduction to what we will soon call a *quantum group*. Leaning on the mechanical interpretation of the braid group 2.2.4 and inspired by [Dri87], [Tur94] and [PS97], we oppose classical to quantum observables.

The basic mathematical model for a classical mechanical system composed of n particles is a symplectic $2n$-dimensional manifold $\mathcal{M}^{2n}$ (that is a smooth manifold equipped with a closed, nondegenerate, skew-symmetric 2-form), called *phase space*. In general, a phase space represents all possible states of a system, each one corresponding to one unique *point* on the manifold. Usually, a state is characterized by two parameters in classical mechanics, namely the position $q_j(t)$ of a moving point together with its velocity $\dot{q}_j(t)$.

In the space of functions on $\mathcal{M}^{2n}$, a multiplication, called *Poisson bracket*, is induced by the symplectic structure. The observables are *functions* on $\mathcal{M}^{2n}$ and form an associative *commutative algebra* with respect to this bracket. The time evolution of the system depends on the choice of the *Lagrangian L*, which summarizes the dynamics of the system and for which the *Euler-Lagrange equation* holds

$$\frac{\partial L}{\partial q_j(t)} - \frac{d}{dt}\frac{\partial L}{\partial \dot{q}_j(t)} = 0.$$

A dual construction is obtained if we consider the *Legendre transform* of the Lagrangian $\sum_{j=1}^{n} \dot{q}_j(t)\frac{\partial L}{\partial \dot{q}_j(t)} - L = H$ which corresponds to the *Hamiltonian* of the system. Instead of the velocity vectors $\dot{q}_j(t)$, we consider now the momentum covectors $p_j(t)$ and the equivalent to the Euler-Lagrange equation is given by the *Hamilton's equations*

$$\dot{q}_j(t) = \frac{\partial H}{\partial p_j}, \quad \dot{p}_j(t) = \frac{\partial H}{\partial q_j}.$$

In the treatment of quantum mechanics, the Hamilton formalism is used. The states no longer form a finite-dimensional manifold, but they give rise to a *Hilbert space* $\mathcal{H}$ (not to be confused with a Hopf algebra!). Contrary to the classical states that can be given by a pair $(q_j(t), \dot{q}_j(t))$, the quantum states are described by a density function that expresses the probability of a particle

to have a certain location and velocity. The *observables* are now *operators* on $\mathcal{H}$ and they form an associative *noncommutative algebra* with respect to the usual *commutator* of operators $[P, Q] = P \circ Q - Q \circ P$. The time evolution of the state ψ (it is a wave function) satisfies the *Schrödinger equation* of the form

$$i\hbar \frac{\partial \psi}{\partial t} = \hat{H}\psi,$$

where $\hat{H}$ is the Hamiltonian operator.

From an algebraic point of view, *quantization* can be seen as a replacement of commutative algebras by noncommutative ones, as illustrated by the Lagrangian and Hamiltonian approaches. Performing a refinement of the algebra of observables in quantum mechanics leads to a new structure that is neither commutative, nor cocommutative. Anticommutativity and quantum physics being closely related, V.G. Drinfeld introduced in 1986 the term of *quantum groups* to refer to this new structure.

3.3.2. Mathematical approach. The theory of *quantum groups* was originally conceived as a machinery that produces solutions to the YBE. Later on, they found applications in several areas, particularly in the theory of link invariants as we will see.

A rough construction of quantum groups is given by the following procedure: one starts with a Lie group G whose elements are states. The complex-valued smooth functions on G can be interpreted as observables and they form an associative, commutative algebra $\mathcal{A} = \text{Func}(G)$ equipped with the Poisson bracket, as seen above. It turns out, that $\mathcal{A}$ is endowed with a Hopf algebra structure. Indeed, the multiplication on G induces a comultiplication on $\mathcal{A} \; \Delta : \mathcal{A} \longrightarrow \mathcal{A} \otimes \mathcal{A}$ where $\mathcal{A} \otimes \mathcal{A} = \text{Func}(G \times G)$. In general, this correspondence defines a functor (map between categories) from the category (that is an algebraic structure consisting of a collection of "objects", linked together by maps, called morphisms, that can be composed associatively and that contain an identity map for each object) of "groups" to the category of associative, commutative algebras that induces the Hopf algebra structure on $\mathcal{A}$. For more details, we refer to [Dri87]. A quantum group is defined to be a realization of such a Hopf algebra $\mathcal{A}$. Moreover if it is quasitriangular, then the YBE is satisfied. In general, the commutativity and cocommutativity of the Hopf algebra are not required conditions for having a quantum group. Anyway, quantum groups were proposed in the framework of the QISM and the underlying corresponding examples were neither commutative nor cocommutative. The reason is simply, that cocommutative Hopf algebras are trivially quasitriangular and thus not very interesting for the study of invariants, since the YBE which takes the form (see (♣) p.36)

$$R_{12} R_{13} R_{23} = R_{13} R_{23} R_{12}$$

is satisfied for $R = \text{id}_{\mathcal{A}} \otimes \text{id}_{\mathcal{A}}$. In that context, the method used to construct noncommutative and noncocommutative Hopf algebras is based on the concept of *quantization*.

Definition 3.16.
A *quantization* of a Hopf algebra $\mathcal{A}$ over the field $\mathbb{F}$ is a deformation of $\mathcal{A}$ depending on a parameter $h \in \mathbb{C}$ giving rise to a Hopf algebra $\mathcal{A}_h$ over $\mathbb{F}[[h]]$ such that $\mathcal{A}_h \cong \mathcal{A}[[h]]$ as modules and $\mathcal{A}_h / h\mathcal{A}_h \cong \mathcal{A}$ as Hopf algebras.

Remarks.

- $\mathbb{F}[[h]] := \left\{ \sum_{n=0}^{\infty} k_n h^n \,|\, k_n \in \mathbb{F} \right\}$ is the set of formal power series in h with coefficients in $\mathbb{F}$. $\mathcal{A}[[h]]$ is a $\mathbb{F}[[h]]$-module.

- We may think of the parameter h as Planck's constant. In the classical limit $h \to 0$, $\mathcal{A}_h \cong \mathcal{A}$, which agrees with the vanishing quantization.

- For our interest, it is sufficient to choose $\mathbb{F} = \mathbb{C}$.

Drinfeld showed that one can combine any Hopf algebra with its dual algebra to get a larger Hopf algebra, called the *quantum double*, which is quasitriangular, henceforth admits a universal R-matrix. For a proof, which is quite tricky, we refer to [Dri87, 13], [KRT97, chapter 3] or [Kass95, chapter IX]. A very important class of noncommutative, noncocommutative quantum groups is composed of *quantum universal enveloping algebras*. Therefore, we shall look at the following example.

Example 3.17.
Let $\mathfrak{g}$ be a finite-dimensional Lie algebra over $\mathbb{C}$. We first need to define the *tensor algebra* over $\mathfrak{g}$ by

$$T(\mathfrak{g}) := \bigoplus_{n=0}^{\infty} \mathfrak{g}^{\otimes n},$$

where $\mathfrak{g}^{\otimes 0} = \mathbb{C}$. This is an associative algebra with multiplication coming from the natural tensor product in $\mathfrak{g}$ and with unit $\mathbb{1}_{\mathbb{C}}$. Let $i : \mathfrak{g} \longrightarrow T(\mathfrak{g})$ be the canonical inclusion map and let the elements in the image of this inclusion be called *primitive*. Then we can define a Hopf algebra structure on $T(\mathfrak{g})$ by specifying the comultiplication, counit and antipode only on these primitive elements, the extension to all elements happens via linearity. We get for a primitive element $X \in T(\mathfrak{g})$

$$\Delta(X) := X \otimes \mathbb{1}_{T(\mathfrak{g})} + \mathbb{1}_{T(\mathfrak{g})} \otimes X,$$
$$\epsilon(X) := 0,$$
$$S(X) := -X.$$

The definition of the universal enveloping algebra includes one more notion, we have not yet encountered. A *two-sided ideal* I of the noncommutative algebra $T(\mathfrak{g})$ is a subset that is both a right ideal (i.e. $\forall\, k \in I, \forall\, X \in T(\mathfrak{g}) : kX \in I$) and left ideal (i.e. $\forall\, k \in I, \forall\, X \in T(\mathfrak{g}) : Xk \in I$). We consider more precisely the two-sided ideal $I(\mathfrak{g})$ generated by $XY - YX - [X, Y]$, for all primitive elements $X, Y \in \mathfrak{g} \subset T(\mathfrak{g})$. The *universal enveloping algebra* of $\mathfrak{g}$ is then defined to be

$$U(\mathfrak{g}) := T(\mathfrak{g})/I(\mathfrak{g}).$$

$U(\mathfrak{g})$ inherits the Hopf algebra structure from $T(\mathfrak{g})$. Furthermore, $U(\mathfrak{g})$ is cocommutative, since for the permutation operator P on $U(\mathfrak{g}) \otimes U(\mathfrak{g})$, we have

$$P(\Delta(X)) = P(X \otimes \mathbb{1}_{U(\mathfrak{g})} + \mathbb{1}_{U(\mathfrak{g})} \otimes X) = \mathbb{1}_{U(\mathfrak{g})} \otimes X + X \otimes \mathbb{1}_{U(\mathfrak{g})} = \Delta(X).$$

Cocommutative Hopf algebras are not interesting for our later study of link invariants, since they are always quasitriangular. Consequently, we try to deform this algebra hoping to cancel out cocommutativity. Thus we get the *quantized universal enveloping algebra*

$$U_h(\mathfrak{g})/hU_h(\mathfrak{g}) \cong U(\mathfrak{g}).$$

Notice that the trivial quantization is not a good choice, since it still results in a cocommutative algebra. $U_h(\mathfrak{g})$ is again a Hopf algebra for reasons related to the quantum double construction of Drinfeld, that we will not comment here. We illustrate the quantized universal enveloping algebra in the next section for one of the simplest and neatest cases $\mathfrak{g} = \mathfrak{sl}_2(\mathbb{C})$.

Up to now, we have not yet clarified how quantum groups shall induce link invariants. Their formal construction will be the subject of the next chapter, but in order to have all the required tools at our disposal, we need to address to representation theory. We study the case of the quantum universal enveloping algebra $U_h(\mathfrak{sl}_2(\mathbb{C}))$ below, a general theory being an exaggerated ambition in the scope of this work.

3.4. The Lie Algebra $\mathfrak{sl}_2(\mathbb{C})$

The discovery of the colored Jones polynomial is based on the study of the Lie algebra $\mathfrak{sl}_2(\mathbb{C})$. The aim of this section is to apply the previous theory, producing the quantum group $U_h(\mathfrak{sl}_2(\mathbb{C}))$ and to explain the precise connection to the R-matrix.

3.4.1. Generalities. We start by recalling the definition of $\mathfrak{sl}_2(\mathbb{C})$. First notice that the Lie algebra of the general linear Lie group $\mathrm{GL}(2, \mathbb{C})$ is given

$$\mathfrak{gl}_2(\mathbb{C}) := \left\{ \begin{pmatrix} a & b \\ c & d \end{pmatrix} \middle| a, b, c, d \in \mathbb{C} \right\}.$$

This is a 4-dimensional algebra generated by $X, Y, H, \mathbb{1}_2$

$$X := \begin{pmatrix} 0 & 1 \\ 0 & 0 \end{pmatrix}, \quad Y := \begin{pmatrix} 0 & 0 \\ 1 & 0 \end{pmatrix}, \quad H := \begin{pmatrix} 1 & 0 \\ 0 & -1 \end{pmatrix}, \quad \mathbb{1}_2 := \begin{pmatrix} 1 & 0 \\ 0 & 1 \end{pmatrix},$$

with the commutator satisfying the obvious relations

$$[\mathbb{1}_2, X] = [\mathbb{1}_2, Y] = [\mathbb{1}_2, H] = 0,$$

as well as

$$[X, Y] = H, \quad [H, X] = 2X, \quad [H, Y] = -2Y. \tag{3.6}$$

The Lie algebra $\mathfrak{sl}_2(\mathbb{C})$ is defined to be

$$\mathfrak{sl}_2(\mathbb{C}) := \left\{ a \in \mathfrak{gl}_2(\mathbb{C}) \,\middle|\, \mathrm{Sp}(a) = 0 \right\},$$

where Sp denotes the usual trace of matrices. Thus $\mathfrak{sl}_2(\mathbb{C})$ corresponds to the 3-dimensional subalgebra of $\mathfrak{gl}_2(\mathbb{C})$ spanned by X, Y, H, satisfying (3.6).

The finite-dimensional irreducible representations of $\mathfrak{sl}_2(\mathbb{C})$ are given by $(V_N, \tilde{\rho}_N)$, where V_N is the space of homogeneous complex polynomials in two variables z_1, z_2 of degree $N \in \mathbb{N}$

$$V_N := \mathrm{span}_{\mathbb{C}} \left(z_1^N, z_1^{N-1} z_2, \ldots, z_1 z_2^{N-1}, z_2^N \right),$$

and the continuous linear action

$$\tilde{\rho}_N : \mathfrak{sl}_2(\mathbb{C}) \times V_N \to V_N$$

is explicitly defined by

$$\begin{aligned}
\tilde{\rho}_N(X) v_j &= (j+1) v_{j+1}, \\
\tilde{\rho}_N(Y) v_j &= j v_{j-1}, \\
\tilde{\rho}_N(H) v_j &= (2j - N + 1) v_j,
\end{aligned}$$

where $\{v_0, v_1, \ldots, v_N\}$ denotes the basis $\{z_1^N, z_1^{N-1} z_2, \ldots, z_1 z_2^{N-1}, z_2^N\}$ of V_N. Since a representation $(V_N, \tilde{\rho}_N)$ of $\mathfrak{sl}_2(\mathbb{C})$ defines on V_N the structure of a $\mathbb{C}[\mathfrak{sl}_2(\mathbb{C})]$-module, we also call it a $\mathfrak{sl}_2(\mathbb{C})$-module. For more details, see for instance [EW06, chapter 8].

3.4.2. The quantum universal enveloping algebra $\mathbf{U_h}(\mathfrak{sl}_2(\mathbb{C}))$. The co-commutative universal enveloping algebra of $\mathfrak{sl}_2(\mathbb{C})$ is defined as in 3.17 by

$$U(\mathfrak{sl}_2(\mathbb{C})) := T(\mathfrak{sl}_2(\mathbb{C})) / I(\mathfrak{sl}_2(\mathbb{C})),$$

and is generated by X, Y, H, which satisfy (3.6). From this follows that $U(\mathfrak{sl}_2(\mathbb{C})) \cong \mathfrak{sl}_2(\mathbb{C})$. The Hopf algebra structure can be seen through (cf. 3.17)

$$\Delta(a) = a \otimes \mathbb{1}_{T(\mathfrak{sl}_2(\mathbb{C}))} + \mathbb{1}_{T(\mathfrak{sl}_2(\mathbb{C}))} \otimes a, \quad \epsilon(a) = 0, \quad S(a) = -a,$$

with $a \in \{X, Y, H\}$.

For the quantum universal enveloping algebra, the following isomorphisms hold (see 3.17)

$$\begin{aligned}
U(\mathfrak{sl}_2(\mathbb{C})) &\cong U_h(\mathfrak{sl}_2(\mathbb{C})) / h U_h(\mathfrak{sl}_2(\mathbb{C})), \\
U_h(\mathfrak{sl}_2(\mathbb{C})) &\cong U(\mathfrak{sl}_2(\mathbb{C}))[[h]].
\end{aligned}$$

A priori, $U(\mathfrak{sl}_2(\mathbb{C}))[[h]]$ may contain divergent power series in h. In order to get rid of them, we restrict the quantum universal enveloping algebra to a

subalgebra containing only the convergent power series in h. This new algebra is denoted by $U_q(\mathfrak{sl}_2(\mathbb{C}))$ where q replaces h by $q := \exp(h)$. The generator H undergoes a substitution too, namely $K := \exp\left(\frac{hH}{4}\right)$. Moreover, we are interested in the case of a quantization by a root of unity, therefore we set $h := \frac{2\pi i}{N}$. Clearly, the classical limit becomes $q \to 1$.

With respect to these restrictions, the generators X, Y, K of $U_q(\mathfrak{sl}_2(\mathbb{C}))$ are subject to the relations (cf. [KM91])

$$KX = sXK, \quad KY = s^{-1}YK, \quad [X, Y] = XY - YX = \frac{K^2 - K^{-2}}{s - s^{-1}},$$

$$X^N = Y^N = 0, \quad K^{4N} = \mathbb{1}_{U_g(\mathfrak{sl}_2(\mathbb{C}))},$$

where we used $s := \exp\left(\frac{i\pi}{N}\right)$. The Hopf algebra structure on $U_h(\mathfrak{sl}_2(\mathbb{C}))$, which is a module over $\mathbb{C}[[h]]$ according to (3.16), is inherited by $U_q(\mathfrak{sl}_2(\mathbb{C}))$ and is explicitly given by (cf. [KM91])

$$\Delta(X) = X \otimes K + K^{-1} \otimes X,$$
$$\Delta(Y) = Y \otimes K + K^{-1} \otimes Y,$$
$$\Delta(K) = K \otimes K,$$
$$S(X) = -sX, \quad S(Y) = -s^{-1}Y, \quad S(K) = K^{-1},$$
$$\epsilon(X) = \epsilon(Y) = 0, \quad \epsilon(K) = 1.$$

3.4.3. Representation theory of $U_q(\mathfrak{sl}_2(\mathbb{C}))$. According to the algebra isomorphism over $\mathbb{C}[[h]]$

$$U_h(\mathfrak{sl}_2(\mathbb{C})) \cong U(\mathfrak{sl}_2(\mathbb{C}))[[h]]$$

we deduce that the irreducible finite-dimensional representations of $U_q(\mathfrak{sl}_2(\mathbb{C}))$ can be derived from those of $U(\mathfrak{sl}_2(\mathbb{C}))$ (which coincide with those of $\mathfrak{sl}_2(\mathbb{C})$)). This leads us to the following theorem.

THEOREM 3.18
The finite-dimensional irreducible representations of $U_q(\mathfrak{sl}_2(\mathbb{C}))$ are given by (V_N, ρ_N), $N \geq 0$, where $V_N = \text{span}_{\mathbb{C}}\left(z_1^N, z_1^{N-1}z_2, \ldots, z_1 z_2^{N-1}, z_2^N\right)$, and the continuous linear action

$$\rho_N : U_q(\mathfrak{sl}_2(\mathbb{C})) \times V_N \to V_N$$

is explicitly defined by

$$\rho_N(X)v_j = [j+1]v_{j+1},$$
$$\rho_N(Y)v_j = [j]v_{j-1}, \quad\quad,$$
$$\rho_N(K)v_j = s^{j-(N-1)/2}v_j,$$

where $\{v_0, v_1, \ldots, v_N\}$ denotes the basis $\{z_1^N, z_1^{N-1}z_2, \ldots, z_1 z_2^{N-1}, z_2^N\}$ of V_N and

$$[n] := \frac{s^n - s^{-n}}{s - s^{-1}}$$

which is called quantum integer for $s := \exp\left(\frac{i\pi}{N}\right)$.

Finally, it can be shown that for this quantum group, there is a solution $\check{R} \in U_q(\mathfrak{sl}_2(\mathbb{C})) \otimes U_q(\mathfrak{sl}_2(\mathbb{C}))$ for the YBE (see [KM91, theorem 2.18]). Thus, we conclude that $U_q(\mathfrak{sl}_2(\mathbb{C}))$ is quasitriangular and the connection to topological link invariants can now be established by the action of this $\check{R}$-matrix on the module $V_N \otimes V_N$ ($N \in \mathbb{N}$) via (see [KM91, corollary 2.32])

$$(\check{R})^{ij}_{kl} = \sum_{n=0}^{\min(N-1-i,j)} \delta_{l,i+n}\delta_{k,j-n} \frac{(s-s^{-1})^n[i+n]![N-1+n-j]!}{[n]![i]![N-1-j]!}$$
$$\times s^{2(i-(N-1)/2)(j-(N-1)/2)-n(i-j)-n(n+1)/2},$$

where

$$[n]! := \prod_{k=1}^{n}[k]$$

is called the *quantum factorial*.

In the next chapter we will see how this R-matrix enters into the definition of the colored Jones polynomial.

4. The Colored Jones Polynomial

Contrary to the previous chapters, we have now reached the marvellous stage where we are able to apply and - above all - combine the prior acquired knowledge to build a topological link invariant. Important contributions to the field were achieved in 1991 by N. Reshetikhin and V.G. Turaev, who published in [RT91] a detailed method for the construction of invariants of 3-manifolds via modular Hopf algebras. The colored Jones polynomial is one of these striking discoveries that we will concentrate on. This chapter is organized as follows:

- introduce the original definition of the colored Jones polynomial by means of the irreducible complex representations of the quantum group $U_q(\mathfrak{sl}_2(\mathbb{C}))$ (4.1),
- allude to the link invariant defined by R. Kashaev using quantum dilogarithm (4.2),
- formalize the definition of the colored Jones polynomial, inspired on the works of H. Murakami and J. Murakami (4.3),
- conclude that the two types of link invariants encountered in this chapter coincide (4.4).

4.1. The Colored Jones polynomial

The decisive idea behind the theory of the colored Jones polynomial, which is nothing but a generalization of the Jones polynomial of section 2.1.5, is the following: given a planar oriented link diagram and the quantum group $U_q(\mathfrak{sl}_2(\mathbb{C}))$, we associate to the components of the link a *color* through an r-dimensional irreducible complex representation of $U_q(\mathfrak{sl}_2(\mathbb{C}))$, that is an $U_q(\mathfrak{sl}_2(\mathbb{C}))$-module. Obeying certain assignment rules for the arcs and the crossings that we will soon explain, we end up with a polynomial in one variable, denoted by $J_r(L)$. The importance of working with quasitriangular Hopf algebras (or quantum groups) is due to the fact that the set of representations needs to be closed under taking tensor products and duals over $\mathbb{C}$ and that the existence of an $\check{R}$-matrix is necessary.
Let us proceed systematically in 6 steps.

1st step. We start with an oriented link L with corresponding diagram D and arrange it by stretching in a way such that it fits with a pattern of horizontal parallels - two consecutive lines surrounding exactly one elementary tangle diagram of type $R, L, \cap$ or $\cup$ from section 2.2.6.
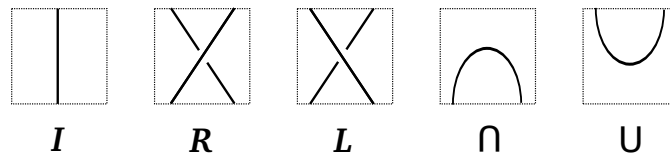
With respect to these elementary diagrams, we assign to each cross section a tensor product by tensoring the diagrams at a given level from left to right. We illustrate this process with the knot 5_2 in Figure 34 (actually, at this stage, the orientation given in the picture is not yet important). The assignment of elementary tangle diagrams becomes in this case

(1) : $\cup \circ \cup$,   (2) : $I \otimes L \otimes I$,   (3) : $I \otimes L \otimes I$,   (4) : $I \otimes L \otimes I$,

(5) : $I \otimes I \otimes R$,   (6) : $I \otimes I \otimes R$,   (7) : $I \otimes \cap \otimes I$,   (8) : $\cap$.
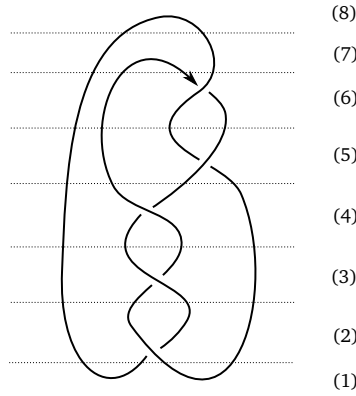
Figure 34: *Oriented knot 5_2 with assigned cross sections (1)-(8)*

2$^{\text{nd}}$ step.   Next, we take into account the orientation of the diagram and the fact, that in each cross section, we actually have a tangle (with typically more than one component). Henceforth, we shall apply the theory of tangle operators (see [KM91, section 3]): between two parallel lines, we decorate each adjacent arc of D with a color given by an r-dimensional irreducible $U_q(\mathfrak{sl}_2(\mathbb{C}))$-module V_r or its dual V_r^*, $r \in [2, N]$ (N is such that for the generators of $U_q(\mathfrak{sl}_2(\mathbb{C}))$, the relations $X^N = Y^N = 0, K^{4N} = 1$ hold). This induces a coloring of the two endpoints of each arc, where the rule to be respected is the following:
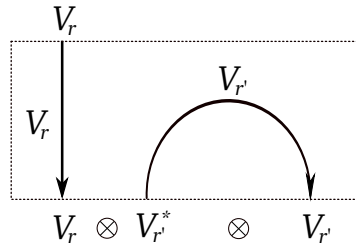
if the arc colored by V_r is oriented downwards, we choose V_r to be assigned to each of its endpoints, we choose the dual V_r^* if the arc is oriented upwards. Tensoring from left to right results in a *boundary $U_q(\mathfrak{sl}_2(\mathbb{C}))$-module* at each

line. By convention, the empty tensor product is $\mathbb{C}$.

3rd step.   At this point, we are going to mark the elementary tangle diagrams that we discretized in step 1 by a function with regard to the subsequent prescription (cf. [KM91, theorem 3.6]).

$$\text{id} \qquad \check{R} \qquad \check{R}^{\text{-1}}$$

$$E \qquad E_{K^2} \qquad N \qquad N_{K^{-2}}$$
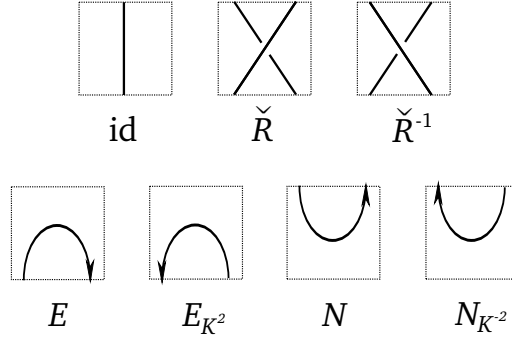
For a basis $\{e_0, e_1, \ldots, e_{r-1}\}$ of V_r with associated dual basis $\{e^0, e^1, \ldots, e^{r-1}\}$ of V_r^*, and regarding the $\check{R}$-matrix as a linear invertible operator, we make use of the following functions:

$$\text{id} : V_r \longrightarrow V_r \quad \text{is the identity map,}$$

$$\check{R} : V_r \otimes V_r \longrightarrow V_r \otimes V_r \quad \text{is defined by the } \check{R}\text{-matrix,}$$

$$\check{R}^{-1} : V_r \otimes V_r \longrightarrow V_r \otimes V_r \quad \text{is defined by the inverse } \check{R}\text{-matrix,}$$

$$E : V_r^* \otimes V_r \longrightarrow \mathbb{C} \quad \text{is defined by } E(f \otimes x) := f(x) \text{ for } f \in V_r^*, x \in V_r,$$

$$E_{K^2} : V_r \otimes V_r^* \longrightarrow \mathbb{C} \quad \text{is defined by } E(x \otimes f) := f(K^2 x) \text{ for } f \in V_r^*, x \in V_r,$$

$$N : \mathbb{C} \longrightarrow V_r \otimes V_r^* \quad \text{is defined by } N(1) := \sum_j e_j \otimes e^j,$$

$$N_{K^{-2}} : \mathbb{C} \longrightarrow V_r^* \otimes V_r \quad \text{is defined by } N_{K^{-2}}(1) := \sum_j e^j \otimes K^{-2} e_j.$$

Notice that for id, $\check{R}$ and $\check{R}^{-1}$, definitions involving V_r^* are also possible. Caution is now required, because our whole link diagram is in fact a $(0,0)$-tangle and therefore the map by ascending along the side of the diagram is an endomorphism of $\mathbb{C}$. We apply this method to the example of the knot 5_2 by passing from (1) to (8). We get the following endomorphism of $\mathbb{C}$

$$E(\text{id} \otimes E \otimes \text{id})(\text{id} \otimes \text{id} \otimes \check{R})(\text{id} \otimes \text{id} \otimes \check{R})(\text{id} \otimes \check{R}^{-1} \otimes \text{id})$$

$$(\text{id} \otimes \check{R}^{-1} \otimes \text{id})(\text{id} \otimes \check{R}^{-1} \otimes \text{id})(N_{K^{-2}} \otimes N_{K^{-2}}).$$

4th step.   Even though a knot or link is a priori a $(0,0)$-tangle, we may transform it into a $(1,1)$-tangle by merely cutting up some arc. In this way, we can apply the theory of tangles, although there will be only one coloring V_r for the single component of the diagram. Reconsidering a similar map, we explained before, we get now an endomorphism of V_r which is a complex
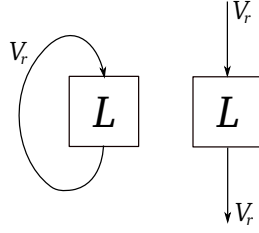
Figure 35: *From a closed link to a (1, 1)-tangle*

multiple of id_{V_r} (as a consequence of Schur's lemma). The complex multiple is defined to be the rth-Colored Jones polynomial of the link L, denoted by $J_r(L)$. This is effectively an element of $\mathbb{C}[[q]]$, as seen in the previous chapter (3.16), thus a convergent power series in a variable q, which is a root of unity. However we have not yet specified how this complex scalar is defined.

5$^{\text{th}}$ step.   The colored Jones polynomial is a $(1, 1)$-tangle invariant, wherefore we continue in this setting. Recalling the basis $\{e_0, e_1, \ldots, e_{r-1}\}$ of V_r and its dual basis $\{e^0, e^1, \ldots, e^{r-1}\}$, we choose a *state* of the diagram by matching complex indices to each arc following
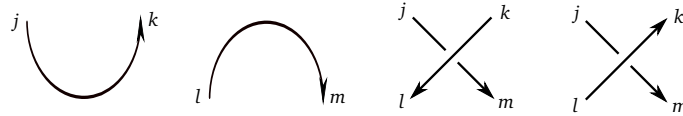
satisfying the relations below.

Now, for $q := s^2 = \exp\left(\frac{2\pi i}{N}\right)$, we define the following product

$$(q)_n := \prod_{l=1}^{n}(1 - q^l),$$

and we recall the $\check{R}$-matrix for V_N from the previous section

$$(\check{R})_{kl}^{ij} = \sum_{n=0}^{\min(N-1-i,j)} \delta_{l,i+n}\delta_{k,j-n} \frac{(s-s^{-1})^n[i+n]![N-1+n-j]!}{[n]![i]![N-1-j]!}$$

$$\times s^{2(i-(N-1)/2)(j-(N-1)/2)-n(i-j)-n(n+1)/2},$$

where $[n]! := \prod_{k=1}^{n}[k]$ and $[n] := \frac{s^n - s^{-n}}{s - s^{-1}}$.

Accordingly to this $\check{R}$-matrix, the following formulas

$(1):\ \delta_{j,k}q^{j-(N-1)/2}$,

$(2):\ \delta_{l,m}q^{-l+(N-1)/2}$,

$(3):\ \delta_{m,j+h}\delta_{l,k-h}(-1)^{j+l+1}\dfrac{(q)_j^{-1}(q)_k}{(q)_h(q)_l(q)_m^{-1}}q^{jl+(j+l)/2+(N^2+1)/4}$,

$(4):\ \delta_{j,m+h}\delta_{k,l-h}(-1)^{k+m+1}\dfrac{(q)_k^{-1}(q)_j}{(q)_h(q)_m(q)_l^{-1}}q^{km+(k+m)/2+(N^2+1)/4}$,

$(5):\ \delta_{m,j-h}\delta_{l,k+h}(-1)^{k+m+1}\dfrac{(q^*)_k^{-1}(q^*)_j}{(q^*)_h(q^*)_m(q^*)_l^{-1}}q^{-km-(k+m)/2-(N^2+1)/4}$,

$(6):\ \delta_{j,m-h}\delta_{k,l+h}(-1)^{j+l+1}\dfrac{(q^*)_j^{-1}(q^*)_k}{(q^*)_h(q^*)_l(q^*)_m^{-1}}q^{-jl-(j+l)/2-(N^2+1)/4}$,

$(7):\ \delta_{k,l-h}\delta_{m,j+h}(-1)^{j+k+1}\dfrac{(q^*)_j^{-1}(q^*)_k^{-1}}{(q^*)_h(q^*)_l^{-1}(q^*)_m^{-1}}q^{-jk-(l+m)/2-(N^2+1)/4}$,

$(8):\ \delta_{l,k-h}\delta_{j,m+h}(-1)^{l+m+1}\dfrac{(q^*)_j(q^*)_k}{(q^*)_h(q^*)_l(q^*)_m}q^{-lm-(j+k)/2-(N^2+1)/4}$,

$(9):\ \delta_{k,l+h}\delta_{m,j-h}(-1)^{l+m+1}\dfrac{(q)_j(q)_k}{(q)_h(q)_l(q)_m}q^{lm+(j+k)/2+(N^2+1)/4}$,

$(10):\ \delta_{l,k+h}\delta_{j,m-h}(-1)^{j+k+1}\dfrac{(q)_j^{-1}(q)_k^{-1}}{(q)_h(q)_l^{-1}(q)_m^{-1}}q^{jk+(l+m)/2+(N^2+1)/4}$,

match with the diagrams on Figure 36.

6$^{\text{th}}$ step.   Finally, we multiply all the involved elements from Figure 36, and then sum over all the coloring indices that occur in the diagram. This provides the colored Jones polynomial of the link.
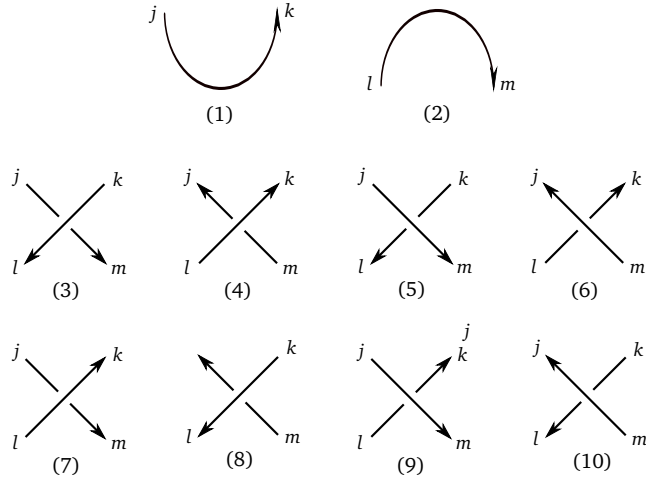
Figure 36: *Assignment of the R-matrix to the oriented crossings in a diagram*

In order to exemplify, we pursue the case of the knot 5_2 with color N. We choose a non-degenerate state of the diagram (for a systematical procedure of such a choice, [Mur10, p.10-16] may be consulted), say
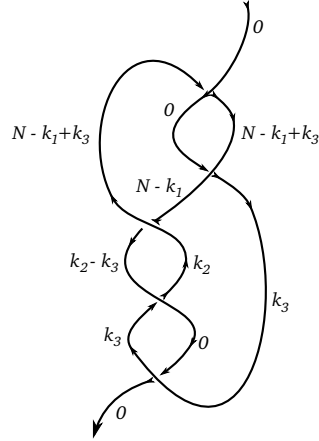
With respect to the previous assignment rules, we get

(a) : $q^{k_1-k_3+(N-1)/2}$,

(b) : $(-1)^{N-k_1-k_3+1}q^{(N-k_1+k_3)/2+(N^2+1)/4}$,

(c) : $(-1)^{N-k_1+1}\dfrac{(q)_{N-k_1+k_3}}{(q)_{N-k_1}}q^{(N-k_1)/2+(N^2+1)/4}$,

(d) : $(-1)^{k_3+1}\dfrac{(q^*)_{k_2-k_3}(q)_{k_2}}{(q^*)_{k_2+k_1-k_3-N}(q)_{N-k_1+k_3}(q^*)_{N-k_1}}q^{(N-k_1)/2+(N^2+1)/4}$,

(e) : $(-1)^{k_3+1}\dfrac{(q)_{k_2}}{(q)_{k_3}}q^{(2k_2-k_3)/2+(N^2+1)/4}$,

(f) : $(-1)^{k_3+1}q^{k_3/2+(N^2+1)/4}$,

corresponding to these components.
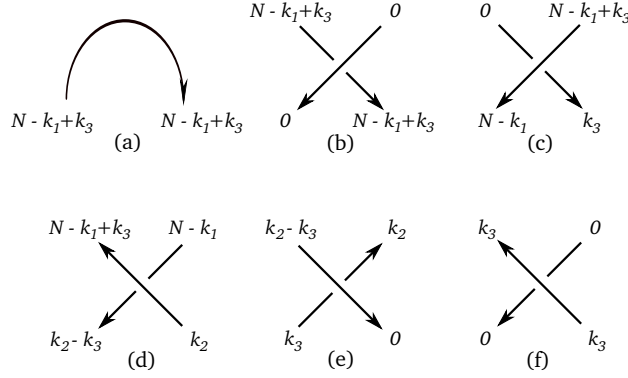
The resulting colored Jones polynomial is given by

$$J_N(5_2) = \sum_{k_1,k_2,k_3} (a)(b)(c)(d)(e)(f).$$

It is obvious that the computation of the colored Jones polynomial is an exhaustive task.

Remarks.

- It is important to notice that this construction of the colored Jones polynomial is independent of the choice of the orientation of the diagram and of the state for which we use the above formulas. Indeed, precisely these properties turn it into a link invariant; for more details consult [KM91, theorem 2.13, remark 3.26].

- The well-known Jones polynomial is obtained for the choice $N = 2$.

4.2. A link invariant defined by R. Kashaev

In 1994, R. Kashaev first introduced in his paper [Ka94] an invariant of *triangulated links* in triangulated 3-manifolds. His construction resembles the quantum mechanical approach we exposed in 3.3. We give just an overwiew of his procedure, because the details immediately involve a considerable amount of calculations and formulas. We refer to [Ka94] and [Ka95] for more specifications.

The pivotal point in Kashaev's theory was the study of the *quantum dilogarithm function*, which corresponds to a quantum version of the dilogarithm function reviewed in (2.8) and is defined for $x \in \mathbb{C}$ by

$$\Psi(x) := \prod_{n=1}^{\infty} (1 - xq^n),$$

where q is a fixed complex quantization parameter with $|q| \leq 1$. His goal consisted in producing a quantum analogue of the *pentagon identity* by L.J.

Rogers

$$L(x) + L(y) - L(xy) = L\left(\frac{x - xy}{1 - xy}\right) + L\left(\frac{y - xy}{1 - xy}\right),$$

where $x, y, z \in \mathbb{C}$ such that $|x|, |y|, |z| \leq 1$ and L denotes the *Rogers' dilogarithm function* defined by means of the dilogarithm function

$$L(z) = Li_2(z) + \log(1 - z) \log\left(\frac{z}{2}\right).$$

Indeed Kashaev succeeded to show the existence of a quantized pentagon identity through the properties of a certain subalgebra of the Hopf algebra $U_q(\mathfrak{sl}_2(\mathbb{C}))$. The stunning consequence was its relation to quantum groups, similarly to the case of the YBE as previously shown in 3.3.

Thereafter, Kashaev discovered that the quantum $6j$-symbols in $U_q(\mathfrak{sl}_2(\mathbb{C}))$ satisfy the generalized pentagon identity. Recall briefly that the quantum $6j$-symbol

$$\begin{Bmatrix} i & j & k \\ l & m & n \end{Bmatrix},$$

is a number defined for 6 spins i, j, k, l, m, n assigned to the edges of a tetrahedron. These spins correspond to representations of $U_q(\mathfrak{sl}_2(\mathbb{C}))$. The classi-
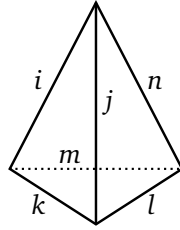
Figure 37: *Six parameters i, j, k, l, m, n*

cal analogue are $6j$-symbols that occur in the representations of $\mathfrak{sl}_2(\mathbb{C})$. For precise formulas, see [Ka94, section 1,2].

Needless to say that this coherence between topology and quantum physics stimulated the study of 3-manifolds $\mathcal{M}^3$ on the one side and of R-matrices on the other side. These investigations culminated first in the construction of an invariant of triangulated links that Kashaev derived from a partition function of the complement of a link L in a 3-manifold. This partition function $\langle L \rangle_{\mathcal{M}^3}$ raised to the Nth-power for some integer $N > 1$, is shown to be an invariant of links. We do not give the explicit form here (see [Ka94, (4.4)]).

Soon after, Kashaev determined another link invariant through a solution to the YBE and he showed that it coincides with the previous one for odd N. The following R-matrix is due to Kashaev.

THEOREM 4.1
The Kashaev R_K-matrix, with respect to components $(R_K)_{ab}^{cd}$ is defined by the

following formula (see [Ka95, (2.12)])

$$N q^{1+d-b+(a-c)(d-b)} \frac{\theta\left(res\,(b-a-1)+res\,(d-c)\right)\theta\left(res\,(a-d)+res\,(c-b)\right)}{(q_{res(b-a-1)})(q^*_{res(a-d)})(q_{res(d-c)})(q^*_{res(c-b)})},$$

where $N \geq 2$, $q := s^2 = exp\left(\frac{2i\pi}{N}\right)$, $q^* = \bar{q} = q^{-1}$, $(q)_n := \prod_{l=1}^{n}(1-q^l)$ *for* $n \geq 0$, $res\,(x) \in \mathbb{Z}_N = \{0, 1, ..., N-1\}$ *is the residue modulo* N *of* $x \in \mathbb{Z}$ *and*

$$\theta : \mathbb{Z} \longrightarrow \{0, 1\}$$

is defined by values $\theta(n)$ *equal to*

$$\begin{cases} 1 & if \quad 0 \leq n \leq N-1, \\ 0 & otherwise. \end{cases}$$

Similarly to the definition of the colored Jones polynomial, we can interpret these factors on diagrams in the following way.
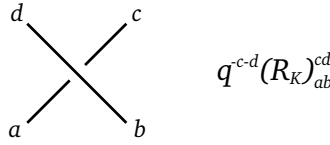
Figure 38: *Assignment of* $(R_K)^{cd}_{ab}$ *to a crossing in a diagram*

In order to derive the Kashaev invariant from this R-matrix, we need to imagine the following situation: suppose we have a $(2, 2)$-tangle planar representation of a link L in the 3-sphere. We define the sets of edges, vertices and faces of this diagram by $\mathcal{E}, \mathcal{V}$ and $\mathcal{F}$ respectively. Then we introduce two maps

$$\gamma : \mathcal{E} \longrightarrow \mathbb{Z}_N, \quad \alpha : \mathcal{V} \times \mathcal{F} \longrightarrow \mathbb{Z}_N,$$

with the restrictions

$$\gamma(e_1) = \gamma(e_2) = 0$$

for the outer strands of the tangle e_1, e_2, and for $v \in \mathcal{V}$, $f \in \mathcal{F}$

$$\alpha(v, f_0) = 0, \quad \text{for } f_0 \text{ the outer region of the plane,}$$
$$\alpha(v, f) = 0, \quad \text{for } v \notin f,$$
$$\sum_{f \in \mathcal{F}} \alpha(v, f) = \sum_{v \in \mathcal{V}} \alpha(v, f) = 1, \quad \text{for } f \neq f_0.$$

Moreover, to each vertex, we associate an element based on the previous figure and depending on α, say $r_\alpha(v) \in \mathbb{C}$. A partition function on this diagram is then defined by

$$\langle L \rangle := \sum_{\gamma} \prod_{v \in \mathcal{V}} r_\alpha(v) \prod_{e \in \mathcal{E}} q^{\gamma(e)}.$$

It turns out that, up to N^{th} roots of unity, different choices of the map α lead to the same partition function. This yields the following theorem, which combines $\langle L \rangle_{\mathcal{M}^3}$ and $\langle L \rangle$.

THEOREM 4.2
The quantity $\langle L \rangle^N$ is an invariant of links. For odd N it coincides with the invariant of triangulated links $\langle L \rangle^N_{\mathcal{M}^3}$ in an oriented 3-manifold $\mathcal{M}^3$.

Examples 4.3 ([Ka94],[Ka97]).
For $M := \mathbb{S}^3$ and writing now $\langle L \rangle_N := \langle L \rangle^N$, we get:

- $\langle \bigcirc \rangle_N = 1$,

- $\langle \oslash \rangle_N = \sum\limits_{a=0}^{N-1} (q)_a$,

- $\langle 4_1 \rangle_N = \sum\limits_{a=0}^{N-1} |(q)_a|^2$,

- $\langle 5_2 \rangle_N = \sum\limits_{0 \leq a \leq b \leq N-1} \dfrac{(q)_b^2}{(q^*)_a} q^{-(b+1)a}$.

This summary reflects the amazing ideas inspired by mathematical physics and an admirable ability of combining a priori non related fields. At the same time, however, the definitions are not quite rigorous from a mathematical point of view and difficult to develop further.

4.3. The Colored Jones polynomials by H. and J. Murakami

The family of link invariants introduced by Kashaev in section 4.2 arises from a quite enigmatic procedure, where he uses the quantum dilogarithm. From a mathematical point of view, his definition, even though only involving elementary tools, still lacks clarity. In the sequel, we are going to study the connection between the link invariant established by Kashaev and the colored Jones polynomial introduced in 4.1, a connection that was first suggested in 2001 by H. Murakami and J. Murakami in their famous article [MM01]. In order to see a clear structure, let us briefly expose our approach:

- state the general definitions of an enhanced Yang-Baxter operator (4.3.1) and the operator trace (4.3.2),
- define a link invariant (that is, the colored Jones polynomial) based on the prior definitions (4.3.3),
- introduce and justify two concrete Yang-Baxter operators (4.4.1),
- analyse the resulting enhanced Yang-Baxter operators (4.4.2),
- identify the corresponding link invariants (4.4.3).

4.3.1. Enhanced Yang-Baxter operator. First, let us recall the definition of an enhanced Yang-Baxter operator.

Definition 4.4.
Let $\alpha, \beta \in \mathbb{C}$ and consider the following maps

- id : $\mathbb{C}^N \longrightarrow \mathbb{C}^N$ the identity map on $\mathbb{C}^N$,

- $R : \mathbb{C}^N \otimes \mathbb{C}^N \longrightarrow \mathbb{C}^N \otimes \mathbb{C}^N$ an invertible linear map,

- $\mu : \mathbb{C}^N \longrightarrow \mathbb{C}^N$ a homomorphism,

- $\mathrm{Sp}_2 : \mathrm{End}(\mathbb{C}^N \otimes \mathbb{C}^N) \longrightarrow \mathrm{End}(\mathbb{C}^N)$ defined by
  $\mathrm{Sp}_2(f)(v_i) = \sum\limits_{j,k=0}^{N-1} f_{i,k}^{j,k}(v_j)$ where the coefficients $f_{i,k}^{j,k}$ correspond to
  the entries of the matrix associated to f with respect to a basis
  $\{v_0, v_1, ..., v_{N-1}\}$ of $\mathbb{C}^N$.

If they satisfy the equations:

(i) $(R \otimes \mathrm{id})(\mathrm{id} \otimes R)(R \otimes \mathrm{id}) = (\mathrm{id} \otimes R)(R \otimes \mathrm{id})(\mathrm{id} \otimes R)$,

(ii) $(\mu \otimes \mu)R = R(\mu \otimes \mu)$,

(iii) $\mathrm{Sp}_2(R^{\pm 1}(\mathrm{id} \otimes \mu)) = \alpha^{\pm 1}\beta \, \mathrm{id}$,

where the first condition is the Yang-Baxter equation, then the quadruple
$S = (R, \mu, \alpha, \beta)$ is called an *enhanced Yang-Baxter operator* (EYBO).

Example 4.5 ([Tur88]).
Recall the R-matrix from example 3.15

$$R := -q \sum_j E_{j,j} \otimes E_{j,j} + \sum_{j \neq k} E_{j,k} \otimes E_{k,j} + (q^{-1} - q) \sum_{j < k} E_{j,j} \otimes E_{k,k},$$

where we consider now the more general case $V = \mathbb{C}^N$, $N \geq 1$ and the
maps $E_{j,k} : \mathbb{C}^N \longrightarrow \mathbb{C}^N$ are defined by $E_{j,k}(v_l) = \delta_{j,l}v_k$ for $1 \leq j, k, l \leq N$.
According to Turaev, R enters into the definition of an EYBO by setting

$$\mu := \mathrm{diag}(\mu_1, \mu_2, \ldots, \mu_N),$$
$$\alpha := -q^N$$
$$\beta := 1,$$

where $\mathrm{diag}(\mu_1, \mu_2, \ldots, \mu_N)$ is the diagonal matrix with entries $\mu_j := q^{2j-N-1}$
for any $1 \leq j \leq N$. For the proof of the fact that (R, μ, α, β) with the choices
above forms an EYBO, [Tur88, theorem 4.2.1] may be consulted. Notice, that
this EYBO gives rise to the HOMFLY-PT polynomial introduced in 2.1.5.

4.3.2. Operator trace. Another ingredient we need for the definition of
the link invariant is the operator trace Sp_k. We have already encountered it
in one of the conditions of an EYBO (for $k = 2$), but here we give a general
definition.

Definition 4.6.

Let f be an endomorphism of $(\mathbb{C}^N)^{\otimes k}$, $k \in \mathbb{N}$, $\{v_0, v_1, ..., v_{N-1}\}$ a basis of $\mathbb{C}^N$ and consider the coordinate expression

$$f(v_{i_1} \otimes v_{i_2} \otimes ... \otimes v_{i_k}) = \sum_{j_1, j_2, ..., j_k = 0}^{N-1} f_{i_1, i_2, ..., i_k}^{j_1, j_2, ..., j_k} (v_{j_1} \otimes v_{j_2} \otimes ... \otimes v_{j_k}).$$

giving rise to the k-dimensional N^2-matrix

$$((f_{i_1, i_2, ..., i_k}^{j_1, j_2, ..., j_k})_{0 \leq i_1, i_2, ..., i_k, j_1, j_2, ..., j_k \leq N-1}) \in \mathbb{C}^{2kN}.$$

The kth *operator trace*

$$\mathrm{Sp}_k : \mathrm{End}((\mathbb{C}^N)^{\otimes k}) \longrightarrow \mathrm{End}((\mathbb{C}^N)^{\otimes k-1}) \quad \text{is defined to be}$$

$$\mathrm{Sp}_k(f)(v_{i_1} \otimes v_{i_2} \otimes ... \otimes v_{i_{k-1}}) = \sum_{j_1, j_2, ..., j_{k-1}, j = 0}^{N-1} f_{i_1, i_2, ..., i_{k-1}, j}^{j_1, j_2, ..., j_{k-1}, j} (v_{j_1} \otimes v_{j_2} \otimes ... \otimes v_{j_{k-1}}).$$

Remark. To reach our goal, which consists in determining the colored Jones polynomials explicitly, we need a method to compute the operator trace, which constitutes the essential part in the definition of the link invariant. Given a basis $\{v_0, v_1, ..., v_{N-1}\}$ of $\mathbb{C}^N$, the identification $(\mathbb{C}^N)^{\otimes k} \cong \mathbb{C}^{N^k}$ through the map

$$v_{i_1} \otimes v_{i_2} \otimes ... \otimes v_{i_k} \longmapsto V_t,$$

where $t := \sum_{l=0}^{k-1} N^l i_{k-l}$, $i_l \in \{0, 1, ..., N-1\}$ for $1 \leq l \leq k$, is the key to the subsequent procedure. Namely, instead of working with k-dimensional N^2-matrices, we are going to deal with 2-dimensional N^k-matrices for the sake of keeping track of the calculations. For $f \in \mathrm{End}((\mathbb{C}^N)^{\otimes k})$ and $\overline{f}$ the matrix associated to f in the basis $\{V_0, ..., V_{N^k-1}\}$, the following coefficient relationship holds:

$$f_{i_1, i_2, ..., i_k}^{j_1, j_2, ..., j_k} = \overline{f}_{t_1, t_2},$$

where $t_1 := \sum_{l=0}^{k-1} N^l j_{k-l}$, $t_2 := \sum_{l=0}^{k-1} N^l i_{k-l}$. Moreover, a straightforward calculation shows that the matrix $\overline{\mathrm{Sp}_k}$ associated to Sp_k with respect to the basis $\{W_0, W_1, ..., W_{N^{k-1}-1}\}$ constructed in a similar way to the above, is given by

$$(\overline{\mathrm{Sp}_k})_{i,j} = \sum_{l=0}^{N-1} \overline{f}_{l+iN, l+jN}, \quad 0 \leq i, j \leq N^{k-1} - 1.$$

We look at an example to clarify this method.

Example 4.7.

We choose $N = 3, k = 2$ and consider the following bases:

  - $\{v_0, v_1, v_2\}$ basis of $\mathbb{C}^3$,

- $\{V_0, V_1, ..., V_8\}$ basis of $\mathbb{C}^9 \cong (\mathbb{C}^3)^{\otimes 2}$,
  where $V_0 = v_0 \otimes v_0, V_1 = v_0 \otimes v_1, V_2 = v_0 \otimes v_2, V_3 = v_1 \otimes v_0, V_4 = v_1 \otimes v_1, V_5 = v_1 \otimes v_2, V_6 = v_2 \otimes v_0, V_7 = v_2 \otimes v_1, V_8 = v_2 \otimes v_2$.

For $f \in \text{End}((\mathbb{C}^3)^{\otimes 2})$, the associated matrix $\overline{f} \in \text{Mat}(9, \mathbb{C})$ with respect to the above basis is defined by

$$\overline{f}_{0,0} = f_{0,0}^{0,0}, \quad \overline{f}_{0,1} = f_{0,1}^{0,0}, \dots \quad \overline{f}_{0,8} = f_{2,2}^{0,0},$$

$$\overline{f}_{1,0} = f_{0,0}^{0,1}, \quad \overline{f}_{1,1} = f_{0,1}^{0,1}, \dots \quad \overline{f}_{1,8} = f_{2,2}^{0,1},$$

$$\vdots$$

$$\overline{f}_{8,0} = f_{0,0}^{2,2}, \quad \overline{f}_{8,1} = f_{0,1}^{2,2}, \dots \quad \overline{f}_{8,8} = f_{2,2}^{2,2}.$$

In this example the basis $\{W_0, W_1, W_2\}$ coincides with the initial basis $\{v_0, v_1, v_2\}$ of $\mathbb{C}^3$, thus the matrix $\overline{\text{Sp}_2(f)}$ is given by:

$$\begin{pmatrix} \overline{f}_{0,0} + \overline{f}_{1,1} + \overline{f}_{2,2} & \overline{f}_{0,3} + \overline{f}_{1,4} + \overline{f}_{2,5} & \overline{f}_{0,6} + \overline{f}_{1,7} + \overline{f}_{2,8} \\ \overline{f}_{3,0} + \overline{f}_{4,1} + \overline{f}_{5,2} & \overline{f}_{3,3} + \overline{f}_{4,4} + \overline{f}_{5,5} & \overline{f}_{3,6} + \overline{f}_{4,7} + \overline{f}_{5,8} \\ \overline{f}_{6,0} + \overline{f}_{7,1} + \overline{f}_{8,2} & \overline{f}_{6,3} + \overline{f}_{7,4} + \overline{f}_{8,5} & \overline{f}_{6,6} + \overline{f}_{7,7} + \overline{f}_{8,8} \end{pmatrix}.$$

Clearly, $\text{Sp}_1(\text{Sp}_2(f)) = \sum_{i=0}^{8} \overline{f}_{i,i} \in \mathbb{C}$.

4.3.3. A link invariant.
What do we need more for constructing a link invariant? In fact, we have an enhanced Yang-Baxter operator $S = (R, \mu, \alpha, \beta)$ as well as a method for computing the operator trace at our disposal. However, we have not yet explained rigorously any connection to links, except from the brief paragraph in 3.1.3. As we know from section 2.2 that every link L can be obtained as the closure of some braid, we are henceforth only considering braids and their generators $\sigma_i^{\pm 1}$. To a braid $\sigma \in \mathcal{B}_n$ whose closure may give a link L we associate the following map

$$\begin{array}{rcl} \mathcal{B}_n & \longrightarrow & \text{Hom}((\mathbb{C}^N)^{\otimes n}) \\ \sigma_i^{\pm 1} & \longmapsto & \underbrace{\text{id} \otimes ... \otimes \text{id}}_{i-1} \otimes R^{\pm 1} \otimes \underbrace{\text{id} \otimes ... \otimes \text{id}}_{n-i-1}. \end{array}$$

In other words, we associate to a braid $\sigma \in \mathcal{B}_n$ a homomorphism $b_R(\sigma) \in \text{Hom}((\mathbb{C}^N)^{\otimes n})$ according to the above identification. This allows us to define a candidate for a link invariant

$$T_S(\sigma) := \alpha^{-\omega(\sigma)} \beta^{-n} \text{Sp}_1(\text{Sp}_2(...(\text{Sp}_n(b_R(\sigma)(\mu^{\otimes n}))))) \in \text{End}(\mathbb{C}) \qquad (4.1)$$

where $\omega(\sigma)$ is the sum of the exponents appearing in the expression of σ as product of generators, thus $-n \leq \omega(\sigma) \leq n$. Assuming that the closure of σ produces the link L, we write $T_S(L)$.

PROPOSITION 4.8
Let L be a link and let $S = (R, \mu, \alpha, \beta)$ be an enhanced Yang-Baxter operator. Then $T_S(L) \in \text{End}(\mathbb{C})$ is an invariant of links.

Proof. We need to show that for a given enhanced Yang-Baxter operator S, $T_S(L)$ is invariant under the three Reidemeister moves. Since equivalent links L and L' have the same braid representation, it is straightforward that the corresponding homomorphisms $b_R(\sigma)$ and $b_R(\sigma')$ coincide and henceforth $T_S(L) = T_S(L')$. $\qquad\square$

Despite this property, T_S has some deficiencies. The reason for this was worked out by Turaev in [Tur88, theorem 3.2.1 and corollary 3.2.2]. To sum up, he shows that this invariant is annihilated by a polynomial of degree $\leq N^2$. Thus we consider a slightly modified version of T_S:

$$T_{S,1}(\sigma) := \alpha^{-\omega(\sigma)}\beta^{-n}\,\mathrm{Sp}_2(\mathrm{Sp}_3(...(\mathrm{Sp}_n(b_R(\sigma)(\mathrm{id}\otimes\mu^{\otimes n-1})))))) \in \mathrm{End}(\mathbb{C}^N).$$
$$(4.2)$$

PROPOSITION 4.9
If for $\lambda_{S,1}(\sigma) \in \mathbb{C}$ and any $\sigma \in \mathcal{B}_n$ the following conditions hold:

(i) $T_{S,1}(\sigma) = \lambda_{S,1}(\sigma)\,id$,

(ii) $Sp_1(\mu)\lambda_{S,1}(\sigma) = T_S(\sigma)$,

then $\lambda_{S,1}(\sigma)$ is a link invariant.

Proof. The argumentation is the same as in the proof of 4.8. $\qquad\square$

Remarks.
- By abuse of notation, if we are talking about the link invariant $T_{S,1}$, we actually refer to $\lambda_{S,1}$. For the same reason as above, we might write $T_{S,1}(L)$, respectively $\lambda_{S,1}(L)$. In section 4.4, we will write $T_{S,1} =: J_N$ (actually meaning $\lambda_{S,1} =: J_N$) to mention its connection to the colored Jones polynomial.
- $T_{S,1}(L)$ can be regarded as an invariant of $(1,1)$-tangles (see 4.1 and [KM91, lemma 3.9]), which, together with the omission of Sp_1, explains the additional index 1.

4.4. Equivalence between Kashaev's link invariant and the Colored Jones polynomials

4.4.1. Two Yang-Baxter operators. After this formal study of the link invariant J_N, we intend to analyse it more concretely.
On the one hand, recall from section 3 (or see [KM91, corollary 2.32 and definition 2.35]) the R-matrix R_J with the $((i,j),(k,l))^{\text{th}}$ entry $(R_J)^{ij}_{kl}$ given by

$$\sum_{n=0}^{\min(N-1-i,j)} \delta_{l,i+n}\delta_{k,j-n}\frac{(s-s^{-1})^n[i+n]![N-1+n-j]!}{[n]![i]![N-1-j]!}$$
$$\times s^{2(i-(N-1)/2)(j-(N-1)/2)-n(i-j)-n(n+1)/2},$$

where $N \geq 2$, $s := \exp\left(\frac{i\pi}{N}\right)$, $[k] := \frac{s^k-s^{-k}}{s-s^{-1}}$ for $k \in \mathbb{C}$, $[k]! := \prod_{l=1}^{k}[l]$.

Remark. R_J corresponds to the "R-flip matrix" $\check{R}_J$ ([KM91, definition 2.35]), that is, consider R_J to be the matrix associated in a fixed basis to the operator $P \circ R$, where P is the permutation homomorphism

$$P : \mathbb{C}^N \otimes \mathbb{C}^N \longrightarrow \mathbb{C}^N \otimes \mathbb{C}^N$$
$$a \otimes b \longmapsto b \otimes a,$$

and R the operator given in [KM91, corollary 2.32]). We omit the $\check{}$-sign in the sequel, since there will be many more other, indispensable symbols in the upcoming formulas.

On the other hand, consider the R-matrix R_K introduced by Kashaev in 4.2 (or [Ka95]) with the $((c,d),(a,b))^{\text{th}}$ entry $(R_K)^{cd}_{ab}$ given by

$$N q^{1+c-b+(a-d)(c-b)} \frac{\theta\left(\text{res}\,(b-a-1)+\text{res}\,(c-d)\right)\theta\left(\text{res}\,(a-c)+\text{res}\,(d-b)\right)}{(q_{\text{res}(b-a-1)})(q^{-1}_{\text{res}(a-c)})(q_{\text{res}(c-d)})(q^{-1}_{\text{res}(d-b)})},$$

where $N \geq 2$, $q := s^2 = \exp\left(\frac{2i\pi}{N}\right)$, $(q)_n := \prod_{l=1}^{n}(1-q^l)$ for $n \geq 0$, $\text{res}\,(x) \in \{0,1,...,N-1\}$ is the residue modulo N of $x \in \mathbb{Z}$ and $\theta : \mathbb{Z} \longrightarrow \{0,1\}$ is defined by values $\theta(n)$ equal to

$$\begin{cases} 1 & \text{if} \quad 0 \leq n \leq N-1, \\ 0 & \text{otherwise.} \end{cases}$$

Remark. Again R_K corresponds to the "R-flip matrix", that is $R_K = P \circ R'$, where R' is the R-matrix given in theorem 4.1.

In order to be able to show afterwards that R_J and R_K both satisfy the YBE (up to now, we only know that it is fulfilled by R'), we first give a characterization of their matrix entries. Actually, H. Murakami and J. Murakami, inspired by the observation that R_J and R_K have the same Jordan canonical form for $N = 2, 3$, established the connection between these two R-matrices. For the sake of avoiding a clumsy notation, rather than analyzing R_J, we are interested in $\tilde{R}_J$:

$$\tilde{R}_J := (W \otimes W)(\mathbb{1}_N \otimes D)R_J(\mathbb{1}_N \otimes D^{-1})(W^{-1} \otimes W^{-1}),$$

where $W, D \in \text{Mat}(N, \mathbb{C})$ are defined by $(W)_{i,j} = s^{2ij}$ and $(D)_{i,j} = \delta_{i,j}s^{(N-1)i}$ respectively and $\mathbb{1}_N \in \text{Mat}(N, \mathbb{C})$ is the identity matrix. $\tilde{R}_J$ is again an R-matrix that features the following properties.

PROPOSITION 4.10

$$(\tilde{R}_J)^{cd}_{ab} = \begin{cases} \rho(a,b,c,d)(-1)^{a+b+1}\frac{[d-c-1]![N-1+c-a]!}{[d-b]![b-a-1]!} & \text{if } d \geq b > a \geq c, \\[2mm] \rho(a,b,c,d)(-1)^{a+c}\frac{[b-d-1]![N-1+c-a]!}{[c-d]![b-a-1]!} & \text{if } b > a \geq c \geq d, \\[2mm] \rho(a,b,c,d)(-1)^{b+d}\frac{[c-a-1]![N-1+b-d]!}{[c-d]![b-a-1]!} & \text{if } c \geq d \geq b > a, \\[2mm] \rho(a,b,c,d)(-1)^{c+d}\frac{[a-b]![N-1+b-d]!}{[c-d]![a-c]!} & \text{if } a \geq c \geq d \geq b, \\[2mm] 0 & \text{otherwise,} \end{cases}$$

where $\rho(a,b,c,d) = \frac{1}{N^2} s^{-N^2/2+1/2+c+d-2b+(a-d)(c-b)} (s-s^{-1})^{2(N-1)} [N-1]!$.

Proof. A thorough proof may be consulted in [MM01] p.90-94.   □

A similar result can be worked out for the matrix R_K.

PROPOSITION 4.11

$$(R_K)^{cd}_{ab} = \begin{cases} \lambda(a,b,c,d)(-1)^{a+b+1} \frac{[d-c-1]![N-1+c-a]!}{[d-b]![b-a-1]!} & \text{if } d \geq b > a \geq c, \\[2mm] \lambda(a,b,c,d)(-1)^{a+c} \frac{[b-d-1]![N-1+c-a]!}{[c-d]![b-a-1]!} & \text{if } b > a \geq c \geq d, \\[2mm] \lambda(a,b,c,d)(-1)^{b+d} \frac{[c-a-1]![N-1+b-d]!}{[c-d]![b-a-1]!} & \text{if } c \geq d \geq b > a, \\[2mm] \lambda(a,b,c,d)(-1)^{c+d} \frac{[a-b]![N-1+b-d]!}{[c-d]![a-c]!} & \text{if } a \geq c \geq d \geq b, \\[2mm] 0 & \text{otherwise}, \end{cases}$$

where $\lambda(a,b,c,d) = \frac{N}{([N-1]!)^2} s^{N^2/2-N/2+2+c+d-2b+(a-d)(c-b)} (s-s^{-1})^{1-N}$.

Proof. For the proof, [MM01] p.95-96 may be looked up.   □

Consequently to the two previous propositions, we conclude that R_J and R_K differ only by a constant depending on N. We have

PROPOSITION 4.12
For any $N \geq 2$, the R-matrices R_K and R_J are related by:

$$\begin{aligned} R_K &= s^{-(N+1)(N-3)/2} (W \otimes W)(\mathbb{1}_N \otimes D) R_J (\mathbb{1}_N \otimes D^{-1})(W^{-1} \otimes W^{-1}) \\ &= c^{-1} \tilde{R}_J, \end{aligned}$$

where $c := s^{(N+1)(N-3)/2}$.

Proof. From the propositions 4.10 and 4.11, and the fact that $s = \exp\left(\frac{\pi i}{N}\right)$, we know that

$$\begin{aligned} \frac{(\tilde{R}_J)^{cd}_{ab}}{(R_K)^{cd}_{ab}} &= \frac{\rho(a,b,c,d)}{\lambda(a,b,c,d)} \\ &= s^{-N^2} s^{(N-3)/2} \left(\frac{(s-s^{-1})^{N-1}[N-1]!}{N}\right)^3 \\ &= (-1)^N s^{(N-3)/2} \left(\frac{(s-s^{-1})^{N-1}[N-1]!}{N}\right)^3. \end{aligned}$$

In order to prove the proposition, we thus only need to check that

$$\frac{(\tilde{R}_J)^{cd}_{ab}}{(R_K)^{cd}_{ab}} = s^{(N+1)(N-3)/2} = (-1)^N s^{(N-3)/2} \left(\frac{(s-s^{-1})^{N-1}[N-1]!}{N}\right)^3.$$

On the one hand, using that $2i\sin(x) = (\exp(ix) - \exp(-ix))$, $\forall x \in \mathbb{R}$, we have

$$
\begin{aligned}
(s - s^{-1})^{N-1}[N-1]! &= (s - s^{-1})^{N-1} \prod_{k=1}^{N-1} \frac{s^k - s^{-k}}{s - s^{-1}} \\
&= \prod_{k=1}^{N-1} (s^k - s^{-k}) \\
&= \prod_{k=1}^{N-1} \left(\exp\left(\frac{k\pi i}{N}\right) - \exp\left(-\frac{k\pi i}{N}\right) \right) \\
&= \prod_{k=1}^{N-1} \left(2i \sin\left(\frac{k\pi}{N}\right) \right) \\
&= (2i)^{N-1} \prod_{k=1}^{N-1} \sin\left(\frac{k\pi}{N}\right).
\end{aligned}
$$

On the other hand, from [GR07] p.33, we employ the formula

$$
\sin(Nx) = 2^{N-1} \prod_{k=0}^{N-1} \sin\left(\frac{x + k\pi}{N}\right)
$$

to get

$$
\begin{aligned}
\lim_{x \to 0} \frac{\sin(Nx)}{\sin(x)} = N &= \lim_{x \to 0} \frac{2^{N-1} \prod_{k=0}^{N-1} \sin\left(\frac{x+k\pi}{N}\right)}{\sin(x)} \\
&= 2^{N-1} \lim_{x \to 0} \prod_{k=1}^{N-1} \sin\left(\frac{x + k\pi}{N}\right) \\
&= 2^{N-1} \prod_{k=1}^{N-1} \sin\left(\frac{k\pi}{N}\right).
\end{aligned}
$$

Finally, this results in

$$
\begin{aligned}
(-1)^N s^{(N-3)/2} \left(\frac{(s - s^{-1})^{N-1}[N-1]!}{N} \right)^3 &= (-1)^N s^{(N-3)/2} \, i^{3(N-1)} \\
&= (s^N)^N s^{(N-3)/2} s^{(N/2)3(N-1)} \\
&= s^{5N^2/2 - N - 3/2} \\
&= s^{N^2/2 - N - 3/2} \\
&= s^{(N+1)(N-3)/2}.
\end{aligned}
$$

$\square$

Eventually, we get the answer to one question, that is whether R_J and R_K satisfy the YBE. For R_J, we refer to [KM91, lemma 2.35], for a thorough proof. However, to see that R_K satisfies the YBE, we need the following lemma

LEMMA 4.13

Let $D \in Mat(N, \mathbb{C})$ be the matrix with the $(i, j)^{th}$ entry $D_j^i = \delta_{i,j} s^{(N-1)j}$. Then the following equality holds:

$$(\mathbb{1}_N \otimes D) R_J (\mathbb{1}_N \otimes D^{-1}) = (D^{-1} \otimes \mathbb{1}_N) R_J (D \otimes \mathbb{1}_N). \qquad (4.3)$$

Proof. Note that (4.3) is equivalent to $(D \otimes D) R_J = R_J (D \otimes D)$. Using the definitions of D and R_J, one easily checks that

$$((D \otimes D) R_J)_{kl}^{ij} = (R_J (D \otimes D))_{kl}^{ij}.$$

$\square$

PROPOSITION 4.14

Kashaev's R-matrix R_K satisfies the YBE, that is

$$(R_K \otimes \mathbb{1}_N)(\mathbb{1}_N \otimes R_K)(R_K \otimes \mathbb{1}_N) = (\mathbb{1}_N \otimes R_K)(R_K \otimes \mathbb{1}_N)(\mathbb{1}_N \otimes R_K). \quad (4.4)$$

Proof. In order to compare the two sides of the equation, we transform each of them using proposition 4.12, lemma 4.13 as well as the following properties:

$$
\begin{aligned}
W \mathbb{1}_N W^{-1} &= D \mathbb{1}_N D^{-1} = \mathbb{1}_N, \\
D^2 \mathbb{1}_N &= D \mathbb{1}_N D.
\end{aligned}
$$

A direct calculation then leads to the following expressions for the left and right hand side of (4.4)

- $(R_K \otimes \mathbb{1}_N)(\mathbb{1}_N \otimes R_K)(R_K \otimes \mathbb{1}_N)$
$= c^{-3}(W \otimes W \otimes W)(\mathbb{1}_N \otimes D \otimes D^2)(R_J \otimes \mathbb{1}_N)(\mathbb{1}_N \otimes R_J)(R_J \otimes \mathbb{1}_N)$
$\times (\mathbb{1}_N \otimes D^{-1} \otimes D^{-2})(W^{-1} \otimes W^{-1} \otimes W^{-1})$

- $(\mathbb{1}_N \otimes R_K)(R_K \otimes \mathbb{1}_N)(\mathbb{1}_N \otimes R_K)$
$= c^{-3}(W \otimes W \otimes W)(\mathbb{1}_N \otimes D \otimes D^2)(\mathbb{1}_N \otimes R_J)(R_J \otimes \mathbb{1}_N)(\mathbb{1}_N \otimes R_J)$
$\times (\mathbb{1}_N \otimes D^{-1} \otimes D^{-2})(W^{-1} \otimes W^{-1} \otimes W^{-1}).$

As the YBE has been shown to be satisfied for R_J, that is

$$(R_J \otimes \mathbb{1}_N)(\mathbb{1}_N \otimes R_J)(R_J \otimes \mathbb{1}_N) = (\mathbb{1}_N \otimes R_J)(R_J \otimes \mathbb{1}_N)(\mathbb{1}_N \otimes R_J),$$

we conclude that the two sides of equation (4.4) coincide, thus the YBE is fulfilled by R_K too. $\square$

4.4.2. Two enhanced Yang-Baxter operators. Remembering that our aim consists in proving that R_J and R_K define the same link invariant, we should now focus on establishing enhanced Yang-Baxter operators involving precisely R_J and R_K. Thus, let us have a look at a possible candidate for S_J given by the quadruple

$$S_J = (R_J, \mu_J, \alpha_J, \beta_J)$$

where $\mu_J \in Mat(N, \mathbb{C})$, $(\mu_J)_j^i := \delta_{i,j} s^{2i-N+1}$, $\alpha_J := s^{(N^2-1)/2}$ and $\beta_J := 1$.

Lemma 4.15
$S_J = (R_J, \mu_J, s^{(N^2-1)/2}, 1)$ *is an enhanced Yang-Baxter operator, that is*

$$(\mu_J \otimes \mu_J)R_J = R_J(\mu_J \otimes \mu_J) \quad (4.5)$$

$$Sp_2(R_J^{\pm 1}(\mathbb{1}_N \otimes \mu_J)) = (s^{(N^2-1)/2})^{\pm 1}\mathbb{1}_N. \quad (4.6)$$

Proof. Similarly to lemma 4.13, we check that the entries

$$((\mu_J \otimes \mu_J)R_J)_{kl}^{ij} = (R_J(\mu_J \otimes \mu_J))_{kl}^{ij}$$

coincide. For the verification of the second equality, we check that the following identities hold in $\mathbb{C}$:

$$\sum_{j=0}^{N-1}(R_J(\mathbb{1}_N \otimes \mu_J))_{N-1,j}^{N-1,j} = s^{(N^2-1)/2},$$

$$\sum_{j=0}^{N-1}((R_J)^{-1}(\mathbb{1}_N \otimes \mu_J))_{0,j}^{0,j} = (s^{(N^2-1)/2})^{-1}.$$

This is sufficient, because the right-hand side of (4.6) equals a scalar multiple of $\delta_{i,k}$, henceforth if the relation is satisfied in the special cases $i = k = N-1$ (for the positive power) and $i = k = 0$ (for the negative power), it will be so in the general case. Recall that $(\mu_J)_j^i = \delta_{i,j}s^{2i-N+1}$ and

$$(R_J)_{kl}^{ij} = \sum_{n=0}^{\min(N-1-i,j)}\delta_{l,i+n}\delta_{k,j-n}\frac{[i+n]![N-1+n-j]!}{[i]![n]![N-1-j]!}$$
$$\times (s-s^{-1})^n s^{2(i-(N-1)/2)(j-(N-1)/2)-n(i-j)-n(n+1)/2},$$

$$(R_J^{-1})_{kl}^{ij} = \sum_{n=0}^{\min(N-1-j,i)}\delta_{l,i-n}\delta_{k,j+n}\frac{[j+n]![N-1+n-i]!}{[j]![n]![N-1-i]!}$$
$$\times (-1)^n(s-s^{-1})^n s^{-2(i-(N-1)/2)(j-(N-1)/2)-n(i-j)+n(n+1)/2}.$$

Consequently, in the first case, we get

$$\sum_{j=0}^{N-1}(R_J(\mathrm{id}\otimes\mu_J))_{N-1,j}^{N-1,j} = \sum_{j=0}^{N-1}\sum_{a,b=0}^{N-1}(R_J)_{a,b}^{N-1,j}\delta_{a,N-1}(\mu_J)_b^j$$

$$= \sum_{j=0}^{N-1}(R_J)_{N-1,j}^{N-1,j}s^{2j-N+1}$$

$$= \sum_{j=0}^{N-1}\delta_{j,N-1}s^{(N-1)(j-\frac{N-1}{2})+2j-N+1}$$

$$= s^{(N^2-1)/2}.$$

The second case involves

$$\sum_{j=0}^{N-1} (R_J^{-1}(\mathrm{id} \otimes \mu_J))_{0,j}^{0,j} = \sum_{j=0}^{N-1} \sum_{a,b=0}^{N-1} (R_J^{-1})_{a,b}^{0,j} \delta_{a,0} (\mu_J)_b^j$$

$$= \sum_{j=0}^{N-1} \delta_{j,0} s^{(N-1)(j-\frac{N-1}{2})+2j-N+1}$$

$$= s^{-(N^2-1)/2}.$$

$\square$

Example 4.16.
As a wonderful consequence of lemma 4.15, we dispose now of an EYBO (note that it is up to normalization and reparametrization equivalent to the one suggested by Turaev in [Tur88]). We shall consider the case of the figure-eight knot (recall Figure 20)
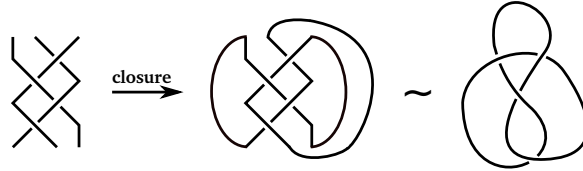
as an example. Since computations are very exhaustive, we just write down the principal results. More details may be found in [Mur10].

- Let $S := (R_J, \mu_J, s^{(N^2-1)/2}, 1)$ be the EYBO from lemma 4.15.

- Denote by $\sigma \in \mathcal{B}_3$ a braid representative of the figure-eight knot, as reviewed on this picture from chapter 2. We have that $\sigma := \sigma_1 \sigma_2^{-1} \sigma_1 \sigma_2^{-1}$.

- The corresponding homomorphism is therefore given by

$$b_{R_J}(\sigma) = (R_J \otimes \mathrm{id})(\mathrm{id} \otimes R_J^{-1})(R_J \otimes \mathrm{id})(\mathrm{id} \otimes R_J^{-1}).$$

- The sum of the exponents appearing in the generator expression of σ being equal to 0 in our case, the colored Jones polynomial for the figure-eight knot, according to the definition (4.2), takes the form

$$T_{S,1}(\sigma) = \mathrm{Sp}_2(\mathrm{Sp}_3\left((R_J \otimes \mathrm{id})(\mathrm{id} \otimes R_J^{-1})(R_J \otimes \mathrm{id})(\mathrm{id} \otimes R_J^{-1})\right).$$

This formula looks quite nice and not so complicated, which is the admirable benefit from the rigorous formalism of J. Murakami and H. Murakami. Nonetheless the calculations involved are not straightforward at all because of the expression for R_J. We give immediately the result that will play an important role in chapter 5. Notice that we use $q = s^2$.

$$T_{S,1}(4_1) = \frac{1}{q^{N/2} - q^{-N/2}} \sum_{k=0}^{N-1} \frac{[N+k]!}{[N-1-k]!} \left(q^{1/2} - q^{-1/2}\right)^{2k+1}.$$

Next, we introduce another EYBO S_K, based on R_K

$$S_K = (R_K, \mu_K, \alpha_K, \beta_K)$$

where $\mu_K \in \mathrm{Mat}(N, \mathbb{C})$, $(\mu_K)_j^i := -\delta_{i,j+1}s$, $\alpha_K := -s$ and $\beta_K := 1$. The following result is the main key for proving that S_K is an enhanced Yang-Baxter operator.

LEMMA 4.17
For W, D, μ_J and μ_K defined as above, the following equality holds:

$$W D \mu_J D^{-1} W^{-1} = \mu_K.$$

Proof. Since the diagonality of D and μ_J implies that they commute, we need to show that $W \mu_J W^{-1} = \mu_K$. In this regard, we calculate the $(i,j)^{\text{th}}$ component of $W \mu_J W^{-1}$:

$$
\begin{aligned}
(W \mu_J W^{-1})_j^i &= \sum_{a,b=0}^{N-1} W_j^a (\mu_J)_a^b (W^{-1})_b^i \\
&= \frac{1}{N} \sum_{a=0}^{N-1} s^{2aj+2a-N+1-2ai} \\
&= \frac{1}{N} \sum_{a=0}^{N-1} s^{1-N} s^{2a(j+1-i)} \\
&= \frac{-s}{N} N \delta_{i,j+1} = (\mu_K)_j^i.
\end{aligned}
$$

$\square$

By this, we are able to show

LEMMA 4.18
$S_K = (R_K, \mu_K, -s, 1)$ *is an enhanced Yang-Baxter operator, that is*

$$
\begin{aligned}
(\mu_K \otimes \mu_K) R_K &= R_K (\mu_K \otimes \mu_K) & (4.7) \\
Sp_2(R_K^{\pm 1}(\mathbb{1}_N \otimes \mu_K)) &= (-s)^{\pm 1} \mathbb{1}_N. & (4.8)
\end{aligned}
$$

Proof. The two equalities are consequences of lemma 4.15. Indeed, the verification follows from proposition 4.12, lemma 4.17 and the fact that μ_J and D commute. $\square$

4.4.3. Correspondence between the two link invariants.   Finally, we can reap the fruit of our calculatory preparations. We introduce the following notations for the link invariants arising from S_J and S_K respectively,

$$J_N(L) := T_{S_{J,1}}(L); \quad \langle L \rangle_N := T_{S_{K,1}}(L).$$

$J_N(L)$ is nothing but the colored Jones polynomial at the Nth root of unity and $\langle L \rangle_N$ corresponds to the Kashaev invariant. We now conclude

Theorem 4.19

For any link L and any integer $N \geq 2$, the link invariants $J_N(L)$ and $\langle L \rangle_N$ coincide.

Proof. The proof is divided into 3 steps.

1$^{\text{st}}$ step.   First, we show that lemma 4.13 generalizes to

$$R_J^{\pm 1} = (D^k \otimes D^k) R_J^{\pm 1} (D^{-k} \otimes D^{-k}). \qquad (4.9)$$

Proof. (1$^{\text{st}}$ step.) The identity is immediately obtained by performing the same computations as in lemma 4.13 on the components of $R_J^{\pm 1}(D^k \otimes D^k)$ and $(D^k \otimes D^k) R_J^{\pm 1}$. $\qquad\qquad\square$

2$^{\text{nd}}$ step.   The braid homomorphisms b_{R_K} and b_{R_J} are related in the following way; for any $\xi \in \mathcal{B}_n$

$$b_{R_K}(\xi) = c^{-w(\xi)}(W^{\otimes n})(\bigotimes_{l=0}^{n-1} D^l) b_{R_J}(\xi)(\bigotimes_{l=0}^{n-1} D^{-l})((W^{-1})^{\otimes n}), \qquad (4.10)$$

where $c := s^{(N+1)(N-3)/2}$.

Proof. (2$^{\text{nd}}$ step.) It is sufficient to show that the above relation holds on the generators of $\mathcal{B}_n$, that is, for any $1 \leq i \leq n-1$

$$b_{R_K}(\sigma_i^{\pm 1}) = c^{\mp 1}(W^{\otimes n})(\bigotimes_{l=0}^{n-1} D^l) b_{R_J}(\sigma_i^{\pm 1})(\bigotimes_{l=0}^{n-1} D^{-l})((W^{-1})^{\otimes n}).$$

Accordingly to proposition 4.12 and (4.9), we get

$$\begin{aligned}
R_K^{\pm 1} &= c^{\mp 1}(W \otimes W)(\mathbb{1}_N \otimes D) R_J^{\pm 1} (\mathbb{1}_N \otimes D^{-1})(W^{-1} \otimes W^{-1}) \\
&= c^{\mp 1}(W \otimes W)(D^{i-1} \otimes D^i) R_J^{\pm 1} (D^{1-i} \otimes D^{-i})(W^{-1} \otimes W^{-1}).
\end{aligned}$$

Recalling that $b_R(\sigma_i^{\pm 1}) = \mathbb{1}_N^{\otimes(i-1)} \otimes R^{\pm 1} \otimes \mathbb{1}_N^{\otimes(n-i-1)}$ (amongst others valid for b_{R_K}, b_{R_J}), we have

$$\begin{aligned}
b_{R_K}(\sigma_i^{\pm 1}) &= c^{\mp 1}\mathbb{1}_N^{\otimes(i-1)} \otimes (W \otimes W)(D^{i-1} \otimes D^i) R_J^{\pm 1} \\
&\quad \times (D^{1-i} \otimes D^{-i})(W^{-1} \otimes W^{-1}) \otimes \mathbb{1}_N^{\otimes(n-i-1)} \\
&= c^{\mp 1}(W^{\otimes n})(\bigotimes_{l=0}^{n-1} D^l) b_{R_J}(\sigma_i^{\pm 1})(\bigotimes_{l=0}^{n-1} D^{-l})((W^{-1})^{\otimes n}).
\end{aligned}$$

$\qquad\qquad\square$

3$^{\text{rd}}$ step.   Ultimately, we conclude that the link invariants defined by S_J and S_K coincide, that is for any link L and for $N \geq 2$:

$$\langle L \rangle_N = J_N(L).$$

Proof. (3$^{\text{rd}}$ step.) As a result of step 2 (4.10) as well as by the facts that $W\mu_J W^{-1} = \mu_K$ and that μ_J commutes with D^k (for any $k \in \mathbb{R}$), we end up with the identity

$$b_{R_K}(\xi)(\mathbb{1}_{\text{N}} \otimes \mu_K^{\otimes(n-1)}) = c^{-w(\xi)}(AB)b_{R_J}(\xi)(\mathbb{1}_{\text{N}} \otimes \mu_J^{\otimes(n-1)})(AB)^{-1},$$

where $A := (W^{\otimes n})$, $B := (\overset{n-1}{\underset{l=0}{\bigotimes}} D^l)$ and ξ is the braid representation of L. Applying now successively the trace operators $\text{Sp}_k (n \geq k \geq 2)$ on both sides and using the conjugacy invariance of traces, we get

$$\alpha_K^{w(\xi)} \beta_K^n T_{S_{K,1}}(\xi) = c^{-w(\xi)} \alpha_J^{w(\xi)} \beta_J^n T_{S_{J,1}}(\xi)$$

$$\Longleftrightarrow \quad (-s)^{w(\xi)} T_{S_{K,1}}(\xi) = s^{-w(\xi)(N+1)(N-3)/2} s^{w(\xi)(N^2-1)/2} T_{S_{J,1}}(\xi)$$

$$\Longleftrightarrow \quad (-s)^{w(\xi)} T_{S_{K,1}}(\xi) = s^{w(\xi)(N+1)} T_{S_{J,1}}(\xi)$$

$$\Longleftrightarrow \quad T_{S_{K,1}}(\xi) = T_{S_{J,1}}(\xi).$$

Thus the conclusion $\langle L \rangle_N = J_N(L)$. $\qquad\qquad\qquad\qquad\qquad\qquad\qquad\square$

This accomplishes the proof of theorem 4.19. $\qquad\qquad\qquad\qquad\qquad\quad\square$

We now learnt that there are different methods to calculate the same invariant of colored links. This is a great achievement, not only on the computational level, but most of all on the level of comprehension of a link invariant based on an enhanced Yang-Baxter operator.

5. THE VOLUME CONJECTURE

The knowledge we have acquired up to here will soon culminate in the famous Volume Conjecture that was first raised by R. Kashaev in 1996. Amazingly, the world of quantum invariants with its appeal to algebra, topology and knot theory is unified by this Conjecture with the world of hyperbolic geometry. This chapter will take us back to the traces of Kashaev's major inspiration sources, present the mathematical tools that were necessary to the establishment of the Volume Conjecture, shed light onto its proved and yet unproved parts and finally discusses its latest generalizations. We mainly rely on the original article of R. Kashaev [Ka97] as well as on the proofs given in [Mur10] by T. Ekholm and in [Yok03] by Y. Yokota. The milestones are the following:

- introduction of the Volume Conjecture by R. Kashaev in 1996 (5.1),
- generalization of the Volume Conjecture using the Gromov norm, after H. Murakami and J. Murakami in 2001, (5.2),
- general numerical method for proving the Volume Conjecture (5.3),
- proof of the Volume Conjecture for the figure-eight knot (5.4),
- proof of the Volume Conjecture for the knot 5_2 (5.5),
- comments on the Volume Conjecture (5.6).

5.1. The Volume Conjecture by R. Kashaev

Motivated by the quest for a quantum generalization of the hyperbolic volume invariant, R. Kashaev introduced a family of link invariants $\langle L \rangle_N$ via 3-dimensional interpretation of the quantum dilogarithm and depending on a natural number N. To understand why these means justify the end, we need to refer to topological quantum field theories (TQFT) (that is a quantum field theory that computes topological invariants), since the construction of $\langle L \rangle_N$ can be regarded as an example of such a combinatorial TQFT. A detailed clarification of these theories would exceed the aim of the present work, therefore we just retain the following crucial ideas: On the one hand, Kashaev knew that the partition function of the hyperbolic knot's complement in an important case of TQFT (in quantum Chern-Simons theory with a non-compact gauge group) leads to a topological invariant, whose classical limit provides the hyperbolic volume of the knot. On the other hand, he was aware of the fact, that the hyperbolic volume of a 3-manifold can be calculated using a smartly chosen triangulation of the latter into ideal tetrahedra. The volume of these simplices can be expressed in terms of Lobachevsky's function, which is the imaginary part of Euler's dilogarithm.

These arguments inspired Kashaev to define a corresponding topological link invariant using quantum dilogarithm, expecting his invariant to reproduce the knot's hyperbolic volume in the classical limit (that is $N \to \infty$). Unfortunately, this problem is not straightforward to solve. Indeed, the discovery of an ever-working algorithm still lacks and in each case, the computation of the limit reveals to be quite laborious. So it comes that the Conjecture

has only been proved for some few hyperbolic knots and links up to date (cf. 5.6).

In his notorious paper [Ka97], Kashaev analyses the growth behaviour of his link invariant for the prime knots 4_1, 5_2 and 6_1 and suggests that the absolute value of the latter increases exponentially as N goes to infinity, the hyperbolic volume of the knot complement being the growth rate. The formulation of the Volume Conjecture phrases as follows.

VOLUME CONJECTURE 5.1 (Kashaev, 1996)
For any hyperbolic link L with corresponding invariant $\langle L \rangle_N$ and hyperbolic volume $Vol(L)$, the following asymptotic behaviour holds:

$$2\pi \lim_{N \to \infty} \frac{\log |\langle L \rangle_N|}{N} = Vol(L). \tag{5.1}$$

In sections 5.4 and 5.5, we are going to show that (5.1) holds for the figure-eight knot and the knot 5_2 by studying numerically the asymptotic behaviour of the Kashaev invariant and by giving a rigorous proof as well. However, before approaching this rather technical part, we focus on J. Murakami's and H. Murakami's formulation of the Volume Conjecture.

5.2. The modified Volume Conjecture by H. Murakami and J. Murakami

For the sake of clarifying the link invariant $\langle - \rangle_N$ introduced by Kashaev, J. Murakami and H. Murakami showed in 2001 its coincidence with the N-dimensional colored Jones polynomial $J_N(-)$ evaluated at the Nth root of unity. In this same spirit ([MM01, conjecture 5.1]), they generalized Kashaev's Volume Conjecture, using the Gromov norm, which can be regarded as a natural generalization of the hyperbolic volume.

VOLUME CONJECTURE 5.2 (J. Murakami, H. Murakami, 2001)
For any knot K with colored Jones polynomial $J_N(K)$ and Gromov norm $\|K\|$, the following asymptotic behaviour holds:

$$\frac{2\pi}{\upsilon_3} \lim_{N \to \infty} \frac{\log |J_N(K)|}{N} = \|K\|, \tag{5.2}$$

where υ_3 is the volume of the ideal regular tetrahedron in the 3-dimensional hyperbolic space $\mathbb{H}^3$.

Remark. If 5.1 is true, then 5.2 holds for any hyperbolic knot (not for links in general!) and connected sums of such knots, since Gromov's simplicial volume (or the Gromov norm) is additive under the connected sum

$$
\begin{aligned}
\frac{2\pi}{\upsilon_3} \lim_{N \to \infty} \frac{\log |J_N(K_1 \# K_2)|}{N} &= \frac{2\pi}{\upsilon_3} \lim_{N \to \infty} \frac{\log |J_N(K_1) J_N(K_2)|}{N} \\
&= \frac{2\pi}{\upsilon_3} \lim_{N \to \infty} \frac{\log |J_N(K_1)| + \log |J_N(K_2)|}{N} \\
&\overset{(5.2)}{=} \|K_1\| + \|K_2\| = \|K_1 \# K_2\|.
\end{aligned}
$$

Accordingly, it is sufficient to verify the Volume Conjecture for prime knots.

A remarkable consequence of the Volume Conjecture is

COROLLARY 5.3
If the Volume Conjecture 5.2 is true, then a knot K is trivial if and only if all of its colored Jones polynomials $J(K)_N$ are trivial.

Proof. The arguments for the proof may be found in [MM01] p.102-103. □

In the next section, we concentrate on a method which enables us to check the Volume Conjecture numerically.

5.3. Numerical evidence

In order to get a flavour of the complexity of the calculations required to study the asymptotic behaviour of the colored Jones polynomial or equivalently of the Kashaev invariant, we start by exposing numerical evidence for the Volume Conjecture. Afterwards, we turn to a rigorous analytical proof for 2 knots.

Inspired by the works of Kashaev in [Ka97] and of Hikami in [Hik03], we give here a general procedure for comparing the classical limit of the Kashaev invariant for hyperbolic knots to the hyperbolic volume of the corresponding complement. We illustrate the technique with the figure-eight knot 4_1 and the knot 5_2 in 5.4 and 5.5 respectively.

5.3.1. 1st Approach: trial function. Given a knot K, its Kashaev invariant can be computed numerically for different values of N using PARI/GP. Studying the quantity $2\pi \frac{\log(|\langle K \rangle_N|)}{N}$ is equivalent to examining the real part $\Re\left(2\pi \frac{\log(\langle K \rangle_N)}{N}\right)$ since for $\langle K \rangle_N =: r \exp(i\theta) \in \mathbb{C}$, we have

$$\Re\left(2\pi \frac{\log(\langle K \rangle_N)}{N}\right) = \Re\left(2\pi \frac{\log(r \exp(i\theta))}{N}\right)$$

$$= \Re\left(2\pi \frac{\log r + i\theta}{N}\right)$$

$$= 2\pi \frac{\log r}{N} = 2\pi \frac{\log(|\langle K \rangle_N|)}{N}.$$

We plot $\Re\left(2\pi \frac{\log(\langle K \rangle_N)}{N}\right)$ as a function of N (for examples, see Figure 39 and Figure 41) and resort to the least-squares method to achieve a trial function $v_K(N)$ that may be expressed as follows

$$v_K(N) = \Re\left(2\pi \frac{\log(\langle K \rangle_N)}{N}\right) = c_1(K) + c_2(K)\frac{2\pi \log N}{N} + \frac{c_3(K)}{N} + \frac{c_4(K)}{N^2}.$$
$$(5.3)$$

The motivation for choosing this trial function goes back to the asymptotic expansion of Kashaev's invariant for torus knots $T(p, q)$. More details may

be read in [Hik03, section 3]. In the classical limit, we therefore have

$$\lim_{N \to \infty} \Re \left(2\pi \frac{\log \left(\langle K \rangle_N \right)}{N} \right) = \lim_{N \to \infty} v_K(N) = c_1(K).$$

In other words, numerical results for $c_1(K)$ should reproduce the value of the K-associated hyperbolic volume. Clearly, this method corresponds to an experimental verification of the Volume Conjecture rather than to a rigorous proof, but it is quite satisfactory in itself as long as the number of crossings does not exceed a certain treshold of computational costs. Nonetheless, we browse another numerical approach, that supports the present one.

5.3.2. 2nd Approach: potential and saddle point. In order to study the asymptotic behaviour of the Kashaev invariant, we need to know the maximum summand which dominates the limit. Unfortunately, this task can not be accomplished in a direct way. We rather need to pass to an approximate integral expression that we manage to evaluate in a best possible way. Thus, the objective consists now in the determination of a *potential $V_K(x)$, $x \in \mathbb{C}^p$,* p being the number of summations appearing in $\langle K \rangle_N$, such that the invariant can be represented as an integral of this potential, namely

$$\langle K \rangle_N \sim \iint \cdots \int \prod_{j=1}^{p} dx_j \, \exp \left(\frac{\mathrm{i}N}{2\pi} V_K(x) \right). \tag{5.4}$$

In order to define such a potential, recall the following definitions

$$(q)_n := \prod_{j=1}^{n} (1 - q^j) \quad \text{and} \quad (q)_n^* := \prod_{j=1}^{n} (1 - q^{-j}),$$

where $q = \exp \left(\frac{2\pi \mathrm{i}}{N} \right)$. With respect to the asymptotic behaviour (very rough!)

$$\lim_{N \to \infty} \frac{2\pi \mathrm{i}}{N} \log(q)_n = \lim_{N \to \infty} \frac{2\pi \mathrm{i}}{N} \sum_{j=1}^{n} \log \left(1 - q^j \right)$$

$$= \lim_{N \to \infty} \frac{2\pi \mathrm{i}}{N} \sum_{j=1}^{n} \log \left(1 - \exp \left(\frac{2\pi \mathrm{i} j}{N} \right) \right)$$

$$= \int_0^{\frac{2\pi \mathrm{i} n}{N}} \log \left(1 - \exp \left(t \right) \right) dt$$

$$= \mathrm{Li}_2(1) - \mathrm{Li}_2 \left(q^n \right)$$

$$= \frac{\pi^2}{6} - \mathrm{Li}_2 \left(q^n \right)$$

the following approximate expressions for q^{ab}, $(q)_n$ and $(q)_n^*$ result for large N

$$q^{ab} \sim \exp\left(-\frac{iN}{2\pi} \log q^a \log q^b\right) \tag{5.5}$$

$$(q)_n \sim \exp\left(\frac{iN}{2\pi}\left(\mathrm{Li}_2(q^n) - \frac{\pi^2}{6}\right)\right) \tag{5.6}$$

$$(q)_n^* \sim \exp\left(\frac{iN}{2\pi}\left(-\mathrm{Li}_2(q^{-n}) + \frac{\pi^2}{6}\right)\right), \tag{5.7}$$

with $a, b, n \in \{0, 1, \ldots, N-1\}$. The substitution of the factors $(q)_n$ and $(q)_n^*$ in the Kashaev invariant $\langle K\rangle_N$ by formulas (5.5), (5.6) and (5.7) as well as a careful replacement of the summation by a contour integral lead to the desired expression (5.4).

For the evaluation of integral (5.4) in the large N-limit, we can apply a stationary phase approximation and obtain a saddle point x_0 as a solution to

$$\left.\frac{\partial}{\partial x_j} V_K(x)\right|_{x=x_0} = 0, \quad \forall j = 1, \ldots, n.$$

With this solution, we obtain (cf. [Hik03])

$$\langle K\rangle_N \sim \exp\left(\frac{iN}{2\pi} V_K(x_0)\right),$$

and therefore

$$\lim_{N\to\infty} 2\pi \frac{\log(\langle K\rangle_N)}{N} \overset{(5.4)}{=} iV_K(x_0).$$

Hopefully, the real part of this limit releases the value of the K-associated hyperbolic volume. Such a limit is called *optimistic limit* and to give special emphasis to this characterization, it is sometimes denoted by

$$o - \lim_{N\to\infty} \Re\left(2\pi \frac{\log(\langle K\rangle_N)}{N}\right) := \Re\left(iV_K(x_0)\right),$$

but we often omit it in the sequel.

5.4. Proof of the Volume Conjecture for the figure-eight knot 4_1

The figure-eight knot is he first (with respect to an ascending crossing number order) non-trivial knot that admits a complete hyperbolic structure on its complement and is subject to the Volume Conjecture. The fact that $\mathbb{S}^3 \setminus 4_1$ is a complete hyperbolic 3-manifold is known and explicitly shown by M. Jacquement in [Jac10].

5.4.1. Numerical evidence involving the Kashaev invariant.

Proof. **1st Approach: trial function.** We start by reviewing the Kashaev invariant for the figure-eight knot 4_1 from chapter 4, more precisely

$$\langle 4_1\rangle_N = \sum_{a=0}^{N-1} |(q)_a|^2. \tag{5.8}$$

After computations of $\langle 4_1 \rangle_N$ for different values of N, we plot $\Re \left(2\pi \frac{\log(\langle 4_1 \rangle_N)}{N} \right)$ and fit the numerical data, marked by a •, by the trial function (5.3), which leads to the illustration below.
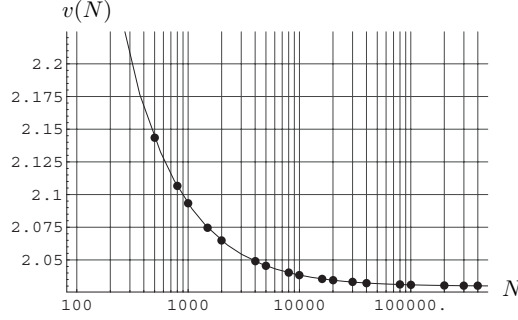

Figure 39: *Numerical data for the figure-eight knot (extracted from [Hik03])*

The numerical result (extracted from [Hik03]) shows

$$c_1(4_1) = 2.029883193056962 \pm 7.77 \times 10^{-9}.$$

2nd Approach: potential and saddle point.   The next goal consists in calculating the potential $V_{4_1}(x)$, where $x \in \mathbb{C}$ ($p = 1$, since there is one sum) satisfying $\log x = \frac{2\pi i}{N} a$. Using relations (5.6) and (5.7) in (5.8), we get

$$|(q)_a|^2 = (q)_a (q)_a^*$$
$$= \exp \left(\frac{iN}{2\pi} \left(\mathrm{Li}_2(x) - \frac{\pi^2}{6} \right) \right) \exp \left(\frac{iN}{2\pi} \left(- \mathrm{Li}_2(x^{-1}) + \frac{\pi^2}{6} \right) \right)$$
$$= \exp \left(\frac{iN}{2\pi} \left(\mathrm{Li}_2(x) - \mathrm{Li}_2(x^{-1}) \right) \right),$$

thus the potential $V_{4_1}(x) = \mathrm{Li}_2(x) - \mathrm{Li}_2(x^{-1})$ and the approximation

$$\langle 4_1 \rangle_N \sim \int dx \exp \left(\frac{iN}{2\pi} V_{4_1}(x) \right). \tag{5.9}$$

By use of the integral expression of the dilogarithm, we end up with the following saddle point equation

$$\frac{d}{dx} V_{4_1}(x) = 0$$
$$\iff -\frac{\log(1-x)}{x} + \frac{\log(1-x^{-1})}{x^{-1}}(-x^{-2}) = 0$$
$$\iff x^2 - x + 1 = 0$$
$$\iff x_0 = e^{\pm i\pi/3}.$$

As the maximal contribution to the integral (5.9) comes from the root $x_0 = e^{-i\pi/3}$, the other solution is neglected.

Comparison. Finally, we compare $c_1(4_1)$ and $\Re\left(iV_{4_1}(x_0)\right)$ to the hyperbolic volume $\mathrm{Vol}(\mathbb{S}^3 \setminus 4_1)$.

$$c_1(4_1) = 2.029883193056962 \pm 7.77 \times 10^{-9},$$

$$\Re\left(iV_{4_1}(x_0)\right) = 2.02988\ldots,$$

$$\mathrm{Vol}(\mathbb{S}^3 \setminus 4_1) = 6\Lambda\left(\frac{\pi}{3}\right) = 2.029883212819307\ldots$$

These results only differ by a value smaller than 10^{-5} which is in agreement with the Volume Conjecture 5.1. □

5.4.2. Analytical proof. The demonstration we expose here follows the work of T. Ekholm (and rewieved in [Mur10]).

Proof. The proof is organized in 3 steps.

1st step. First, we aim to show the following asymptotic behaviour

$$\lim_{N \to \infty} \frac{\log J_N(4_1)}{N} = \frac{2}{\pi} \int_0^{\frac{5\pi}{6}} \log(2\sin(x))dx \quad \text{where} \tag{5.10}$$

$$J_N(4_1) = \frac{1}{q^{N/2} - q^{-N/2}} \sum_{k=0}^{N-1} \frac{[N+k]!}{[N-1-k]!}\left(q^{1/2} - q^{-1/2}\right)^{2k+1}, \tag{5.11}$$

with $q = \exp\left(\frac{2\pi i}{N}\right)$ and $[k] := \frac{q^{k/2} - q^{-k/2}}{q^{1/2} - q^{-1/2}}$.

Proof. (1st step.) The basic idea of the proof is to use the Sandwich theorem, that is, to confine the limit (5.10) with the limit of another function, that can be computed more easily. In order to find this function, we transform (5.11) according to

$$J_N(4_1) = \frac{1}{q^{N/2} - q^{-N/2}} \sum_{j=0}^{N-1} \frac{[N+j]!}{[N-1-j]!}\left(q^{1/2} - q^{-1/2}\right)^{2j+1}$$

$$= \frac{1}{q^{N/2} - q^{-N/2}} \sum_{j=0}^{N-1} \frac{\prod_{m=1}^{N+j}\left(q^{m/2} - q^{-m/2}\right)}{\prod_{m=1}^{N-j-1}\left(q^{m/2} - q^{-m/2}\right)}$$

$$= \sum_{j=0}^{N-1} \prod_{m=N-j}^{N+j}\left(q^{m/2} - q^{-m/2}\right)\left(q^{N/2} - q^{-N/2}\right)^{-1}$$

$$= \sum_{j=0}^{N-1} \prod_{m=N-j}^{N-1}\left(q^{m/2} - q^{-m/2}\right) \prod_{m=N+1}^{N+j}\left(q^{m/2} - q^{-m/2}\right)$$

$$= \sum_{j=0}^{N-1} \prod_{k=1}^{j}\left(q^{(N-k)/2} - q^{-(N-k)/2}\right) \prod_{l=1}^{j}\left(q^{(N+l)/2} - q^{-(N+l)/2}\right)$$

$$= \sum_{j=0}^{N-1} \prod_{k=1}^{j}\left(q^{(N-k)/2} - q^{-(N-k)/2}\right)\left(q^{(N+k)/2} - q^{-(N+k)/2}\right)$$

where we put $k := -m + N$, $l := m - N$ and $k, l \geq 0$. Replacing q by $\exp\left(\frac{2\pi i}{N}\right)$ and using the relation $2i \sin(x) = (\exp(ix) - \exp(-ix))$ for any $x \in \mathbb{R}$, we get

$$
\begin{aligned}
J_N(4_1) &= \sum_{j=0}^{N-1} \prod_{k=1}^{j} \left(2i \sin\left(\pi - \frac{k\pi}{N}\right)\right)\left(2i \sin\left(\pi + \frac{k\pi}{N}\right)\right) \\
&= \sum_{j=0}^{N-1} \prod_{k=1}^{j} \left(2\sin\left(\frac{k\pi}{N}\right)\right)^2 \\
&= \sum_{j=0}^{N-1} \prod_{k=1}^{j} f(N;k)
\end{aligned}
$$

where $f(N;k) := \left(2\sin\left(\frac{k\pi}{N}\right)\right)^2$. Next, we set $g(N;j) := \prod_{k=1}^{j} f(N;k)$. From the graph of the function $f(N;k)$ (see Figure 40), we deduce that $g(N;j)$ is decreasing for $j \in \left]0, \frac{N}{6}\right[\cup \left]\frac{5N}{6}, N-1\right[$ and increasing for $j \in \left]\frac{N}{6}, \frac{5N}{6}\right[$. Since j does only take integer values, we actually refer to the integer part of the fractions $\frac{N}{6}, \frac{5N}{6}$. The table below summarizes theses observations.
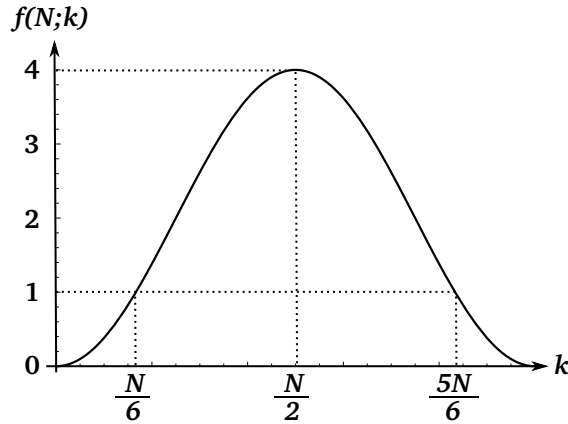
Figure 40: *Graph of $f(N;k)$*

k, j	0	...	$\frac{N}{6}$	...	$\frac{N}{2}$	...	$\frac{5N}{6}$	...	N
$f(N;k)$	0	↗	1	↗	4	↘	1	↘	0
$g(N;j)$	1	↘		↗		↗	⋆	↘	

The star $\star$ stands for $g(N; \frac{5N}{6})$, that is, for the maximum value reached by $g(N, j)$.

As a consequence to the positive terms in $J_N(4_1) = \sum_{j=0}^{N-1} g(N;j)$, the following inequality holds

$$
g\left(N, \frac{5N}{6}\right) \leq J_N(4_1) \leq N g\left(N, \frac{5N}{6}\right) \tag{5.12}
$$

and since the logarithm function is strictly increasing, (5.12) becomes

$$\frac{\log\left(g\left(N,\frac{5N}{6}\right)\right)}{N} \leq \frac{\log\left(J_N(4_1)\right)}{N} \leq \frac{\log N}{N} + \frac{\log\left(g\left(N,\frac{5N}{6}\right)\right)}{N}.$$

The function we were looking for can be defined as

$$h(N;j) := \frac{\log\left(g\left(N,j\right)\right)}{N}.$$

Using the fact that $\lim_{N\to\infty} \frac{\log N}{N} = 0$, the following comparison results

$$\lim_{N\to\infty} h\left(N;\frac{5N}{6}\right) \leq \lim_{N\to\infty} \frac{\log\left(J_N(4_1)\right)}{N} \leq \lim_{N\to\infty} h\left(N;\frac{5N}{6}\right).$$

By virtue of the Sandwich theorem, we conclude

$$\lim_{N\to\infty} \frac{\log\left(J_N(4_1)\right)}{N} = \lim_{N\to\infty} h\left(N;\frac{5N}{6}\right). \qquad (5.13)$$

Of course, we have not yet reached our goal, because the limit on the right hand side of (5.13) still needs to be evaluated. Before doing so, let us transform this limit according to

$$\begin{aligned}
\lim_{N\to\infty} h\left(N;\frac{5N}{6}\right) &= \lim_{N\to\infty} \frac{\log\left(g\left(N,\frac{5N}{6}\right)\right)}{N} \\
&= \lim_{N\to\infty} \frac{1}{N} \sum_{k=1}^{5N/6} \log\left(f(N;k)\right) \\
&= 2 \lim_{N\to\infty} \frac{1}{N} \sum_{k=1}^{5N/6} \log\left(2\sin\left(\frac{k\pi}{N}\right)\right) \\
&= \frac{2}{\pi} \int_0^{\frac{5\pi}{6}} \log(2\sin(x))dx.
\end{aligned}$$

This accomplishes the proof of the first step (the integral computation being the objective of step 2). $\qquad\square$

2nd step. Using the Lobachevsky function Λ, the evaluation of the limit (5.10) gives

$$\frac{2}{\pi} \int_0^{\frac{5\pi}{6}} \log(2\sin(x))dx = \frac{3}{\pi}\Lambda\left(\frac{\pi}{3}\right). \qquad (5.14)$$

Proof. (2nd step.) The key for the demonstration lies in the definition and properties of the Lobachevsky function. Recall that

$$\Lambda(\theta) := -\int_0^{\theta} \log|2\sin(x)|dx \quad \text{for} \quad \theta \in \mathbb{R}.$$

As for $x \in [0, \frac{5\pi}{6}]$, the sine is always positive, the integral becomes

$$\frac{2}{\pi} \int\limits_0^{\frac{5\pi}{6}} \log(2\sin(x))dx = -\frac{2}{\pi} \Lambda\left(\frac{5\pi}{6}\right).$$

From the properties 2.34 of Λ and (2.10) we conclude that

$$\left. \begin{array}{rcl} \Lambda\left(\frac{5\pi}{6}\right) & = & -\Lambda\left(\frac{\pi}{6}\right), \\ \Lambda\left(\frac{\pi}{3}\right) & = & \frac{2}{3}\Lambda\left(\frac{\pi}{6}\right) \end{array} \right\} \Longrightarrow \Lambda\left(\frac{5\pi}{6}\right) = -\frac{3}{2}\Lambda\left(\frac{\pi}{3}\right)$$

and therefore

$$\frac{2}{\pi} \int\limits_0^{\frac{5\pi}{6}} \log(2\sin(x))dx = \frac{3}{\pi} \Lambda\left(\frac{\pi}{3}\right).$$

This finally results in

$$2\pi \lim_{N \to \infty} \frac{\log J_N(K)}{N} = 4 \int\limits_0^{\frac{5\pi}{6}} \log(2\sin(x))dx$$

$$= 6\Lambda\left(\frac{\pi}{3}\right)$$

$\square$

3$^{\text{rd}}$ step.   In the last step, we need to show that

$$\|4_1\| = \frac{6}{\upsilon_3} \Lambda\left(\frac{\pi}{3}\right) \tag{5.15}$$

which finalizes the proof of (5.2).

Proof. (3$^{\text{rd}}$ step.) The proof for the third step is straightforward, once we are aware of the following theorem.

THEOREM 5.4 ([Thu02])
The complement of the figure-eight knot can be obtained by gluing two ideal hyperbolic regular tetrahedra.

Since an ideal hyperbolic regular tetrahedron is isometric to $T\left(\frac{\pi}{3}, \frac{\pi}{3}, \frac{\pi}{3}\right)$, the complement of the figure-eight knot in $\mathbb{S}^3$ is isometric to the union of two copies of $T\left(\frac{\pi}{3}, \frac{\pi}{3}, \frac{\pi}{3}\right)$. Consequently

$$\text{Vol}(\mathbb{S}^3 \setminus 4_1) = 2\,\text{Vol}\left(T\left(\frac{\pi}{3}, \frac{\pi}{3}, \frac{\pi}{3}\right)\right) \stackrel{(2.14)}{=} 6\Lambda\left(\frac{\pi}{3}\right).$$

Using the fact that $\text{Vol}(\mathbb{S}^3 \setminus 4_1) = \upsilon_3 \|4_1\|$, we end up with equality (5.15). $\square$

To sum up, we combine the 3 steps in order to get

$$\frac{2\pi}{\upsilon_3} \lim_{N \to \infty} \frac{\log J_N(4_1)}{N} = \frac{4}{\upsilon_3} \int\limits_0^{\frac{5\pi}{6}} \log(2\sin(x))dx = \frac{6}{\upsilon_3} \Lambda\left(\frac{\pi}{3}\right) = \|4_1\|.$$

$\square$

5.5. Proof of the Volume Conjecture for the knot 5_2

Characterized by its neatness, the proof of the Volume Conjecture for the figure-eight knot is not quite representative for the difficulties we prophesied at the beginning of this chapter. However, in the next proof we will see that, although the number of crossings of the considered knot increases only by 1 compared to the figure-eight knot, the involved arguments will be completely different and of more constructive nature.

5.5.1. Numerical evidence involving the Kashaev invariant.

Proof. **1ˢᵗ Approach: trial function.**   Recall the Kashaev invariant for the knot 5_2

$$\langle 5_2 \rangle_N = \sum_{0 \leq a \leq b \leq N-1} \frac{((q)_b)^2}{(q)_a^*} q^{-(b+1)a}. \tag{5.16}$$

After computations of $\langle 5_2 \rangle_N$ for different values of N, we plot $\Re \left(2\pi \frac{\log(\langle 5_2 \rangle_N)}{N} \right)$ and fit the numerical data, marked by a •, by the trial function (5.3), which leads to the illustration in Figure 41.
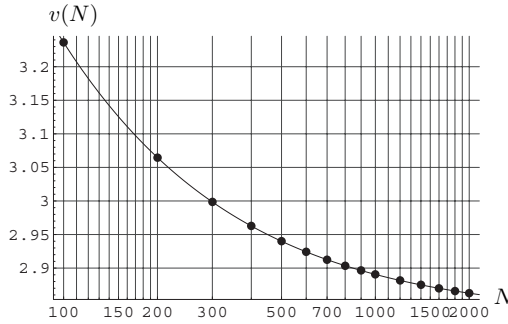

Figure 41: *Numerical data for the knot 5_2 (extracted from [Hik03])*

The numerical result (extracted from [Hik03]) shows

$$c_1(5_2) = 2.8281219744 \pm 1.5571 \times 10^{-8}.$$

2ⁿᵈ Approach: potential and saddle point.   Next, we aim the computation of the potential $V_{5_2}(x)$, where $x = (x_1, x_2) \in \mathbb{C}^2$ ($p = 2$, since there are two sums in $\langle 5_2 \rangle_N$) satisfying $\log x_1 = \frac{2\pi i}{N} a$ and $\log x_2 = \frac{2\pi i}{N} b$ respectively. Using relations (5.5), (5.6) and (5.7) in (5.16), we get

$$\frac{((q)_b)^2}{(q)_a^*} q^{-(b+1)a}$$
$$= \frac{\exp \left(\frac{iN}{2\pi} \left(2 \operatorname{Li}_2 (x_2) - \frac{\pi^2}{3} \right) \right)}{\exp \left(\frac{iN}{2\pi} \left(-\operatorname{Li}_2 (x_1^{-1}) + \frac{\pi^2}{6} \right) \right)} \exp \left(\frac{iN}{2\pi} \log x_1 \log x_2 \right)$$
$$= \exp \left(\frac{iN}{2\pi} \left(2 \operatorname{Li}_2 (x_2) + \operatorname{Li}_2 (x_1^{-1}) + \log x_1 \log x_2 - \frac{\pi^2}{2} \right) \right),$$

thus the potential $V_{5_2}(x_1, x_2) = 2\operatorname{Li}_2(x_2) + \operatorname{Li}_2\left(x_1^{-1}\right) + \log x_1 \log x_2 - \frac{\pi^2}{2}$ and the approximation

$$\langle 5_2 \rangle_N \sim \iint dx_1 dx_2 \exp\left(\frac{iN}{2\pi} V_{5_2}(x_1, x_2)\right). \tag{5.17}$$

Again by use of the integral expression of the dilogarithm, we end up with the following saddle point equations and solutions (with the help of Mathematica)

$$\begin{cases} \frac{\partial}{\partial x_1} V_{5_2}(x) = 0 \\ \frac{\partial}{\partial x_2} V_{5_2}(x) = 0 \end{cases} \iff \begin{cases} \frac{\log\left(1 - x_1^{-1}\right)}{x_1} + \frac{\log x_2}{x_1} = 0 \\ -2\frac{\log(1 - x_2)}{x_2} + \frac{\log x_1}{x_2} = 0 \end{cases}$$

$$\iff \begin{cases} x_{1,0} = 0.122561 + i\,0.744862 \\ x_{2,0} = 0.337641 - i\,0.56228 \end{cases}$$

or

$$\begin{cases} x_{1,0} = 0.122561 - i\,0.744862 \\ x_{2,0} = 0.337641 + i\,0.56228. \end{cases}$$

As the first solution is responsible for the maximum contribution to the integral (5.17), we only retain that root.

Comparison. Finally, we compare $c_1(5_2)$ and $\Re\left(iV_{5_2}(x_{10}, x_{20})\right)$ to the hyperbolic volume $\operatorname{Vol}(\mathbb{S}^3 \setminus 5_2)$.

$$c_1(5_2) = 2.8281219744 \pm 1.5571 \times 10^{-8},$$
$$\Re\left(iV_{5_2}(x_{10}, x_{20})\right) = 2.82812\ldots,$$
$$\operatorname{Vol}(\mathbb{S}^3 \setminus 5_2) = 2.828122088330783\ldots$$

These results support the Volume Conjecture 5.1, since they only differ by a value smaller than 10^{-5}. $\qquad\square$

5.5.2. Analytical proof. The proof we expose for the knot 5_2 is similar to the potential/saddle point method encountered in chapter 5.3. Indeed, we introduce a potential function (but different from the one in 5.3), that was first suggested by Y. Yokota and which allows us to express the Kashaev invariant as an integral solvable with the saddle point method. The crucial difference to the numerical method lies in the connection that is established between the saddle point equations and the hyperbolicity equations for a certain topological triangulation of the knot complement. Indeed they coincide.

Proof. In this proof, we are merely going to explain the essential ideas for showing the Volume Conjecture (version 5.1) for the knot 5_2, for the details of some constructions, we refer to the original articles [Yok03], [Yok] and [Cho10]. Let us proceed in 4 steps.

1ˢᵗ step. The first step is sacrificed to the construction of the potential function V associated to the $(1,1)$-tangle diagram of the knot 5_2 illustrated by Figure 42 (D_b). The potential function can be expressed as

$$V(x,y) = \mathrm{Li}_2\,(x) + \mathrm{Li}_2\left(\frac{1}{x}\right) + \mathrm{Li}_2\,(y) - \mathrm{Li}_2\left(\frac{1}{y}\right) - \mathrm{Li}_2\left(\frac{y}{x}\right) - \frac{\pi^2}{6}. \quad (5.18)$$

Proof. (1ˢᵗ step.) We are going to explain the construction of this potential function following [Cho10].
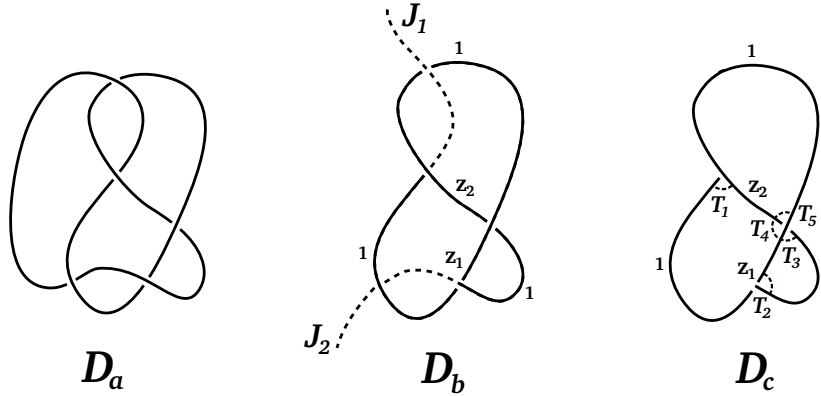

Figure 42: *Construction of the potential V via triangulation*

(a) We start from the reduced (there are no unnecessary crossings) diagram D_a of 5_2 and define *edges* of D_a as arcs connecting two adjacent crossing points. In our case, D_a contains 10 edges.

(b) We transform D_a into a $(1,1)$-tangle diagram D_b by cutting up one arc of D_a in order to obtain the two open edges J_1 and J_2. Yokota assumes several conditions on the $(1,1)$-tangle diagram (see [Yok]), but we retain, that D_b should again be reduced (this is achieved by performing (R1) and (R2)) and that J_1 respectively J_2 should be chosen in a way such that they are first involved in an over-/ undercrossing. Then J_1 and J_2 are extended so that their non-boundary endpoints become the first undercrossing- and first overcrossing points respectively, these two points not being the same. It was shown by Yokota in [Yok] that such a situation is always possible for every hyperbolic knots.

(c) J_1 and J_2 are now removed from D_b and the resulting open edges are glued together with the exception of the trivalent points. 5 edges remain on the new diagram D_c. Next, we associate complex variables z_1, z_2 to *contributing edges* of D_c (that is, edges lying on the bounded regions of D_c) and 1 to the *non-contributing edges*.

At each remaining crossing, we draw a small circle with the part in the

unbounded region of the diagram and the part that was on $J_1 \cup J_2$ omitted. The surviving 5 arcs correspond to ideal tetrahedra and an ideal triangulation of $\mathbb{S}^3 \setminus 5_2$ is obtained by gluing them together. For more details on the gluing rules, again [Yok] may be consulted. The most important rule to guarantee the complete hyperbolic structure are the hyperbolicity equations, appearing in step 3. We denote by $T(t_j)$ (T_j on the figure) these ideal tetrahedra, each of them parametrized by a complex number t_j, $1 \le j \le 5$, with positive imaginary part.

(d) The assignment of a parameter t_j, of a dilogarithm function as well as of a signature σ_j to each tetrahedra $T(t_j)$ is ruled by

$$\text{Li}_2(t_j) - \frac{\pi^2}{6} \qquad\qquad -\text{Li}_2(t_j) + \frac{\pi^2}{6}$$
$$t_j = \frac{y}{x} \;,\;\; \sigma_j = +1 \qquad\qquad t_j = \frac{y}{x} \;,\;\; \sigma_j = -1$$

The reason for the dilogarithm association will be given in step 3 and is quite similar to the argument exposed in the numerical proof 5.3.

(f) Eventually, the potential introduced by Y. Yokota is defined as

$$V(z_1, z_2) := \sum_{j=1}^{5} \sigma_j \left(\text{Li}_2 \left(t_j^{\sigma_j} \right) - \frac{\pi^2}{6} \right).$$

In our case, we find

j	1	2	3	4	5
t_j	z_2	z_1	$\frac{1}{z_1}$	$\frac{z_1}{z_2}$	z_2
σ_j	-1	$+1$	$+1$	-1	$+1$

and thus, by setting $x := z_1$ and $y := z_2$, the resulting potential is given by

$$V(x, y) = -\text{Li}_2 \left(\frac{1}{y} \right) + \frac{\pi^2}{6} + \text{Li}_2 (x) - \frac{\pi^2}{6} + \text{Li}_2 \left(\frac{1}{x} \right) - \frac{\pi^2}{6}$$
$$- \text{Li}_2 \left(\frac{y}{x} \right) + \frac{\pi^2}{6} + \text{Li}_2 (y) - \frac{\pi^2}{6}$$
$$= \text{Li}_2 (x) + \text{Li}_2 \left(\frac{1}{x} \right) + \text{Li}_2 (y) - \text{Li}_2 \left(\frac{1}{y} \right) - \text{Li}_2 \left(\frac{y}{x} \right) - \frac{\pi^2}{6}.$$

$\square$

2$^{\text{nd}}$ step.   In the next step, we can face the computation of the volume of the 5_2 knot complement. It turns out that the following equality holds

$$\text{Vol}(\mathbb{S}^3 \setminus 5_2) = 2\,\text{D}\,(y_0) + \text{D} \left(\frac{x_0}{y_0} \right) = 2.828122088330783\ldots, \qquad (5.19)$$

where D is the Bloch-Wigner function defined in (2.11) and (x_0, y_0) is the unique solution (*geometric solution*) to the hyperbolicity equations arising from the ideal triangulation of step 1.

Proof. (2nd step.) Using the triangulation from step 1, the resulting hyperbolicity equations (standing for the consistency and the cusp conditions) that need to be satisfied for having a complete hyperbolic structure on the 5_2 knot complement, write

$$\frac{\left(1 - \frac{y}{x}\right)(1 - x)}{1 - \frac{1}{x}} = \frac{1 - \frac{y}{x}}{(1 - y)\left(1 - \frac{1}{y}\right)} = 1. \tag{5.20}$$

For their derivation, we refer to [Yok03] p.5-8. They can be reduced to

$$\begin{cases} y & = & (y - 1)^3 \\ x & = & y - 1. \end{cases}$$

With the help of Mathematica, the solutions to these equations are determined (we do not retain the real solution)

$$\begin{cases} x_0 & = & -0.662359 + i\, 0.56228 \\ y_0 & = & 0.337641 + i\, 0.56228 \end{cases} \quad \text{or} \quad \begin{cases} x_0 & = & -0.662359 - i\, 0.56228 \\ y_0 & = & 0.337641 - i\, 0.56228. \end{cases}$$

The last solution is excluded since the imaginary parts should be positive. Consequently, with respect to this solution, the ideal triangulation $T(t_1), \ldots, T(t_5)$ where $t_1 = y$, $t_2 = x$, $t_3 = \frac{1}{x}$, $t_4 = \frac{x}{y}$ and $t_5 = y$ can be reformulated as being composed of the ideal tetrahedra

$$T(y_0), T(x_0), T\left(\frac{1}{x_0}\right), T\left(\frac{x_0}{y_0}\right), T(y_0),$$

with

$$x_0 = -0.662359 + i\, 0.56228, \quad y_0 = 0.337641 + i\, 0.56228.$$

The corresponding hyperbolic volume, according to (2.13), is given by

$$\text{Vol}(\mathbb{S}^3 \setminus 5_2) = \text{D}(y_0) + \text{D}(x_0) + \text{D}\left(\frac{1}{x_0}\right) + \text{D}\left(\frac{x_0}{y_0}\right) + \text{D}(y_0)$$

$$= 2\,\text{D}(y_0) + \text{D}\left(\frac{x_0}{y_0}\right),$$

since $D(z) = -D\left(\frac{1}{z}\right)$ for any $z \in \mathbb{C} \cup \{\infty\}$.   □

3rd step. So far, we handle the right hand side (5.1) for 5_2. In order to enlighten the left hand side and its coherence with the volume formula, we establish a relationship between the classical limit of the Kashaev invariant and the potential $V(x, y)$ abiding by the scheme from section 5.3. Thus, we show

$$2\pi \lim_{N \to \infty} \frac{\log |\langle 5_2 \rangle_N|}{N} = \Im(V(x_0, y_0)), \tag{5.21}$$

(x_0, y_0) being a saddle point of $V(x, y)$ with maximal contribution.

Proof. (3$^{\text{rd}}$ step.) Recall the approximations we deduced in section 5.3 for q^{ab}, $(q)_n$ and $(q)_n^*$ for large N

$$q^{ab} \sim \exp\left(-\frac{iN}{2\pi}\log q^a \log q^b\right)$$

$$(q)_n \sim \exp\left(\frac{iN}{2\pi}\left(\operatorname{Li}_2(q^n) - \frac{\pi^2}{6}\right)\right)$$

$$(q)_n^* \sim \exp\left(\frac{iN}{2\pi}\left(-\operatorname{Li}_2(q^{-n}) + \frac{\pi^2}{6}\right)\right).$$

Almost [1] equivalent to (5.16), the Kashaev invariant for the knot 5_2 can be expressed as (see [Yok03])

$$\langle 5_2 \rangle_N = \pm \sum_{1 \leq a \leq b \leq N-1} \frac{N^3 q^{-b+a}}{(q)_{a-1}(q)_{a-1}^*(q)_{b-1}(q)_{b-a}^*(q)_{-b}}. \tag{5.22}$$

Before substituting the previous approximations in (5.22), we shall transform the latter formula using for $n \in \{0, 1, \ldots, N-1\}$ the identities

$$N = (q)_{n-1}(q)_{N-n}^*,$$

$$(q)_{-n}^* = (q)_{N-n}^*.$$

These modifications lead to (after choosing the $+$ convention)

$$\langle 5_2 \rangle_N = \sum_{1 \leq a \leq b \leq N-1} \frac{(q)_{-a}^*(q)_{-b}^*(q)_{b-1}^* q^{-b+a}}{(q)_{a-1}^*(q)_{b-a}^*}.$$

The replacements (5.5), (5.6) and (5.7) then provide an approximation for the Kashaev invariant

$$\langle 5_2 \rangle_N \sim \sum_{1 \leq a \leq b \leq N-1} \exp\left(\frac{iN}{2\pi}\left(-\operatorname{Li}_2(q^a) - \operatorname{Li}_2(q^b) - \operatorname{Li}_2(qq^{-b}) + \frac{\pi^2}{6}\right)\right)$$

$$\times \exp\left(\frac{iN}{2\pi}\left(\operatorname{Li}_2(qq^{-a}) + \operatorname{Li}_2(q^{a-b}) - \log q \log q^{-b+a}\right)\right)$$

$$\sim \sum_{1 \leq a \leq b \leq N-1} \tilde{\alpha}(q^a, q^b, N) \times \exp\left(\frac{N}{2\pi i}\tilde{V}(q^a, q^b, N)\right),$$

---

[1] In fact, this formula contains a bug: there are seemingly three terms missing! While working on this proof, I tried to understand the correspondence between the Yokota potential and the potential introduced in the framework of the numerical method. The conclusion is that the Kashaev invariant (5.16), known to be true, is not equivalent to (5.22), a contradiction! We communicated the problem to H. Murakami, J. Cho and J. Murakami and they quickly confirmed the inconsistency. J. Cho and J. Murakami forwarded us a preprint on *Optimistic limits of the colored Jones invariants*. A suggestion of H. Murakami states that the term for $a = b = 0$ and twice the term $a = 0, b = 1$ are missing in the formula. A sketchy calculation of my own let me think, that the proof presented here does nonetheless work, since these terms will pass in the realm of the function $\tilde{\alpha}$.

where

$$\tilde{\alpha}(q^a, q^b, N) := \exp\left(-\frac{iN}{2\pi} \log q \log q^{-b+a}\right),$$

$$\tilde{V}(q^a, q^b, N) := \text{Li}_2\left(q^a\right) + \text{Li}_2\left(q^b\right) + \text{Li}_2\left(qq^{-b}\right) - \frac{\pi^2}{6} - \text{Li}_2\left(qq^{-a}\right) - \text{Li}_2\left(q^{a-b}\right).$$

After setting $x := q^b$, $y := q^a$ and by fading to the classical N-limit, the resulting potential is given by

$$V(x, y) = \text{Li}_2\left(y\right) + \text{Li}_2\left(x\right) + \text{Li}_2\left(\frac{1}{x}\right) - \text{Li}_2\left(\frac{1}{y}\right) - \text{Li}_2\left(\frac{y}{x}\right) - \frac{\pi^2}{6},$$

and $\tilde{\alpha}(q^a, q^b, N) \to \alpha(N)$, which is at most of order 1. Notice that the q-factors from the dilogarithm terms $\text{Li}_2\left(qq^{-a}\right)$ and $\text{Li}_2\left(qq^{-a}\right)$ vanish for $N \to \infty$, since $q \to 1$. This potential is in agreement with the potential (5.18) from step 1.

We now focus on the computation of the approximation of $\langle 5_2 \rangle_N$. As the asymptotic behaviour is controlled by the maximum summand, we seek for this term. Therefore, we pass from the summation to an integral

$$\langle 5_2 \rangle_N \sim \iint dx\, dy\; \alpha(N) \exp\left(\frac{N}{2\pi i} V(x, y)\right), \tag{5.23}$$

for lack of clear arguments, we do not detail the integration contours. This shapes up as useful, because the integral can be evaluated by means of the saddle point method, that is, its value is largely dominated by a critical value of $V(x, y)$, reached in some extremum point $(x_0, y_0) \in \mathbb{C}^2$

$$\langle 5_2 \rangle_N \sim \alpha(N) \exp\left(\frac{N}{2\pi i} V(x_0, y_0)\right).$$

As an immediate consequence of this approximation, the classical N-limit becomes

$$2\pi \lim_{N\to\infty} \frac{\log\langle 5_2 \rangle_N}{N} = 2\pi \underbrace{\lim_{N\to\infty} \frac{\log(\alpha(N))}{N}}_{=0} - i \lim_{N\to\infty} V(x_0, y_0)$$

$$= -iV(x_0, y_0).$$

Note that in the Volume Conjecture, we study the growth of the absolute value of the Kashaev invariant. This is reflected in the previous calculation by taking

$$2\pi \lim_{N\to\infty} \frac{\log|\langle 5_2 \rangle_N|}{N} = 2\pi \lim_{N\to\infty} \Re\left(\frac{\log\langle 5_2 \rangle_N}{N}\right)$$

$$= \Re\left(-iV(x_0, y_0)\right)$$

$$= \Im\left(V(x_0, y_0)\right).$$

Despite of the right form, the previous limit makes no sense until the extremum point (x_0, y_0) is specified. Indeed (x_0, y_0) is a complex solution to

$$
\begin{cases}
\frac{\partial V(x,y)}{\partial x} &= 0 \\
\frac{\partial V(x,y)}{\partial y} &= 0
\end{cases}
$$

$$
\Longleftrightarrow
\begin{cases}
\frac{\log(1-x)}{x} - \frac{\log(1-x^{-1})}{x} + \frac{\log(1-yx^{-1})}{x} &= 0 \\
-\frac{\log(1-y)}{y} - \frac{\log(1-y^{-1})}{y} + \frac{\log(1-yx^{-1})}{y} &= 0
\end{cases}
$$

$$
\Longleftrightarrow
\begin{cases}
\frac{(1-x)(1-yx^{-1})}{1-x^{-1}} &= 1 \\
\frac{1-yx^{-1}}{(1-y)(1-y^{-1})} &= 1.
\end{cases}
$$

These are nothing else than the hyperbolicity equations (5.20) and therefore we retain the following numerical solution of maximum contribution to the integral (5.23)

$$
x_0 = -0.662359 + \mathrm{i}\, 0.56228, \quad y_0 = 0.337641 + \mathrm{i}\, 0.56228.
$$

$\square$

4$^{\text{th}}$ step. Let us summarize the previous steps in order to draw the appropriate and intended conclusion, namely

$$
\mathrm{Vol}(\mathbb{S}^3 \setminus 5_2) = \Im\left(V(x_0, y_0)\right). \tag{5.24}
$$

Proof. (4$^{\text{th}}$ step.) The investigation of the right hand side of the Volume Conjecture consisted in the study of the knot diagram and its possible triangulation, providing the potential $V(x, y)$ (5.18), giving rise to the hyperbolicity equations (5.20) and resulting in the volume formula (5.19) for the 5_2 knot complement. For the left hand side of the Volume Conjecture, by means of approximations, we compassed the potential $\tilde{V}(q^a, q^b, N)$ and the saddle point (x_0, y_0) leading to the asymptotic value (5.21) of the Kashaev invariant. The parallels of the two approaches become obvious through the relations

$$
\lim_{N \to \infty} \tilde{V}(q^a, q^b, N) \,\Big|_{\substack{q^a \to y \\ q^b \to x}} = V(x, y),
$$

$$
x \frac{\partial V(x, y)}{\partial x} = 0 \Longleftrightarrow \log(H_1) = 0,
$$
$$
y \frac{\partial V(x, y)}{\partial y} = 0 \Longleftrightarrow \log(H_2) = 0,
$$

where H_1, H_2 correspond to the first and second part of the hyperbolicity equations (5.20). The last missing piece of the puzzle, that is the ultimate connection between the two sides (5.24), is explored by using the Bloch-Wigner function (2.11) in the expression of the classical N-limit of the po-

tential $V(x, y)$. This results in

$$\Im\left(V(x, y)\right) = \Im\left(\mathrm{Li}_2\left(y\right) + \mathrm{Li}_2\left(x\right) + \mathrm{Li}_2\left(\frac{1}{x}\right) - \mathrm{Li}_2\left(\frac{1}{y}\right) - \mathrm{Li}_2\left(\frac{y}{x}\right)\right)$$

$$= \mathrm{D}\left(y\right) + \mathrm{D}\left(x\right) + \mathrm{D}\left(\frac{1}{x}\right) - \mathrm{D}\left(\frac{1}{y}\right) - \mathrm{D}\left(\frac{y}{x}\right)$$

$$+ \log|x|\left(-\arg\left(1 - x\right) + \arg\left(1 - \frac{1}{x}\right) - \arg\left(1 - \frac{y}{x}\right)\right)$$

$$+ \log|y|\left(-\arg\left(1 - y\right) - \arg\left(1 - \frac{1}{y}\right) + \arg\left(1 - \frac{y}{x}\right)\right).$$

At the saddle point, all but the Bloch-Wigner function terms vanish, since

$$\log|x_0|\left(-\arg\left(1 - x_0\right) + \arg\left(1 - \frac{1}{x_0}\right) - \arg\left(1 - \frac{y_0}{x_0}\right)\right)$$

$$+ \log|y_0|\left(-\arg\left(1 - y_0\right) - \arg\left(1 - \frac{1}{y_0}\right) + \arg\left(1 - \frac{y_0}{x_0}\right)\right)$$

$$= \log|x_0|\left(\arg\left(\underbrace{\frac{1 - \frac{1}{x_0}}{(1 - x_0)\left(1 - \frac{y_0}{x_0}\right)}}_{=1}\right)\right) + \log|y_0|\left(\arg\left(\underbrace{\frac{1 - \frac{y_0}{x_0}}{\left(1 - \frac{1}{y_0}\right)(1 - y_0)}}_{=1}\right)\right)$$

$$= 0$$

As a consequence, we get

$$\Im\left(V(x_0, y_0)\right) = \mathrm{D}\left(y_0\right) + \mathrm{D}\left(x_0\right) + \mathrm{D}\left(\frac{1}{x_0}\right) - \mathrm{D}\left(\frac{1}{y_0}\right) - \mathrm{D}\left(\frac{y_0}{x_0}\right)$$

$$= 2\,\mathrm{D}\left(y_0\right) + \mathrm{D}\left(\frac{x_0}{y_0}\right)$$

$$\overset{(5.19)}{=} \mathrm{Vol}(\mathbb{S}^3 \setminus 5_2)$$

$$\square$$

This accomplishes the proof of the Volume Conjecture for the knot 5_2. $\square$

5.6. Comments

The mysterious nature of the Volume Conjecture, which fascinates through its aptitude for establishing a bridge between quantum invariants of knots and hyperbolic geometry, has been highly clarified since its formulation by Kashaev in 1996. An important step in favour of a better understanding was the equivalence between the Kashaev invariant and the colored Jones polynomial shown by Murakami, Murakami in 2001. The proofs and attempts for proofs that have been worked out for the last years lead to a better comprehension of the Volume Conjecture and raised simultaneously new questions. Two of them are commented below. Moreover, we give an up-to-date (according to our information sources [vdV] and [Mur10]) list of knots and links for which, the Conjecture has been proved so far.

5.6.1. Generalization of the Volume Conjecture.   The Volume Conjecture treats the asymptotic behaviour of the absolute value of the Kashaev invariant. A natural question we can ask is: What will happen if we drop this condition and then study the asymptotic behaviour? W. Thurston mentioned that the Chern-Simons invariant can be regarded as an imaginary part of the volume. Again, we will not comment on Chern-Simons invariants in this work, but it is interesting to know that if we involve it, we get a *complexified Volume Conjecture* first pointed out in [MMO$^+$02] in 2002.

VOLUME CONJECTURE 5.5 (Complexification of the Volume Conjecture, 2002)
For any hyperbolic knot K with corresponding colored Jones polynomial $J_N(K)$ and hyperbolic volume Vol(K), the following asymptotic behaviour holds:

$$2\pi \lim_{N \to \infty} \frac{\log(J_N(K))}{N} = Vol(K) + iCS(K) \qquad \mod \pi^2 i\mathbb{Z},$$

where $CS(K)$ is the Chern-Simons invariant defined for a 3-manifold $\mathbb{S}^3 \setminus K$ with torus boundary.

Remark. This complexified version has so far been numerically verified for knots up to 8 crossings as well as for the Whitehead link.

Another factor one can ponder on is the deformation parameter q. Indeed, we considered the colored Jones polynomial evaluated at q, that is the N-root of unity, since this coincides with the Kashaev invariant. The resulting limit (if existing) corresponds to the complete hyperbolic structure of the hyperbolic knot complement. What happens now if the complete hyperbolic structure is deformed to incomplete ones? Is there a way to modify the Volume Conjecture and its complexification in order to get a similar result? The answer is given by studying the "deformed" limit

$$2\pi \lim_{N \to \infty} \frac{\log(J_N(K; \tilde{q}))}{N},$$

where $J_N(K; \tilde{q})$ is the colored Jones polynomial of K evaluated at $\tilde{q} := q \exp\left(\frac{u}{N}\right)$, $u \in \mathbb{C}$. H. Murakami stated the following conjecture in [Mur07] in 2007.

VOLUME CONJECTURE 5.6 (H. Murakami, 2007)
For any knot K, there exits an open set $U \subset \mathbb{C}$ such that if $u \in U$, then the following limit exists

$$\lim_{N \to \infty} \frac{\log\left(J_N\left(K; exp\left(\frac{u + 2\pi i}{N}\right)\right)\right)}{N}.$$

Moreover if we put

$$H(K; u) := (u + 2\pi i) \lim_{N \to \infty} \frac{\log\left(J_N\left(K; exp\left(\frac{u + 2\pi i}{N}\right)\right)\right)}{N},$$

$$v := 2\frac{dH(K; u)}{du} - 2\pi i,$$

then we have

$$Vol(K; u) = \Im(H(K; u)) - \pi \Re(u) - \frac{1}{2} \Re(u) \Im(u),$$

$Vol(K; u)$ being the volume of $\mathbb{S}^3 \setminus K$ with deformed hyperbolic structure.

Remark. The case for the figure-eight knot is verified in [Mur10], whereas the case of torus knots is treated in [Mur07]. More proofs are not yet known.

5.6.2. Knots and links for which the Volume Conjecture is proved.
Through the previous proofs of the Volume Conjecture for particular knots, we recognized how complex and diverse these demonstrations are. Each case needs to be treated individually and requires a lot of geometrical and numerical effort. For the following knots and links, the Volume Conjecture has been shown to be true.

Knots:
- Figure-eight knot 4_1,
- the knot 5_2,
- torus knots,
- iterated torus knots,
- Whitehead doubles of torus knots of type $T(2, 2p)$.

Remark. The complement of a torus knot in the 3-sphere does not admit a complete hyperbolic structure which implies that the hyperbolic volume as well as the Gromov norm vanish. The asymptotic behaviour of the colored Jones polynomial can also be shown to cancel out (see [KT00] or [Hik03]).

Links:
- Whitehead link and twisted Whitehead links,
- torus links of type $T(2, 2p)$,
- iterated torus links,
- Borromean rings,
- Whitehead chains,
- Borromean double of the figure-eight knot.

The theory established by Y. Yokota (cf. proof of the knot 5_2) seems to be rather promising pertaining to the prospect of setting up a general algorithm to verify the Volume Conjecture. It could have been applied in the proof of the figure-eight knot too. However, as noticed in the proof, there are still important arguments missing to justify some steps in the approximation process, even though the latter is known to work numerically. What is more, it remains nebulous how to define the theory on potentials in a way such that it is invariant under the choice of expression for the knot invariant. These are a few open problems on the Volume Conjecture that keep research on this subject and related topics striving forward.

REFERENCES

[Ada94]   C. C. ADAMS. *The knot book*. W. H. Freeman and Company, New York (1994). An elementary introduction to the mathematical theory of knots. 3, 39

[Akt09]   T. AKTOSUN. *Inverse scattering transform and the theory of solitons* (2009). arXiv:0905.4746v1 [nlin.SI]. 39, 43

[Bir74]   J. S. BIRMAN. *Braids, links, and mapping class groups*. Princeton University Press, Princeton, N.J. (1974). Annals of Mathematics Studies, No. 82. 18

[Cho10]   J. CHO. *Yokota theory, the invariant trace fields of hyperbolic knots and the borel regulator map* (2010). arXiv:1005.3094v1 [math.GT]. 86, 87

[Dri87]   V. G. DRINFEL'D. *Quantum groups*. In *Proceedings of the International Congress of Mathematicians, Vol. 1, 2 (Berkeley, Calif., 1986)*. Amer. Math. Soc., Providence, RI, pages 798–820. 45, 46, 47

[EW06]   K. ERDMANN and M. J. WILDON. *Introduction to Lie algebras*. Springer Undergraduate Mathematics Series. Springer-Verlag London Ltd., London (2006). 49

[Fad95]   L. FADDEEV. *Instructive history of the quantum inverse scattering method*. Acta Applicandae Mathematicae (1995). **39**, 69–84. 39, 43

[GR07]   I. S. GRADSHTEYN and I. M. RYZHIK. *Table of integrals, series, and products*. Elsevier/Academic Press, Amsterdam, seventh edition (2007). 68

[Hik03]   K. HIKAMI. *Volume conjecture and asymptotic expansion of q-series*. Experiment. Math. (2003). **12**(3), 319–337. URL http://projecteuclid.org/getRecord?id=euclid.em/1087329235. 77, 79, 80, 85, 95

[Jac10]   M. JACQUEMET. *The Discovery of Hyperbolization of Knot Complements*. Master's thesis, University of Fribourg, Switzerland (2010). 79

[Jim94]   M. JIMBO. *Introduction to the Yang-Baxter equation*. In *Advanced Series in Mathematical Physics*, volume 17. C.N. Yang, M.L.Ge (1994). 39

[Ka94]   R. M. KASHAEV. *Quantum dilogarithm as a 6j-symbol*. Modern Phys. Lett. A (1994). **9**(40), 3757–3768. URL http://dx.doi.org/10.1142/S0217732394003610. 58, 59, 61

[Ka95]   —. *A link invariant from quantum dilogarithm*. Modern Phys. Lett. A (1995). **10**(19), 1409–1418. URL http://dx.doi.org/10.1142/S0217732395001526. 58, 60, 66

[Kass95]   C. KASSEL. *Quantum groups*, volume 155 of *Graduate Texts in Mathematics*. Springer-Verlag, New York (1995). 19, 32, 34, 47

[Ka97]   R. M. KASHAEV. *The hyperbolic volume of knots from the quantum dilogarithm*. Lett. Math. Phys. (1997). **39**(3), 269–275. URL http://dx.doi.org/10.1023/A:1007364912784. 61, 75, 76, 77

[Kel08]   R. KELLERHALS. *Géométrie hyperbolique* (2008). Unpublished lecture notes. 21

[Kel10]   —. *Komplexe hyperbolische Geometrie* (2010). Unpublished lecture notes. 21

[KM91]   R. KIRBY and P. MELVIN. *The 3-manifold invariants of Witten and Reshetikhin-Turaev for* sl(2, **C**). Invent. Math. (1991). **105**(3), 473–545. URL http://dx.doi.org/10.1007/BF01232277. 19, 32, 50, 51, 53, 54, 58, 65, 66, 68

[KaM98]   M. KARBACH and G. MÜLLER. *Introduction to the Bethe Ansatz I* (1998). arXiv:9809 162.1. 39

[KRT97]   C. KASSEL, M. ROSSO and V. TURAEV. *Quantum groups and knot invariants*, volume 5 of *Panoramas et Synthèses [Panoramas and Syntheses]*. Société Mathématique de France, Paris (1997). 19, 47

[KT00]   R. M. KASHAEV and O. TIRKKONEN. *A proof of the volume conjecture on torus knots*. Zap. Nauchn. Sem. S.-Peterburg. Otdel. Mat. Inst. Steklov. (POMI) (2000). **269**(Vopr. Kvant. Teor. Polya i Stat. Fiz. 16), 262–268, 370. URL http://dx.doi.org/10.1023/A:1022608131142. 95

[KT08]   C. KASSEL and V. TURAEV. *Braid groups*, volume 247 of *Graduate Texts in Mathematics*. Springer, New York (2008). URL http://dx.doi.org/10.1007/978-0-387-68548-9. With the graphical assistance of Olivier Dodane. 18

[Lic97]   W. B. R. LICKORISH. *An introduction to knot theory*, volume 175 of *Graduate Texts in Mathematics*. Springer-Verlag, New York (1997). 3, 10

[MM01]   H. MURAKAMI and J. MURAKAMI. *The colored Jones polynomials and the simplicial volume of a knot*. Acta Math. (2001). **186**(1), 85–104. URL http://dx.doi.org/10.1007/BF02392716. 61, 67, 76, 77

[MMO⁺02] H. MURAKAMI, J. MURAKAMI, M. OKAMOTO, T. TAKATA and Y. YOKOTA. *Kashaev's conjecture and the Chern-Simons invariants of knots and links*. Experiment. Math. (2002). **11**(3), 427–435. URL `http://projecteuclid.org/getRecord?id=euclid.em/1057777432`. 94

[Mur07]   H. MURAKAMI. *A version of the volume conjecture*. Adv. Math. (2007). **211**(2), 678–683. URL `http://dx.doi.org/10.1016/j.aim.2006.09.005`. 94, 95

[Mur10]   —. *An introduction to the volume conjecture* (2010). arXiv:1002.0126v1 [math.GT]. 57, 71, 75, 81, 93, 95

[PS97]   V. V. PRASOLOV and A. B. SOSSINSKY. *Knots, links, braids and 3-manifolds*, volume 154 of *Translations of Mathematical Monographs*. American Mathematical Society, Providence, RI (1997). An introduction to the new invariants in low-dimensional topology, Translated from the Russian manuscript by Sossinsky [Sosinskiˇi]. 3, 7, 12, 16, 32, 39, 45

[Rat06]   J. G. RATCLIFFE. *Foundations of hyperbolic manifolds*, volume 149 of *Graduate Texts in Mathematics*. Springer, New York, second edition (2006). 21, 25, 26, 27, 31

[RT91]   N. RESHETIKHIN and V. G. TURAEV. *Invariants of 3-manifolds via link polynomials and quantum groups*. Invent. Math. (1991). **103**(3), 547–597. URL `http://dx.doi.org/10.1007/BF01239527`. 52

[Thu02]   W. P. THURSTON. *The geometry and topology of three-manifolds* (2002). URL `http://www.msri.org/publications/books/gt3m/`. Electronic version 1.1. 31, 84

[Tur88]   V. G. TURAEV. *The Yang-Baxter equation and invariants of links*. Invent. Math. (1988). **92**(3), 527–553. URL `http://dx.doi.org/10.1007/BF01393746`. 37, 62, 65, 71

[Tur94]   —. *Quantum invariants of knots and 3-manifolds*, volume 18 of *de Gruyter Studies in Mathematics*. Walter de Gruyter & Co., Berlin (1994). 45

[Tur09]   P. TURNER. *Selected topics in geometry and topology - knots, links and 3-manifolds* (2009). Unpublished lecture notes. 3, 11

[vdV]   R. VAN DER VEEN. *A collection of all known results of the volume conjecture*. URL `http://staff.science.uva.nl/~riveen/results_on_the_volume_conjecture.htm`. Homepage. 93

[Yok]   Y. YOKOTA. *On the volume conjecture for hyperbolic knots*. URL `http://www.comp.metro-u.ac.jp/~jojo/papers.html`. Preprint. 86, 87, 88

[Yok03]   —. *From the Jones polynomial to the A-polynomial of hyperbolic knots*. In *Proceedings of the Winter Workshop of Topology/Workshop of Topology and Computer (Sendai, 2002/Nara, 2001)*, volume 9. pages 11–21. URL `http://dx.doi.org/10.4036/iis.2003.11`. 75, 86, 89, 90